Universiteit
Leiden
The Netherlands

The effects of triglycerides and fatty acids on T cells: role in atherosclerosis

Reilly, N.A.

Citation
Reilly, N. A. (2024, October 30). *The effects of triglycerides and fatty acids on T cells: role in atherosclerosis*. Retrieved from https://hdl.handle.net/1887/4106896

Version:	Publisher's Version
License:	Licence agreement concerning inclusion of doctoral thesis in the Institutional Repository of the University of Leiden
Downloaded from:	https://hdl.handle.net/1887/4106896

Note: To cite this publication please use the final published version (if applicable).

CHAPTER 3

Oleic acid triggers metabolic rewiring of T cells poising them for T helper 9 differentiation

Nathalie A. Reilly,[1,7] Friederike Sonnet,[2] Koen F. Dekkers,[1] Joanneke C. Kwekkeboom,[3] Lucy Sinke,[1] Stan Hilt,[1] Hayat M. Suleiman,[1] Marten A. Hoeksema,[4] Hailiang Mei,[5] Erik W. van Zwet,[6] Bart Everts,[2] Andreea Ioan-Facsinay,[3] J. Wouter Jukema,[7,8] and Bastiaan T. Heijmans[1]

[1] *Molecular Epidemiology, Department of Biomedical Data Sciences, Leiden, the Netherlands.*
[2] *Leiden University Center for Infectious Diseases (LUCID), Leiden, the Netherlands.*
[3] *Department of Rheumatology Leiden University Medical Center, Leiden, the Netherlands.*
[4] *Department of Medical Biochemistry, Amsterdam UMC, location University of Amsterdam, Amsterdam, the Netherlands.*
[5] *Sequencing Analysis Support Core, Department of Biomedical Data Sciences, Leiden, the Netherlands.*
[6] *Medical Statistics, Department of Biomedical Data Sciences, Leiden, the Netherlands.*
[7] *Department of Cardiology, Leiden University Medical Center, Leiden, the Netherlands.*
[8] *Netherlands Heart Institute, Utrecht, the Netherlands.*

iScience **27**, *(2024).*
DOI: 10.1016/j.isci.2024.109496

Abstract

T cells are the most common immune cells in atherosclerotic plaques, and the function of T cells can be altered by fatty acids. Here, we show that pre-exposure of $CD4^+$ T cells to oleic acid, an abundant fatty acid linked to cardiovascular events, upregulates core metabolic pathways and promotes differentiation into interleukin-9 (IL-9)-producing cells upon activation. RNA sequencing of non-activated T cells reveals that oleic acid upregulates genes encoding key enzymes responsible for cholesterol and fatty acid biosynthesis. Transcription footprint analysis links these expression changes to the differentiation toward T_H9 cells, a pro-atherogenic subset. Spectral flow cytometry shows that pre-exposure to oleic acid results in a skew toward IL-9^+-producing T cells upon activation. Importantly, pharmacological inhibition of either cholesterol or fatty acid biosynthesis abolishes this effect, suggesting a beneficial role for statins beyond cholesterol lowering. Taken together, oleic acid may affect inflammatory diseases like atherosclerosis by rewiring T cell metabolism.

Highlights

- Non-activated T cells upregulate metabolism-related genes in response to oleic acid.
- The expression changes link to PU.1, a key transcription factor of T helper 9 cells.
- Upon activation, preexposure leads to a skew toward interleukin-9-producing cells.
- Inhibition of cholesterol or fatty acid biosynthesis abolishes this effect.

Graphical abstract

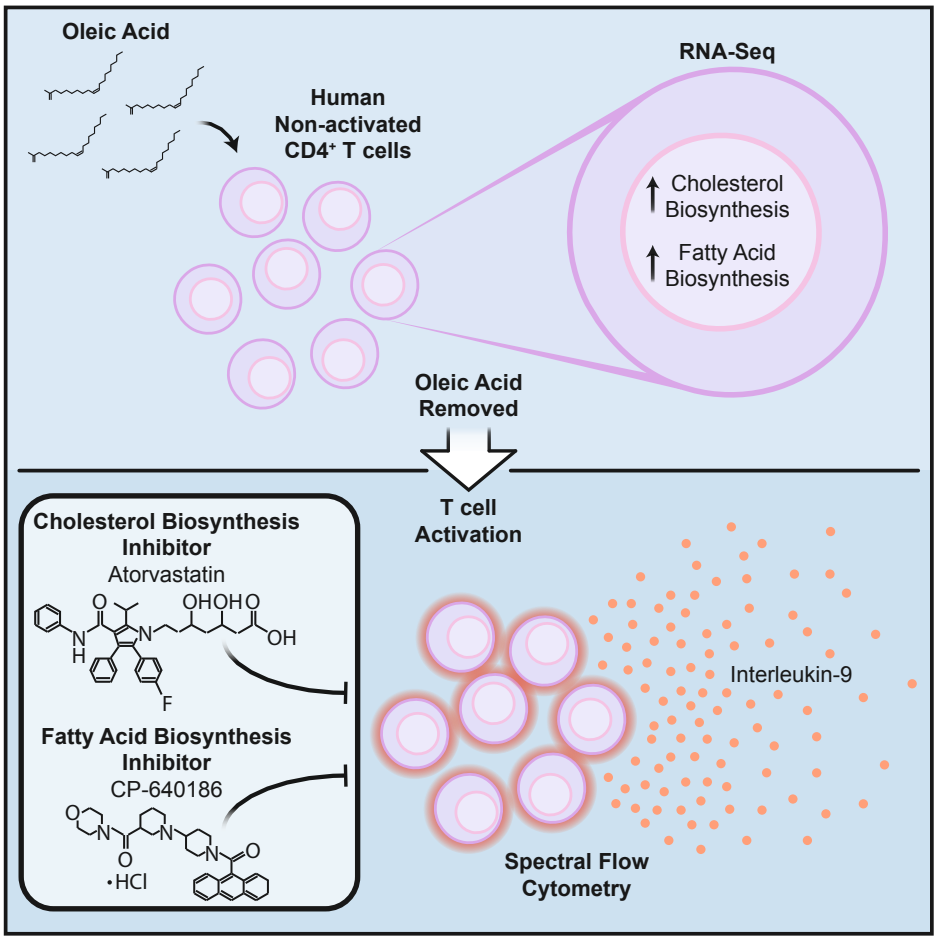

Introduction

Atherosclerosis is the primary underlying cause of cardiovascular disease and is driven by the interactions between the immune system, lipids, and the vascular wall[1, 2]. Recent single-cell RNA sequencing (RNA-seq) and mass cytometry studies showed that T cells make up the majority of immune cells in atherosclerotic plaques, half of which are $CD4^+$ T cells[3-6]. This indicates that the role of $CD4^+$ T cells in atherosclerosis is much greater than previously recognized[7-9]. Lipids and in particular fatty acids are known to have a major influence on the function of $CD4^+$ T cells[2]. While previous research evaluated the effect of fatty acids on $CD4^+$ T cell function during or after activation[2, 10-13], interactions between fatty acids and $CD4^+$ T cells relevant for atherosclerosis can already occur in the circulation, when the cells are in a non-activated state[2]. While the impact of these interactions has not been studied, they may skew the differentiation toward pro- or anti-inflammatory subsets[8, 14] once the $CD4^+$ T cells infiltrate atherosclerotic plaques or other disease sites such as rheumatoid arthritis and become activated[2, 15].

Fatty acids affect $CD4^+$ T cells in multiple ways ranging from activation and proliferation to differentiation[2]. It is thought that these effects are largely mediated by changes in metabolism[16]. In a non-activated state, like in the circulation, $CD4^+$ T cells rely on oxidative phosphorylation and β-oxidation of fatty acids for energy production[17, 18]. However, upon activation, $CD4^+$ T cells switch their metabolism to fatty acid biosynthesis and aerobic glycolysis to support cell growth and proliferation, reminiscent of the Warburg effect[18-20]. Importantly, the generation of specific T cell subset populations is associated with this metabolic reprogramming[10, 21-26]. The generally pro-inflammatory[14, 27, 28] T helper 1 (T_H1) and T helper 17 (T_H17) cells, but also T helper 2 (T_H2) cells that can be both pro- and anti-inflammatory, rely on pathways of aerobic glycolysis upon activation[29-35]. In contrast, the generally anti-inflammatory regulatory T (T_{reg}) cells mainly remain reliant on oxidative phosphorylation even after activation, indicating that the metabolic state of the cell may influence T cell effects in disease[18, 22, 23, 34]. Therefore, fatty acid-mediated metabolic reprogramming of $CD4^+$ T cells may affect the initiation and progression of atherosclerosis by skewing $CD4^+$ T cells toward a pro- or anti-inflammatory phenotype.

In this study, we characterized the effects of oleic acid on non-activated $CD4^+$ T cell function. Oleic acid is a monounsaturated fatty acid that is of particular interest since it is one of the most abundant fatty acids in the circulation[36], is independently associated with an increased risk of cardiovascular events[37, 38], and has been reported to elicit both pro- and anti-inflammatory effects on $CD4^+$ T cells[10-12, 39-43]. To do so, we performed RNA-sequencing on non-activated $CD4^+$ T cells exposed to oleic acid at 5 different time points. Furthermore, we performed spectral cytometry post-activation for various $CD4^+$ T cell markers. We find that oleic acid exposure leads to a metabolic reprogramming and generates a profile that becomes skewed toward T_H2, T_H17, and, notably, T_H9 $CD4^+$ T cells after activation. This skewed profile post-activation is blocked by the addition of metabolic inhibitors during the initial oleic acid exposure.

STAR Methods

Key resources table

REAGENT or RESOURCE	SOURCE	IDENTIFIER
Antibodies		
Anti-human CD4 MicroBeads - lyophilized	Miltenyi Biotec	Cat#130-097-048; RRID:AB_2889919
Anti-human CD3; PE; Isotype Mouse; Clone SK7	BD Biosciences	Cat#345765; RRID:AB_2868796
Anti-human CD4; APC; Isotype Mouse; Clone SK3	BD Biosciences	Cat#345771; RRID:AB_2868799
Anti-human CD8; FITC; Isotype Mouse; Clone HIT8a	BD Biosciences	Cat#555634; RRID:AB_395996
Anti-human CD14; PEcy7; Isotype Mouse; Clone M5E2	BD Biosciences	Cat#557742; RRID:AB_396848
Dynabeads™ Human T-Activator CD3/CD28 for T Cell Expansion and Activation	Thermo Fisher Scientific	Cat#11161D; RRID:AB_2916088
Anti-human CD38; APC/Fire™ 810; Isotype Mouse; Clone HB-7	BioLegend	Cat#356643; RRID:AB_2860936
Anti-human CD8; Pacific Orange™; Isotype Mouse; Clone 3B5	Thermo Fisher Scientific	Cat#MHCD0830; RRID:AB_10372066
Anti-human CD25; BUV563; Isotype Mouse; Clone 2A3	BD Biosciences	Cat#612918; RRID:AB_2870203
Anti-human CD45RA; BUV496; Isotype Mouse; Clone 5H9	BD Biosciences	Cat#741182; RRID:AB_2870749
Anti-human CD45RO; BUV805; Isotype Mouse; Clone UCHL1	BD Biosciences	Cat#748367; RRID:AB_2872786
Anti-human CD4; cFluor® YG584; Isotype Mouse; Clone SK3	Cytek Biosciences	Cat#R7-20042
Anti-human CD3; BUV395; Isotype Mouse; Clone UCHT1	BD Biosciences	Cat#563546; RRID:AB_2744387
Anti-human CD27; APC-H7; Isotype Mouse; Clone M-T271	BD Biosciences	Cat#560222; RRID:AB_1645474
Anti-human CD279 (PD-1); BV750; Isotype Mouse; Clone EH12.1	BD Biosciences	Cat#747446; RRID:AB_2872125
Anti-human CD127; R718; Isotype Mouse; Clone HIL-7R-M21	BD Biosciences	Cat#566967; RRID:AB_2869977

[continued on next page]

Key resources table *[continued]*

REAGENT or RESOURCE	SOURCE	IDENTIFIER
Anti-human CD197 (CCR7); Brilliant Violet 785™; Isotype Mouse; Clone G043H7	BioLegend	Cat#353230; RRID:AB_2561371
Anti-human TNF; PE-Cy™7; Isotype Mouse; Clone MAb11	BD Biosciences	Cat#557647; RRID:AB_396764
Anti-human IL-17A; Pacific Blue™; Isotype Mouse; Clone BL168	BioLegend	Cat#512312; RRID:AB_961392
Anti-human IL-5; APC; Isotype Rat; Clone TRFK5	BioLegend	Cat#504306; RRID:AB_315329
Anti-human IL-4; BUV737; Isotype Rat; Clone MP4-25D2	BD Biosciences	Cat#612835; RRID:AB_2870157
Anti-human IFN-γ; BV650; Isotype Mouse; Clone 4S.B3	BD Biosciences	Cat#563416; RRID:AB_2738193
Anti-human IL-13; BV711; Isotype Rat; Clone JES10-5A2	BD Biosciences	Cat#564288; RRID:AB_2738731
Anti-human IL-9; PE; Isotype Mouse; Clone MH9A4	BioLegend	Cat#507605; RRID:AB_315487
Anti-human IL-10; PerCP-eFluor™ 710; Isotype Rat; Clone JES3-9D7	Thermo Fisher Scientific	Cat#46-7108-42; RRID:AB_2573833
Anti-human CD152; PE-Cy™5; Isotype Mouse; Clone BNI3	BD Biosciences	Cat#555854; RRID:AB_396177
Anti-human IL-21; Alexa Fluor® 647; Isotype Mouse; Clone 3A3-N2.1	BD Biosciences	Cat#560493; RRID:AB_1645421
Anti-human T-bet; KIRAVIA Blue 520™; Isotype Mouse; Clone 4B10	BioLegend	Cat#644838; RRID:AB_2888710
Anti-human FOXP3; PE/Dazzle™ 594; Isotype Mouse; Clone 206D	BioLegend	Cat#320126; RRID:AB_2564024
Anti-human IL-22; Vio® B515; Isotype Human; Clone REA466	Miltenyi Biotec	Cat#130-108-096; RRID:AB_2652431
Anti-human GATA3; BV421; Isotype Mouse; Clone L50-823	BD Biosciences	Cat#563349; RRID:AB_2738152
CompBeads Anti-Mouse Ig, κ/Negative Control Compensation Particles Set	BD Biosciences	Cat#552843; RRID:AB_10051478
CompBeads Anti-Rat Ig, κ/Negative Control Compensation Particles Set	BD Biosciences	Cat#552844; RRID:AB_10055784
MACS® Comp Bead Kit, anti-REA	Miltenyi Biotec	Cat#130-104-693

[continued on next page]

Key resources table *[continued]*

REAGENT or RESOURCE	SOURCE	IDENTIFIER
Biological Samples		
Primary Human $CD4^+$ T cells isolated from buffy coats	Sanquin, Amsterdam, The Netherlands	N/A
Chemicals, Peptides, and Recombinant Proteins		
1% paraformaldehyde	Apotheek LUMC	Cat#120810-001
Fetal Calf Serum	Bodinco BDC	Cat#16941
Dulbecco's Modified Eagle's Medium - high glucose	Sigma-Aldrich	Cat#D5796
Penicillin-Streptomycin	Lonza	Cat#DE17-602E
GlutaMAX™ Supplement	Thermo Fisher Scientific	Cat#35050038
Recombinant Human IL-2	PeproTech	Cat#200-02
CryoSure-Dimethyl Sulfoxide	WAK-Chemie Medical GmbH	Cat#WAK-DMSO-10
Oleic Acid	Sigma-Aldrich	Cat#O1383
HPLC Grade Ethanol	Thermo Fisher Scientific	Cat#64-17-5
Bovine Serum Albumin	Sigma-Aldrich	Cat#A7030
TaqMan™ Fast Advanced Master Mix	Thermo Fisher Scientific	Cat#4444557
Atorvastatin	Sigma-Aldrich	Cat#PHR1422
CP 640,186	Sanbio	Cat#17691-5
RPMI 1640, HEPES, no glutamine	Thermo Fisher Scientific	Cat#42401
Fetal Calf Serum	Serana	Cat#S-FBS-SA-015
Phorbol 12-myristate 13-acetate	Sigma-Aldrich	Cat#P8139
Ionomycin	Sigma-Aldrich	Cat#I0634
Brefeldin A	Sigma-Aldrich	Cat#B7651
LIVE/DEAD™ Fixable Blue Dead Cell Stain	Thermo Fisher Scientific	Cat#L34962

[continued on next page]

Key resources table *[continued]*

REAGENT or RESOURCE	SOURCE	IDENTIFIER
Bovine Serum Albumin Fraction V	Merck	Cat#10735086001
UltraPure™ 0.5M EDTA, pH 8.0	Thermo Fisher Scientific	Cat#15575020
Brilliant Stain Buffer	BD Biosciences	Cat#563794
Critical Commercial Assays		
Quick-DNA/RNA Microprep Plus Kit	Zymo Research	Cat#D7005
Qubit™ RNA, Broad Range (BR), Assay Kits	Thermo Fisher Scientific	Cat#Q10210
Agilent RNA 6000 Nano Kit	Agilent	Cat#5067-1511
Transcriptor First Strand cDNA Synthesis Kit	Roche	Cat#04897030001
Truseq Stranded mRNA Library Prep	Illumina	Cat#20020595
Ribo Zero Gold rRNA Depletion Kit	Illumina	Cat#20037135
eBioscience™ Foxp3 / Transcription Factor Staining Buffer Set	Thermo Fisher Scientific	Cat#00-5523-00
Deposited Data		
Count data of RNA-sequencing	Gene Expression Omnibus repository, GEO	GSE231458
Oligonucleotides		
CPT1A	Thermo Fisher Scientific	Cat#4331182; Assay ID Hs00912671_m1
RPL13A	Thermo Fisher Scientific	Cat#4448892; Assay ID Hs03043887_gH
SDHA	Thermo Fisher Scientific	Cat#4453320; Assay ID Hs00188166_m1
Software and Algorithms		
RStudio	RStudio, Inc.	v4.2.2
BD FACSDiva™ Software	BD Biosciences	v8.0.2
SpectroFlo® Software	Cytek Biosciences	v2.2.0.3
OMIQ	Dotmatics	N/A
BioRender	BioRender	N/A

Resource availability

Materials availability

This study did not generate new unique reagents.

Data and code availability

- RNA sequencing data generated in this study have been deposited at Gene Expression Omnibus repository, accession, GEO, and are publicly available as of the date of publication. Accession numbers are listed in the key resources table.
- This paper does not report original code.
- Any additional information required to reanalyze the data reported in this paper is available from the lead contact upon request.

Experimental model and study participant details

$CD4^+$ T cell isolation and culture conditions

To obtain non-activated $CD4^+$ T cells, peripheral blood mononuclear cells (PBMCs) were isolated from buffy coats of anonymous blood bank donors (Sanquin, Amsterdam, The Netherlands) by Ficoll paque (Apotheek LUMC, 97902861) gradient centrifugation. The sex of the cells could not be determined due to the anonymity of the donors. However, RNA sequencing showed that, of 9 donors sequenced, 8 were female and 1 was male, which was accounted for during the statistical analysis by correcting for donor effect. Next, $CD4^+$ T cells were purified from the PBMCs using lyophilized human anti-$CD4^+$ magnetically labeled microbeads (Miltenyi Biotec, 130-097-048) scaling the manufacturer's instructions to 1/5 of the recommended volumes. $CD4^+$ T cell authentication and purity was assessed on an LSR-II instrument at the Leiden University Medical Center Flow Cytometry Core Facility (https://www.lumc.nl/research/facilities/fcf/) with the BD FACSDiva™ v8.0.2 software (BD Biosciences). Cells were stained with anti-CD3-PE (BD Biosciences, 345765; RRID:AB_2868796), anti-CD4-APC (BD Biosciences, 345771; RRID: AB_2868799), anti-CD8-FITC (BD Biosciences, 555634; RRID:AB_395996), and anti-CD14-PEcy7 (BD Biosciences, 557742; RRID:AB_396848) and resuspended in 1% paraformaldehyde (Apotheek LUMC, 120810-001) to fix the cells prior to acquisition. Purity was >98% for all donors.

Prior to oleic acid exposure,~$8*10^7$ isolated cells were cultured overnight to allow the cells to return to a resting state after the stress of the isolation procedure. This was done in T75 flasks (Greiner Bio-One, 658-175) at a density of ~$2.5*10^6$ cells/mL in 5% fetal calf serum (FCS) (Bodinco BDC, 16941) DMEM (Dulbecco's Modified Eagle's Serum (Sigma-Aldrich, D5796), 1% Pen-Strep (Lonza, DE17-602E), 1% GlutaMAX-1 (100x) (Thermo Fisher Scientific, 35050-038)) medium supplemented with 50 IU/mL IL-2 (PeproTech, 200-02) and incubated at 37°C under 5% CO_2. To keep the cells in a non-activated state, no additional stimulus was added. Any $CD4^+$ T cells not used directly after the isolation were kept in DMEM supplemented with 30% FCS, 1% Pen-Strep, 1% GlutaMAX-1, and 20% Dimethyl Sulfoxide (DMSO) (WAK-Chemie Medical GmbH, WAK-DMSO-10) medium, and stored in liquid nitrogen.

Next, non-activated $CD4^+$ T cells were cultured with or without oleic acid for 0.5, 3, 24, 48, or 72 hours at 37°C under 5% CO_2. To this end, $CD4^+$ T cells from each donor were plated in a 24 wells plate (density of ~$4*10^6$ cells/well) in 2mL 5% FCS DMEM for each time point, one exposed to oleic acid, one to the solvent control, and one to the negative control. Cells were cultured in medium containing FCS to ensure cell viability during culture and to be more comparable to physiological conditions of the circulation where other lipids are also present. Oleic acid (Sigma-Aldrich, O1383) was dissolved in HPLC grade ethanol (Thermo Fisher Scientific, 64-17-5) to a final concentration of 30,000µg/mL and complexed to fatty acid-free (FAF) bovine serum albumin (BSA) (Sigma-Aldrich, A7030) in a 2% FAF BSA DMEM mixture (Dulbecco's Modified Eagle's Serum, 2% FAF BSA, 1% Pen-Strep, 1% GlutaMAX-1 (100x)) to a final concentration of 150µg/mL. Complexing oleic acid mimics physiological conditions as fatty acids are also bound to albumin in the human circulation[68]. Oleic acid was further diluted to the final concentrations of 10, 20, 30, and 50µg/mL. The concentrations tested were determined based on a literature search[10-12, 42-46]. For the solvent control samples, HPLC grade ethanol was diluted in 2% FAF BSA DMEM in the same volume as to dilute oleic acid to 150µg/mL and added to the wells. For the negative control samples, 2% FAF BSA DMEM was added directly to the wells with no additional solvent. The amount of 2% FAF BSA DMEM added to the wells was equal for each condition to keep the volumes equivalent. To assess the additional oleic acid stimulus to the non-activated $CD4^+$ T cells due to FCS in the culture medium, an FCS sample was measured via the Shotgun Lipidomics Assistant (SLA) method[69] to estimate the fraction of oleic acid in the sample. The sample was prepped as previously described[70] but with two modifications, a starting volume of 25µL FCS and 600µL MTBE was added instead of 575µL during the first extraction. After exposure, the cells were flash frozen in liquid nitrogen and stored at -80°C until further use. Cell viability was measured via trypan blue staining (Sigma-Aldrich, T8154).

Spectral cytometry cell prep and activation

To study the effect of oleic acid pre-exposure on $CD4^+$ T cell subset development, cells from 8 out of 9 donors that were previously analyzed using RNA-seq were thawed from liquid nitrogen; 1 donor could not be studied further because too few cells were available. Cells were cultured overnight to allow the cells to return to a resting state after the stress of the thawing, in T75 flasks at a density of ~$2.5*10^6$ cells/mL in 5% FCS DMEM medium supplemented with 50 IU/mL IL-2 at 37°C under 5% CO_2. To keep the cells in a non-activated state, no additional stimulus was added. Following overnight incubation, the cells were divided into 2 conditions, oleic acid and solvent exposed, and plated in a 24 wells plate (density of ~$4*10^6$ cells/well) in 2mL 5% FCS DMEM. The oleic acid and solvent solution were prepared as stated previously, with one modification. To ensure that there was no effect of the solvent on T cell differentiation, the HPLC grade EtOH was evaporated before dissolving the oleic acid in 2% FAF BSA DMEM medium. The HPLC grade EtOH was also evaporated before adding the 2% FAF BSA DMEM medium in the solvent exposed condition, rendering it essentially the same as the negative control. These solutions were each added to the respective wells, where the final concentration of the oleic acid exposed conditions equaled 30µg/mL. The $CD4^+$ T cells were cultured for 48h at 37°C under 5% CO_2.

To ensure that the effect on $CD4^+$ T cell differentiation was due to oleic acid pre-exposure, all medium of each condition was replaced by 5% FCS medium after 48h of exposure, before initiating the activation. Cell viability and diameter were first measured by Via1-Cassette™ (Chemometec, 941-0012) on a NucleoCounter® NC-200™ (Chemometec, 900-0200) and found to be > 90% for each condition. Then, 2 million cells were harvested by flash freezing in liquid nitrogen for *in vitro* model confirmation by RT-qPCR. The remaining cells were plated in a round bottom 96 wells plate (Corning Incorporated, 3799), at a density of 100,000 cells/well, and were activated for 72h using Dynabeads™ Human T-Activator CD3/CD28 for T Cell Expansion and Activation (Thermo Fisher Scientific, 11161D; RRID:AB_2916088) according to the manufacturer's instructions at 37°C under 5% CO_2. Half the cells from each exposure were activated and the other half was left in the non-activated state. Subsequently, the cells from each pre-exposure and activation state were pooled in Eppendorf tubes and the beads were magnetically removed from the activated cells. Cell viability and diameter were measured by Via1-Cassette™ after 72h. Cells were then used for T cell subset identification described in more detail below. All centrifugation steps were performed at 1500 rpm at room temperature.

Inhibitor culture conditions and activation

To study whether the effect of oleic acid pre-exposure on $CD4^+$ T cell subset development could be prevented by metabolic inhibitors, cells from 3 out of 8 donors that were previously analyzed for subset development were thawed from liquid nitrogen; 5 donors could not be studied further because too few cells were available. Cells were cultured overnight to allow the cells to return to a resting state after the stress of the thawing, in T75 flasks at a density of ~$2.5*10^6$ cells/mL in 5% FCS DMEM medium supplemented with 50 IU/mL IL-2 at 37°C under 5% CO_2. To keep the cells in a non-activated state, no additional stimulus was added. Following overnight incubation, the cells were divided into 5 conditions, solvent, oleic acid, oleic acid + atorvastatin (Sigma-Aldrich, PHR1422), oleic acid + CP-640186 (Sanbio, 17691-5), and oleic acid + atorvastatin + CP-640186 exposed, and plated in a 24 wells plate (density of ~$4*10^6$ cells/well) in 2mL 5% FCS DMEM. The oleic acid and solvent solution were prepared as stated previously, with HPLC grade EtOH evaporation. These solutions were each added to the respective wells, where the final concentration of the oleic acid exposed conditions equaled 30µg/mL. Atorvastatin and CP-640186 were added to the respective wells at a concentration of 10µM and 20µM, respectively. The $CD4^+$ T cells were cultured for 48h at 37°C under 5% CO_2.

To ensure that the effect on $CD4^+$ T cell differentiation was due to oleic acid and inhibitor pre-exposure, all medium of each condition was replaced by 5% FCS medium after 48h of exposure, before initiating the activation. Cell viability and diameter were first measured by Via1- Cassette™ on a NucleoCounter® NC-200™ and found to be > 90% for each condition. Then, ~0.5-1.5 million cells were harvested by flash freezing in liquid nitrogen for *in vitro* model confirmation by RT-qPCR. The remaining cells were plated in a round bottom 96 wells plate, at a density of 100,000 cells/well, and were activated for 72h using Dynabeads™ Human T-Activator CD3/CD28 for T Cell Expansion and Activation according to the manufacturer's instructions at 37°C under 5% CO_2. Subsequently, the cells from each pre-exposure were pooled in Eppendorf tubes and the beads

were magnetically removed. Cell viability and diameter were measured by Via1-Cassette™ after 72h. Cells were then used for T cell subset identification described in more detail below. All centrifugation steps were performed at 1500 rpm at room temperature.

Method details

RNA isolation

To isolate total RNA for RNA sequencing and RT-qPCR, RNA was extracted from the cell samples using the Zymo Quick-DNA/RNA Microprep Plus Kit (Zymo Research, D7005) according to manufacturer's instructions. The RNA was quantified using a Qubit® 2.0 Fluorometer (Q32866) with the Qubit® RNA BR Assay Kit (Thermo Fisher Scientific, Q10211) according to manufacturer's instructions. RNA integrity (RIN) values of the samples were on average 8.40 SE 0.14 as determined using an Agilent 2100 Bioanalyzer Instrument (G2939BA) with the Agilent RNA 6000 Nano Reagents (5067-1511). RNA was divided into two samples and stored at -80°C, 1µg for RNA sequencing and the rest for cDNA synthesis and RT-qPCR measurements.

Real time-quantitative PCR

To measure the expression of *CPT1A* in all the cell samples, cDNA was synthesized with 200ng of the stored RNA using the Transcriptor First Strand cDNA Synthesis Kit (Roche, 04897030001) according to the manufacturer's instructions. Quantitative real time PCR's for *CPT1A* (Thermo Fisher Scientific, 4331182; Assay ID: Hs00912671_m1) were performed using the TaqMan™ Fast Advanced Master Mix (Thermo Fisher Scientific, 4444557) with 10ng cDNA per reaction on a QuantStudio 6 Real-Time PCR system (Applied Biosystems). All RT-qPCR reactions were performed in triplicate and outliers were removed if the Ct value measured differed more than 0.5% from the mean. Relative gene expression levels (-ΔCt) were calculated using the average of Ct values of *RPL13A* (Thermo Fisher Scientific, 4448892; Assay ID: Hs03043887_gH) and *SDHA* (Thermo Fisher Scientific, 4453320; Assay ID: Hs00188166_m1) as internal controls[71]. The fold change was determined using the $2^{-\Delta\Delta Ct}$ method, using the negative control as the reference. All statistical analyses were performed in R. Data are expressed as mean of the relative fold change and standard error. The reported P values were determined by applying a paired two-tailed student's T test. P values < 0.05 were considered to be statistically significant.

RNA sequencing

RNA sequencing (RNA-seq) was performed to determine the differences in the transcriptome of oleic acid versus solvent exposed non-activated $CD4^+$ T cells across time. 1µg of total RNA from each of the samples was sent for sequencing (Macrogen, Amsterdam, NL), each with a concentration above 20ng/µL in 50µL solution. RNA-seq libraries were prepared from 200ng RNA using the Illumina Truseq stranded mRNA library prep (Illumina, 20020595) after depletion of ribosomal RNA with Ribo Zero Gold (Illumina, 20037135). Both whole-transcriptome amplification and sequencing library preparations were performed in two 96-well plates with half the samples each, to reduce assay-to-assay variability. Quality control steps were included to determine total RNA quality and quantity, the optimal number of PCR preamplification cycles, and fragment size

selection. No samples were eliminated from further downstream steps. Barcoded libraries were pooled and equally divided across two lanes to ensure an equal distribution of all the samples across the two lanes. Barcoded libraries were sequenced to a read depth of 30 million reads using the Novaseq 6000 (Illumina) to generate 100 base pair paired-end reads.

Spectral cytometry

Prior to FACS analysis, cells were washed in RPMI 1640 medium (Thermo Fisher Scientific, 42401), supplemented with 100U/mL penicillin, 100µg/mL streptomycin, 1mM pyruvate, 2mM glutamate, and 10% FCS (Serana, S-FBS-SA-015), and adjusted to a concentration of $1x10^6$ cells/mL. Cells were then resuspended in 100µL RPMI + 10% FCS and stimulated for 4h with Phorbol 12-myristate 13-acetate (PMA; 100ng/mL, Sigma-Aldrich, P8139) and ionomycin (1µg/mL, Sigma-Aldrich, I0634) at 37°C under 5% CO_2 to promote cytokine production[72]. After 2h of stimulation, 10µg/mL of the protein transport inhibitor Brefeldin A (Sigma-Aldrich, B7651) was added.

After stimulation, the cells were washed twice in phosphate-buffered saline (PBS), stained for viable cells with LIVE/DEAD™ Fixable Blue (Thermo Fisher Scientific, L34962) for 30min at room temperature, then washed twice in fluorescence-activated cell sorting (FACS) buffer (PBS supplemented with 0.5% BSA (Merck, 10735086001) and 2mM EDTA (Thermo Fisher Scientific, 15575020)). The antibody surface cocktail consisted of 11 markers, anti-CD38-APC-Fire810 (BioLegend, 356643; RRID:AB_2860936), anti-CD8-Pacific Orange (Thermo Fisher Scientific, MHCD0830; RRID:AB_10372066), anti-CD25-BUV563 (BD Biosciences, 612918; RRID:AB_2870203), anti-CD45RA-BUV496 (BD Biosciences, 741182; RRID:AB_2870749), anti-CD45RO-BUV805 (BD Biosciences, 748367; RRID:AB_2872786), anti-CD4-cFluor® YG584 (Cytek Biosciences, SKU R7-20041), anti-CD3-BUV395 (BD Biosciences, 563546; RRID:AB_2744387), anti-CD27-APC-H7 (BD Biosciences, 560222; RRID: AB_1645474), anti-PD1-BV750 (BD Biosciences, 747446; RRID:AB_2872125), anti-CD127-R718 (BD Biosciences, 566967; RRID:AB_2869977), and anti-CCR7-BV785 (BioLegend, 353230; RRID:AB_2561371). For the spectral cytometry of the inhibitor experiment, the same surface cocktail was used except for the CD8 marker. The antibody surface cocktail was prepared in FACS buffer containing 20% Brilliant Stain Buffer Plus (BD Biosciences, 563794) was added to the cells and incubated for 30min at room temperature. Cells were then washed twice in FACS buffer and afterwards fixed and permeabilized with the Fixation/Permeabilization solution from the eBioscience™ FoxP3 / Transcription Factor Staining Buffer Set (Thermo Fisher Scientific, 00-5523-00) according to the manufacturer's instructions for 30min at 4°C. Subsequently, cells were washed twice with the Permeabilization buffer from the eBioscience™ FoxP3 / Transcription Factor Staining Buffer Set before being stained with the intracellular/intranuclear antibody cocktail for 30min at 4°C. The intracellular/intranuclear antibody cocktail consisted of 14 markers, anti-TNF-PE-Cy7 (BD Biosciences, 557647; RRID:AB_396764), anti-IL-17A-Pacific Blue (BioLegend, 512312; RRID:AB_961392), anti-IL-5-APC (BioLegend, 504306; RRID:AB_315329), anti-IL-4-BUV737 (BD Biosciences, 612835; RRID:AB_2870157), anti-IFN-γ-BV650 (BD Biosciences, 563416; RRID:AB_2738193), anti-IL-13-BV711 (BD Biosciences, 564288; RRID:AB_2738731), anti-IL-9-PE (BioLegend, 507605; RRID: AB_315487), anti-IL-10-PerCP-eFluor™ 710 (Thermo Fisher Scientific, 46-7108-42; RRID:AB_2573833), anti-CD152-PE-Cy5 (BD Biosciences, 555854; RRID:AB_396177),

anti-IL-21-Alexa Fluor® 647 (BD Biosciences, 560493; RRID:AB_1645421), anti-T-bet-KIRAVIA Blue 520™ (BioLegend, 644838; RRID:AB_2888710), anti-FOXP3-PE/Dazzle™ 594 (BioLegend, 320126; RRID:AB_2564024), anti-IL-22-Vio® B515 (Miltenyi Biotec, 130-108-096; RRID:AB_2652431), and anti-GATA3-BV421 (BD Biosciences, 563349; RRID:AB_2738152). For the spectral cytometry of the inhibitor experiment, the same intracellular/intranuclear antibody cocktail was used except for the IL-5 marker. Lastly, cells were washed with eBioscience™ Permeabilization buffer followed by another wash in FACS buffer. All centrifugation steps before fixation were performed at 300x g at room temperature and after fixation at 800x g at 4°C. Single-stain reference controls were either cells or UltraComp eBeads™ (CompBeads Anti-Mouse Ig, κ/Negative Control Compensation Particles Set (BD Biosciences; 552843; RRID:AB_10051478); CompBeads Anti-Rat Ig, κ/Negative Control Compensation Particles Set (BD Biosciences; 552844; RRID:AB_10055784), or MACS® Comp Bead Kit, anti-REA (Miltenyi Biotec; 130-104-693)). Cells were used as unstained reference control. All reference controls underwent the same protocol as the fully stained samples, including washes, buffers used, and fixation and permeabilization steps.

For acquisition, cells were resuspended in FACS buffer and acquired on a 5L-Cytek Aurora instrument at the Leiden University Medical Center Flow Cytometry Core Facility with the SpectroFlo® v2.2.0.3 software (Cytek Biosciences). Data was manually gated in OMIQ (Dotmatics, 2023). All statistical analyses were performed in R. Data are expressed as mean of the relative fold change and standard error. The reported P values were determined by applying a paired two-tailed student's T test. Differences with $P_{FDR} < 0.05$ (Benjamini-Hochberg) were considered to be significant.

Quantification and statistical analysis

Statistical analyses

All statistical analyses were performed in R (v4.2.2). Statistical details per experiment can be found in the "Method details" section of the "STAR Methods" as well as in the (supplemental) figure and table legends. A detailed description of the methods used to analyze the RNA sequencing data can be found below in the section "RNA Sequencing Analysis". For the analysis of all other experiments, the results are presented as mean ± SEM values. The reported P values were determined by applying a paired two-tailed student's T test between control and oleic acid exposed samples. Differences with $P_{FDR} < 0.05$ (Benjamini-Hochberg) were considered to be significant.

RNA sequencing analysis

RNA-seq reads were processed using the BioWDL RNAseq pipeline (v3.0.0) developed at LUMC (http://zenodo.org/record/3713261#.ZF98HdJBw5k). Quality controls were performed using FastQC (v0.11.7) and MultiQC (v1.7). Cleaned reads were aligned to the human reference genome GRCh38 using STAR aligner (v2.7.3a). Gene count table was generated using Htseq-count (v0.11.2) with Ensembl gene annotation version 99. Based on Ensembl gene biotype annotation, we included only protein coding genes for further downstream analysis (19,916 genes in total). We used the Bioconductor package *DESeq2*[73] (v1.40.1) to test whether oleic acid had an effect on gene expression at any time point. *DESeq2* fits a generalized linear model (GLM) assuming the

negative binomial distribution for the counts. The model expresses the logarithm of the average of the counts in terms of one of more predictors. In this case, we compared two models: The first "null" model has only timepoint (as a categorical variable with 5 levels) and subject identifier as predictors. By including the subject identifier in the model, we account for the dependence between measurements within the same subject. The second "alternative" model also includes the interaction between phenotype (oleic acid as a numerical measurement) and timepoint. We compare the fit of the two models with a likelihood ratio test. As part of the *DESeq2* process lowly expressed genes were automatically removed, resulting in 12,932 analyzed genes[73]. The Benjamini-Hochberg procedure was used to correct for multiple testing and a false discovery rate (FDR) < 0.05 was considered statistically significant.

Next, to identify distinct gene expression patterns in the data, unsupervised K means clustering was performed on the differentially expressed genes using the *factoextra*[74] package (v1.0.7). The number of clusters, *k*, was chosen using the elbow, silhouette, and gap-statistic method. Heatmaps were constructed using *ComplexHeatmap*[75] (v2.14.0) by plotting the log2FoldChange of the DEGs at each time point.

The identified clusters were then mapped for pathway enrichment. 10 human pathway databases (BioPlanet 2019, WikiPathways 2019 Human, KEGG 2019 Human, Elsevier Pathway Collection, BioCarta 2015, Reactome 2016, HumanCyc 2016, NCI-Nature 2016, Panther 2016 and MSigDB Hallmark 2020) were queried using gene symbols, with 430 of 544 queried genes present in at least 1 database. The identified clusters were then mapped for pathway enrichment using *clusterProfiler*[76] (v4.6.2) with the background set to 12,932 expressed genes in the $CD4^+$ T cells based on *DESeq2* filtering. Multiple testing using the Benjamini-Hochberg method at 5% FDR was performed over the combined results from the 10 databases. Pathways that included highly similar gene sets were grouped (Jaccard index > 0.7) and only the most significantly enriched pathway per group was retained. Furthermore, using the UniProt IDs of the enriched genes, the Path-MAP function of the PathBank database[77] was used to visualize the list of matching components within specific canonical pathways. *De novo* motif analysis on promotors of differentially regulated genes was performed using HOMER[78].

Results

Establishing a model to study the effect of oleic acid on non-activated $CD4^+$ T cells

Prior to studying the effect of oleic acid on non-activated $CD4^+$ T cells, we evaluated various experimental conditions in order to establish an *in vitro* exposure model. Cells were cultured in medium containing fetal calf serum (FCS) to ensure cell viability during culture, and oleic acid was complexed to BSA to model physiological conditions of the circulation. The cellular response to oleic acid was assessed by measuring cell viability and the expression of *CPT1A*. The *CPT1A* gene encodes the long-chain fatty acid transporter carnitine palmitoyl transferase 1a, a rate-limiting enzyme in the metabolic process of β-fatty acid oxidation. First, three different

types of culturing conditions for non-activated $CD4^+$ T cells were compared: 5% FCS medium with oleic acid bound to fatty acid-free (FAF) BSA, 5% FCS medium with oleic acid diluted in 5% FCS medium, and FAF medium with oleic acid bound to FAF BSA. However, the latter two conditions led to either undissolved oleic acid or a low cell viability (Supp. Fig. 1a). The first condition produced the largest *CPT1A* response while maintaining a high cell viability (Supp. Fig. 1), presumably because oleic acid bound to BSA and the presence of FCS may be a better approximation of physiological conditions. In addition, various oleic acid concentrations used in previous studies were evaluated[10-12, 42-46]. A concentration of 30 µg/mL was observed to result in the highest *CPT1A* upregulation (9.83-fold, SE 5.60) while maintaining cell viability (84.36%, SE 0.49%; Supp. Fig. 1). Importantly, this concentration is lower than the typical oleic acid concentration in the human circulation (85–904 µg/mL)[47]. The solvent control, ethanol, did not influence the results and was thus used as the control condition for the following analyses (Supp. Fig. 2). Finally, we measured the oleic acid concentration in the medium due to the addition of 5% FCS. This concentration was 0.26 µg/mL of free oleic acid and 4.39 µg/mL oleic acid as components of larger molecules including cholesterol esters and sphingolipids.

Transcriptomic analysis of oleic acid-exposed non-activated $CD4^+$ T cells

In order to identify the molecular features that define the effect of oleic acid exposure on non-activated $CD4^+$ T cells *in vitro*, we exposed nonactivated $CD4^+$ T cells to 30 µg/mL oleic acid for 0.5, 3, 24, 48, or 72 h (n = 9; Fig. 1a). First, we measured *CPT1A* expression and found that its expression consistently increased over time indicating a robust response to oleic acid exposure across donors, while *CPT1A* expression did not change under control conditions (Fig. 1b and Supp. Fig. 2b). Next, we analyzed the transcriptome of non-activated $CD4^+$ T cells after oleic acid exposure using RNA-seq. Oleic acid induced differential expression of 544 genes ($P_{FDR} < 0.05$) that clustered into 310 upregulated genes and 234 downregulated genes (Fig. 1c and Supp. Fig. 3, and Supp. Tables 1a and b). There was no statistical evidence for further subdivisions of the two clusters, for example, in fast- and slow-responding genes.

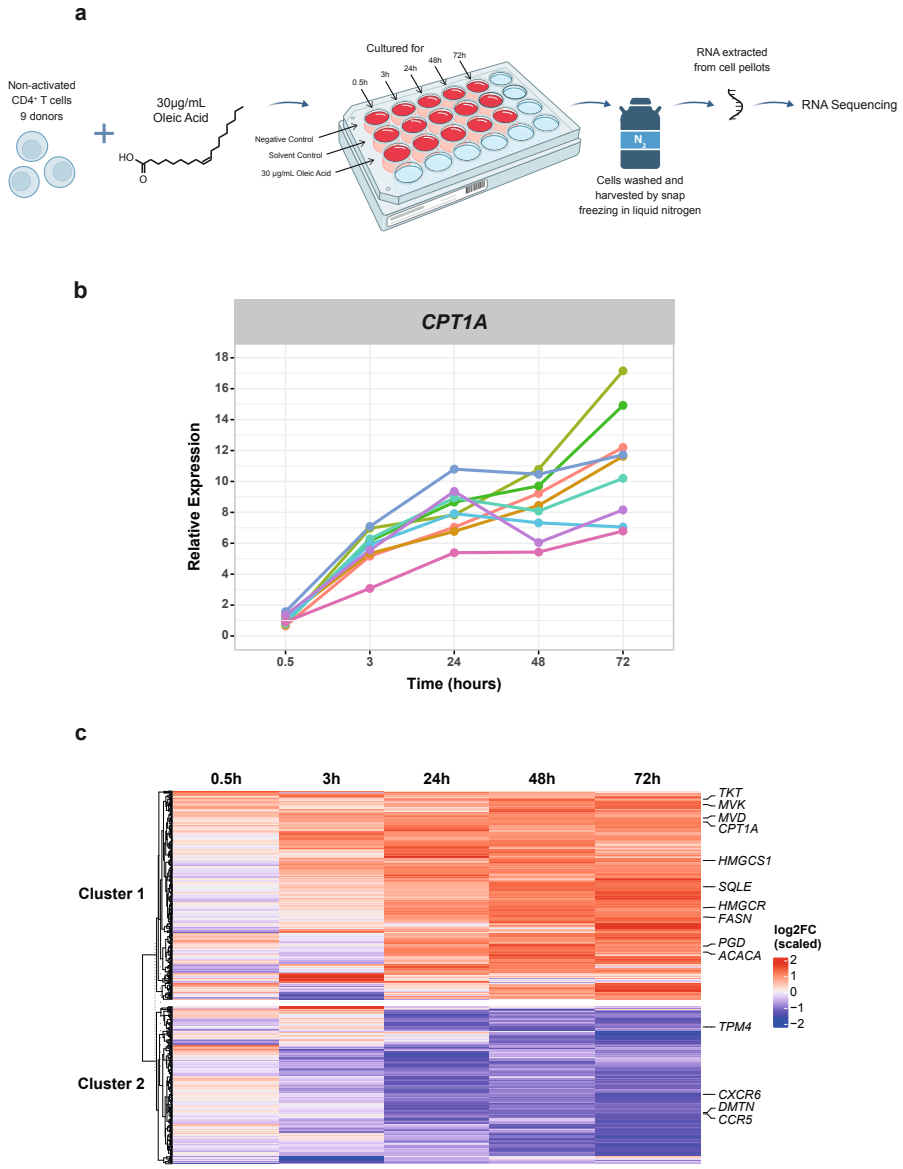

Fig. 1 | Oleic acid exposure in non-activated CD4⁺ T cells induces changes in transcriptomics. (a) Experimental setup for RNA sequencing of oleic acid-exposed non-activated CD4⁺ T cells, n = 9. **(b)** Line plot showing the relative expression of ***CPT1A*** per donor across time as a confirmation of the ***in vitro*** model by RT-qPCR. Values are colored by donor across time. On average ***CPT1A*** was upregulated 1.03 SE 0.10-fold at 0.5 h, 5.73 SE 0.40-fold at 3 h, 8.08 SE 0.53-fold at 24 h, 8.39 SE 0.62-fold at 48 h, and 11.09 SE 1.16-fold at 72 h as compared to the solvent control, n = 9. **(c)** Differentially expressed genes (DEGs) in oleic acid-exposed non-activated CD4⁺ T cells across time as compared to the solvent control. Heatmap obtained from the ***DESeq2*** analysis resulting in 544 DEGs ($P_{FDR} < 0.05$). DEGs were plotted across time to show the genes expression as log2FoldChange at each time point. Unsupervised K-means clustering indicated 2 clusters. Cluster 1 contains 310 of the DEGs, which are generally upregulated and are represented in red, and cluster 2 contains 234 of the DEGs, which are generally downregulated and are represented in blue. Genes of interest are labeled, n = 9.

We first examined the functions of the 310 genes that were upregulated in non-activated $CD4^+$ T cells by oleic acid exposure. We inspected the top differentially expressed genes (Supp. Fig. 3a and Supp. Table 1a). The top differentially expressed gene was *CPT1A* highlighting the involvement of β-fatty acid oxidation. In addition, we found an increased expression of *HMGCR* (3-hydroxy-3-methyl-glutaryl-coenzyme A [CoA] reductase), encoding the rate-limiting enzyme for cholesterol biosynthesis, and *ACACA* (acetyl-coenzyme A carboxylase 1), encoding the rate-limiting enzyme of fatty acid biosynthesis. Furthermore, transcripts of several aerobic glycolysis-related genes, such as *TKT* and *PGD*, were upregulated (Supp. Fig. 3a and Supp. Table 1a). A formal analysis of enriched biological processes among all 310 upregulated genes confirmed the involvement of metabolism. In particular, cholesterol biosynthesis ($P_{FDR} < 0.001$), homeostasis ($P_{FDR} < 0.001$), and signaling of mTORC1 ($P_{FDR} < 0.001$), a key complex of mechanistic target of rapamycin (mTOR) which aids in the switch toward aerobic glycolysis and fatty acid biosynthesis, were enriched (Fig. 2a). Mapping the upregulated genes to canonical metabolic pathways further supported a specific metabolic rewiring of oleic acid-exposed non-activated $CD4^+$ T cells (Fig. 2b). First, oleic acid can first be catabolized through beta oxidation to produce acetyl-CoA, which can then be used as a starting point for cholesterol and fatty acid biosynthesis. In addition to *CPT1A*, we found 4 out of 15 enzymes in b-fatty acid oxidation (including *SLC25A20*, *ACADVL*, and *ACAA2*) and 2 out of 15 enzymes in the aerobic glycolysis pathway to be upregulated (*TKT* and *PGD*; Fig. 2b, Supp. Fig. 4 and 5). Remarkably, on top of *HMGCR*, 15 out of 20 enzymes involved in cholesterol biosynthesis were upregulated in our gene set, including several key rate-limiting genes (such as *HMGCS1*, *SQLE*, *MVD*, and *MVK*). More specifically, 9/11 components of the mevalonate, 6/9 of the Bloch, and 6/9 of the Kandutsch-Russell pathway, together responsible for cholesterol biosynthesis, were upregulated (Fig. 2b and Supp. Fig. 6). The upregulated gene set also included *ACACA* and *FASN* that encode the two enzymes that together are responsible for the 37 reactions making up fatty acid biosynthesis (Fig. 2b and Supp. Fig. 7). Of note, the genes *ACACA* and *FASN* have been implicated in the differentiation toward T_H17 cells, a highly pro-inflammatory subset of $CD4^+$ T cells[46]. Furthermore, aerobic glycolysis and cholesterol and fatty acid biosynthesis are the hallmark metabolic processes of activated T cells and suggest that non-activated $CD4^+$ T cells undergo a metabolic reprogramming upon oleic acid exposure that may poise the cells for a different response to activation.

We then examined the functions of the 234 genes that were downregulated in non-activated $CD4^+$ T cells by oleic acid exposure. We first inspected the top differentially expressed genes (Supp. Fig. 3b and Supp. Table 1b). Among the top downregulated genes, decreased expression of *CXCR6* and *CCR5*, important chemokine receptors in the T cell immune response, was measured. Moreover, expression of *TPM4*, encoding actin-binding proteins involved in the cytoskeleton, and *DMTN*, encoding an actin-binding and bundling protein that stabilizes the actin cytoskeleton, was also downregulated. A formal analysis of the enriched biological processes among all 234 downregulated genes revealed a wide variety of different pathways. In line with the genes observed among the top downregulated genes, this included processes involved in immune response (*CCR2*, *CCR8*, *HLA-DRA*, *SLC2A1*) ($P_{FDR} < 0.001$) and actin cytoskeleton organization (*ACTB*, *RAC2*, *ARPC2*, *IQGAP1*) ($P_{FDR} < 0.001$) (Fig. 2c). In addition, processes involved in chemotaxis

(P_{FDR} < 0.001), chemokine and cytokine signaling (P_{FDR} < 0.001), and Rho GTPase regulation (P_{FDR} < 0.001) were also downregulated (Fig. 2c). Overall, these data point to a broad yet aspecific downregulation of genes in oleic acid-exposed non-activated $CD4^+$ T cells, perhaps to cope with the influx of the fatty acid.

Next, we investigated whether specific transcription factors may underlie the differential expression observed by testing the enrichment of transcription factor binding motifs in upregulated vs. downregulated genes. The top motifs enriched among upregulated genes included key transcription factors PU.1, EGR1, BHLHE40, and SREBP1 (Fig. 2d). Notably, PU.1 is the key transcription factor for the development of T_H9 cells. BHLHE40 has been linked to T_H17 development and pathogenicity in autoimmune encephalomyelitis suggesting an additional possible preference toward T_H17 differentiation post-activation[48, 49]. Furthermore, EGR1 and SREBP1 are involved in either the activation of Tbet or fatty acid and cholesterol biosynthesis, respectively[50, 51]. These data further support the notion that oleic acid-exposed non-activated $CD4^+$ T cells may be poised to differentiate toward T_H9 and T_H17 T cell subsets after activation.

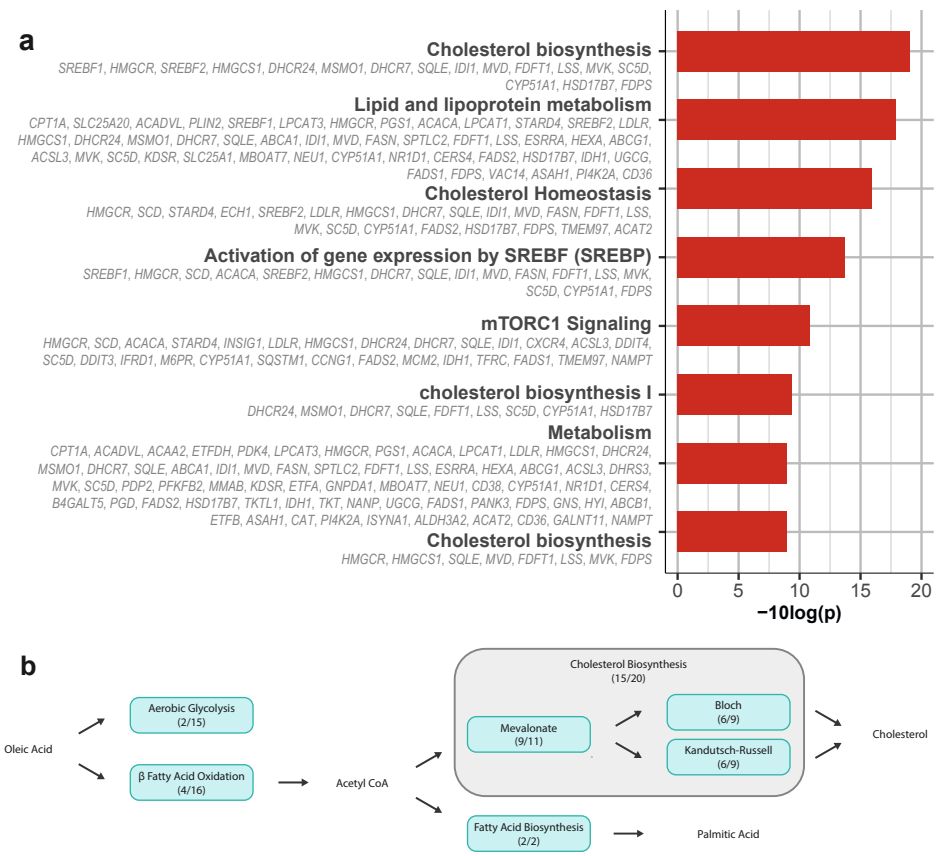

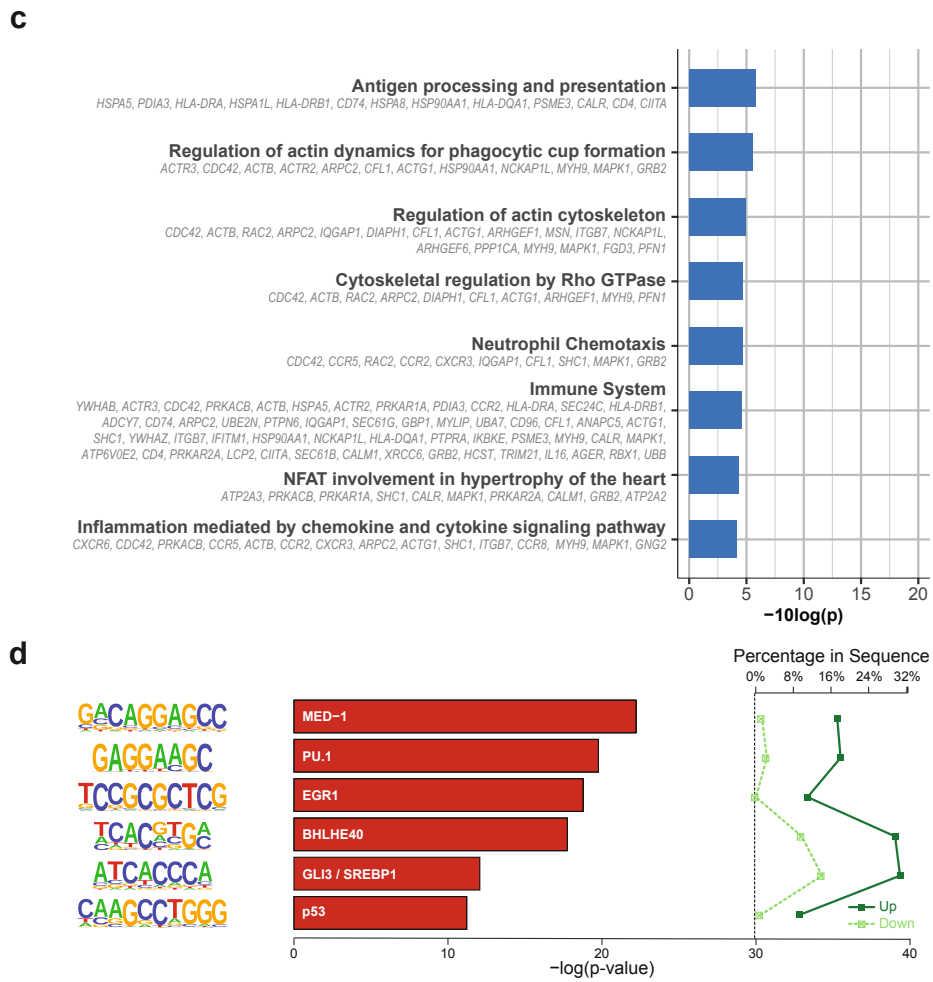

Fig. 2 | Up- and downregulated pathways and transcription factors in oleic acid-exposed non-activated CD4⁺ T cells. (a) Pathway enrichment analysis of cluster 1 DEGs generated using *clusterProfiler* using 10 human pathway databases. Top 8 enrichments are shown. **(b)** Illustration of canonical pathway map of oleic acid metabolism by non-activated CD4⁺ T cells exposed to oleic acid. Blue boxes indicate metabolic pathways with the number of genes present in that particular pathway from cluster 1 of the RNA sequencing. Cholesterol biosynthesis can be divided into 3 separate pathways indicated by the surrounding gray rectangle. **(c)** Pathway enrichment analysis of cluster 2 DEGs generated using *clusterProfiler* using 10 human pathway databases. Top 8 enrichments are shown. **(d)** *De novo* motif analysis on promoters of up- versus down-regulated genes. Enrichment of transcription factor binding motifs was performed using HOMER. 6 motifs are shown with supplementing information on p value, percentage of genes in upregulated gene set and percentage of genes in downregulated gene set, transcription factor name, -log(p value), and percentage in sequence.

Oleic acid induced CD4⁺ T cell phenotypes after activation

To determine the functional impact of the transcriptomic changes identified, we characterized the phenotypes of CD4⁺ T cells that were pre-exposed to oleic acid or control conditions and subsequently activated in the absence of oleic acid. To this end, non-activated CD4⁺ T cells of 8

out of 9 donors, for whom sufficient cells were available, were again exposed to 30 µg/mL oleic acid (Fig. 3a). The effect of exposure was confirmed by an upregulation of *CPT1A* (Supp. Fig. 8a); cell viability was high (>90%), and there was no difference in diameter between cells exposed to oleic acid and control (Supp. Fig. 8b–e).

First, we examined phenotypes after oleic acid exposure without activation (Supp. Fig. 9 and Supp. Table 1c). We observed decreased frequencies of $CD127^{low}CD25^{hi}FoxP3^+$ and $CD27^+$ $CD4^+$ T cells in response to oleic acid pre-exposure ($P_{FDR} < 0.05$; Fig. 3b). In non-activated cells, the $CD127^{low}CD25^{hi}FoxP3^+$ population is representative of T_{reg} cells, and thus the decreased frequencies in the non-activated cells are in line with the lower *FOXP3* expression observed in the RNA-seq analysis. Increased frequencies of interleukin (IL)-5^+ cells were also observed ($P_{FDR} < 0.05$; Fig. 3c) These data suggest that the oleic acid-induced changes in gene expression are reflected in consistent functional characteristics of the $CD4^+$ T cells without activation.

Activation of the $CD4^+$ T cells led to an increased cell size irrespective of pre-exposure to oleic acid (Fig. 3d). In contrast, the expression of surface and intracellular markers was influenced by exposure to oleic acid prior to activation (Supp. Fig. 10 and Supp. Table 1d). Pre-exposure to oleic acid resulted in a higher proportion of IL-9^+ cells ($P_{FDR} < 0.01$) as compared to the control (Fig. 3e). Additional analysis showed that IL-9 was not co-expressed with other T_H2-associated cytokines (Supp. Table 1e). This aligns with our finding that a large percentage of upregulated genes mapped to a PU.1 motif (Fig. 2d), the key transcription factor controlling T_H9 differentiation. Furthermore, increased frequencies of IL-$17A^+$ cells were observed after pre-exposure to oleic acid as compared with control conditions ($P_{FDR} < 0.05$). As IL-17A is mainly produced by T_H17 cells, it was hypothesized that other T_H17-associated cytokines, such as IL-21, may also have been upregulated. Indeed, IL-21^+ cells were increased in frequency ($p < 0.05$), but this effect was no longer significant after correction for multiple testing ($P_{FDR} < 0.08$). This aligns with our finding that a large percentage of upregulated genes mapped to the BHLHE40 motif (Fig. 2d) involved in T_H17 differentiation[48, 49]. Activated $CD4^+$ T cells showed increased frequencies of $CD127^{low}CD25^{hi}FoxP3^+$ and $GATA3^+$ and decreased frequencies of $CD27^+$ and $CD38^+$ cells in response to oleic acid pre-exposure ($P_{FDR} < 0.05$; Fig. 3f). However, FoxP3 can be expressed on activated conventional T cells without a suppressor function[52]; therefore, we are unable to differentiate whether the increased proportion of $CD127^{low}CD25^{hi}FoxP3^+$ cells post-activation is due to increased differentiation toward T_{reg} or an artifact of T cell activation. GATA3 is the key transcription factor involved in T_H2 differentiation, and, as such, frequencies of T_H2-related cytokines IL-5^+ and IL-13^+ were increased ($P_{FDR} < 0.05$; Fig. 3e). Finally, we observed that the effect of oleic acid on differentiation is not secondary to a differential proliferative capacity ($p > 0.92$; Supp. Fig. 11). Together, these data indicate that the metabolic changes in non-activated $CD4^+$ cells upon oleic acid exposure skew the cells toward producing more cytokines characteristic of T_H9, T_H17, and T_H2 subsets upon activation.

In order to reinforce our findings, we repeated the spectral cytometry analysis with 8 independent donors. The effect of oleic acid exposure was confirmed by an upregulation of *CPT1A* (Supp. Fig. 12a). Cell viability was high (>78%), and there was no difference in diameter between cells

exposed to oleic acid and control (Supp. Fig. 12b–e). Without activation, the phenotypes of oleic acid-exposed $CD4^+$ T cells showed increased frequencies of both $IL\text{-}17A^+$ ($P_{FDR} < 0.05$) and $TNF\alpha^+$ cells ($P_{FDR} < 0.05$; Supp. Fig. 13a, b, and 14; Supp. Table 1f). After activation, the phenotypes of oleic acid-exposed $CD4^+$ T cells showed an increased frequency of $IL\text{-}9^+$ ($P_{FDR} < 0.05$) and $GATA3^+$ ($P_{FDR} < 0.05$) cells as well as decreased frequencies of $CD38^+$ cells ($P_{FDR} < 0.05$; Supp. Fig. 13c, d, and 15, and Supp. Table 1g). These findings in non-activated and activated cells confirm results of our experiment and substantiate that oleic acid exposure in non-activated $CD4^+$ cells poised the cells toward producing more cytokines representative of T_H9 cells post-activation.

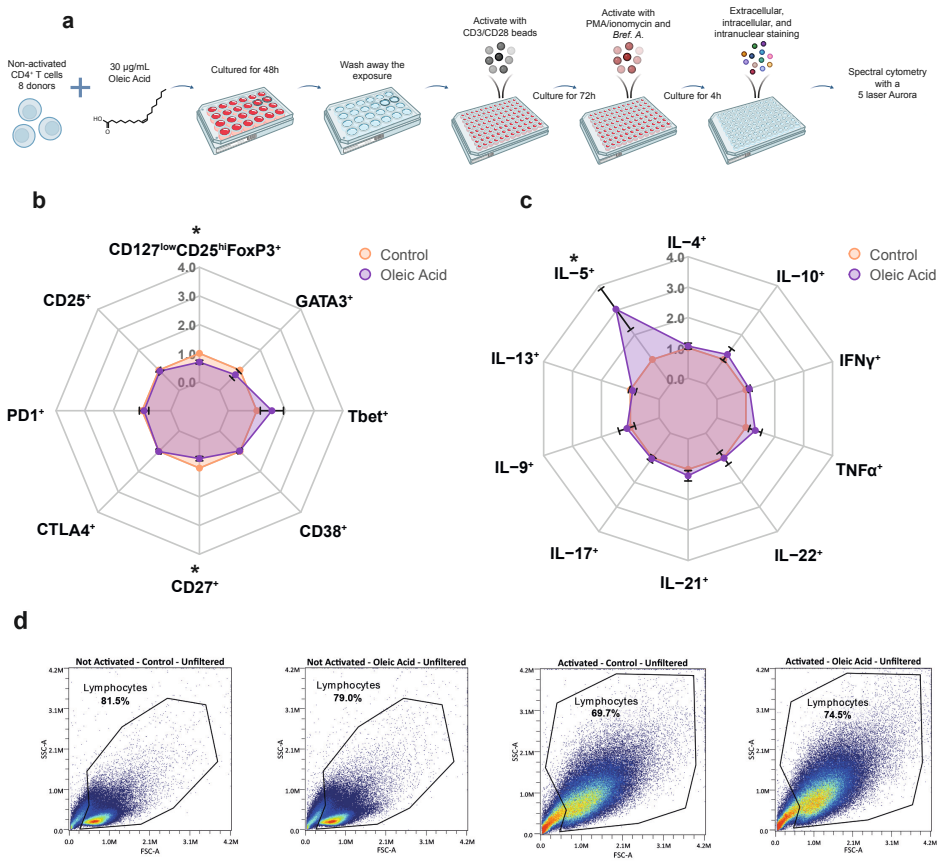

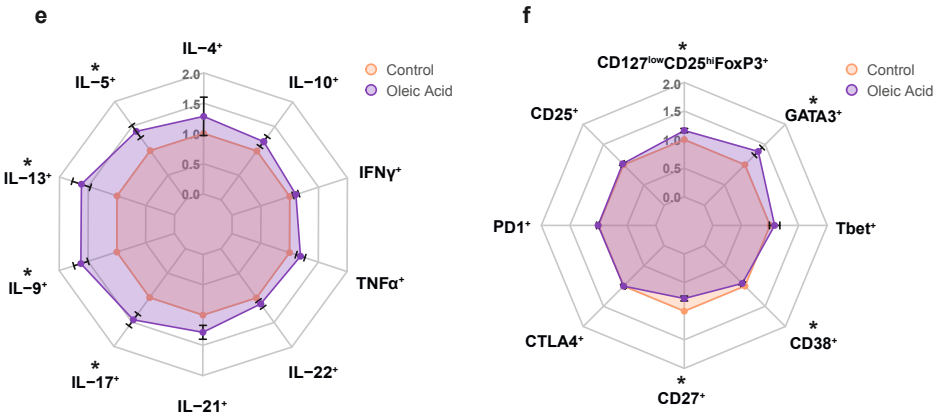

Fig. 3 | Oleic acid pre-exposure leads to changes in expression of extracellular markers, transcription factors, and intracellular cytokines. (*) $P_{FDR} < 0.05$, n = 8. **(a)** Experimental setup for spectral cytometry measurements of oleic acid-exposed non-activated $CD4^+$ T cells for 48 h with and without activation for 72 h post-exposure. **(b)** Radar plot of various $CD4^+$ T cell external markers and transcription factors expressed in $CD4^+$ T cells after 48 h of oleic acid exposure or control followed by 72 h of rest and 4 h stimulus with PMA/ionomycin. Values are expressed as fold change and standard error relative to control. **(c)** Radar plot of various $CD4^+$ T cell internal cytokines expressed in $CD4^+$ T cells after 48 h of oleic acid exposure or control followed by 72 h of rest and 4 h stimulus with PMA/ionomycin. Values are expressed as fold change and standard error relative to control. **(d)** Forward and side scatter of activated vs. non-activated and control vs. oleic acid pre-exposed $CD4^+$ T cells. Large differences in cell shape between the non-activated and activated state were observed, but little difference in cell shape between pre-exposure to control or oleic acid was found. Non-activated control exposed cells are on the far left, non-activated oleic acid-exposed cells are on the center left, activated control-exposed cells are on the center right, and activated oleic acid-exposed cells are on the far right. **(e)** Radar plot of various $CD4^+$ T cell internal cytokines expressed in $CD4^+$ T cells after 48 h of oleic acid exposure or control followed by 72 h of activation with CD3/CD28 activation beads and 4 h additional stimulus with PMA/ionomycin. Values are expressed as fold change and standard error relative to control. **(f)** Radar plot of various $CD4^+$ T cell external markers and transcription factors expressed in $CD4^+$ T cells after 48 h of oleic acid exposure or control followed by 72 h of activation with CD3/CD28 activation beads and 4 h additional stimulus with PMA/ionomycin. Values are expressed as fold change and standard error relative to control.

Oleic acid induced $CD4^+$ T cell phenotypes blocked by metabolic inhibitors

We next determined whether induction of this profile, reminiscent of an increase differentiation toward T_H9, T_H17, and T_H2 subsets, was dependent on an upregulation of cholesterol and fatty acid biosynthesis in line with our RNA-seq data. We inhibited cholesterol synthesis with atorvastatin, targeting 3-hydroxy-3-methylglutaryl (HMG)-CoA reductase (HMGCR), and fatty acid synthesis with CP-640186, targeting both ACC1 and ACC2 (*ACACA* and *ACACB*). To this end, non-activated $CD4^+$ T cells of 3 out of 8 donors, for whom sufficient cells were available, were again exposed to control conditions, oleic acid only, oleic acid +10 µM atorvastatin, oleic acid +20 µM CP-640186, or oleic acid and both atorvastatin and CP-640186 for 48 h. The effect of oleic acid exposure was confirmed by an upregulation of *CPT1A* (Supp. Fig. 16a). Cell viability was high (>88%), and there was no difference in diameter between cells exposed to control, oleic acid, or oleic acid + inhibitors (Supp. Fig. 16b–e).

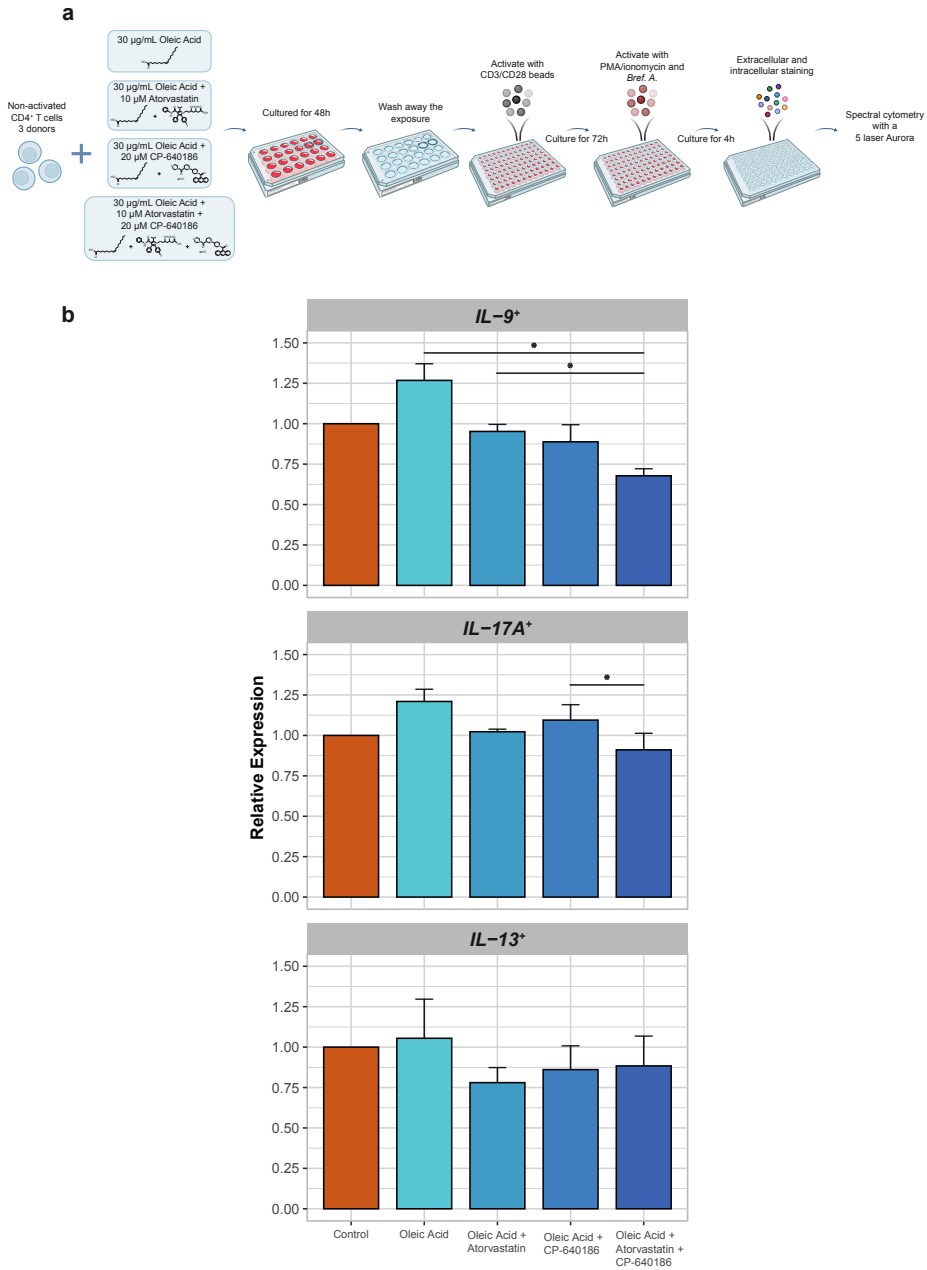

Fig. 4 | Metabolic inhibitors prevent oleic acid pre-exposure-induced changes in expression of IL-9, IL-17A, and IL-13. (*) $p < 0.05$, $n = 3$. **(a)** Experimental setup for spectral cytometry measurements of oleic acid + inhibitor exposed non-activated $CD4^+$ T cells for 48 h with activation for 72 h postexposure. **(b)** Bar plot of IL-9, IL-17A, and IL-13 expression in $CD4^+$ T cell after 48 h of control, oleic acid, oleic acid + atorvastatin, oleic acid + CP-640186, or oleic acid + atorvastatin + CP-640186 exposure followed by 72 h of activation with CD3/CD28 activation beads and 4 h additional stimulus with PMA/ionomycin. Values are expressed as fold change and standard error relative to control.

Subsequently, both oleic acid and the inhibitors were washed away and the pre-exposed $CD4^+$ T cells were activated. We evaluated the expression of one key marker for each subset: IL-9 for T_H9, IL-17A for T_H17, and IL-13 for T_H2 cells (Fig. 4a and Supp. Fig. 17). Remarkably, the ability of oleic acid to increase frequencies of IL-9^+ cells was inhibited by both atorvastatin and CP-640186 (Fig. 4b and Supp. Table 1h). Although similar trends were observed for frequencies of IL-$17A^+$ and IL-13^+ cells, these effects were not statistically significant (Fig. 4b). These data indicate that oleic acid promotes the differentiation to in particular IL-9^+-producing T cells via upregulation of cholesterol and fatty acid biosynthesis.

Discussion

T cells are known to respond to fatty acids[2]. Using an *in vitro* model, we show that sub-physiological concentrations of oleic acid can already influence $CD4^+$ T cells when in a non-activated state by upregulating the expression of genes that encode enzymes involved in core metabolic pathways responsible for cholesterol biosynthesis, fatty acid biosynthesis, and aerobic glycolysis. These metabolic processes are hallmarks of activated T cells[53]. Indeed, upon activation, $CD4^+$ T cells pre-exposed to oleic acid are characterized by increased production of cytokines, including IL-9, IL-17A, IL-5, and IL-13, indicative of a preferential differentiation toward the pro-inflammatory T helper subsets T_H9 as well as T_H17 and T_H2, which can have both pro- and anti-inflammatory effects. Interestingly, this effect is abolished in particular for IL-9^+-producing cells by blocking the cholesterol or the fatty acid biosynthesis pathways during the initial exposure to oleic acid. Our findings imply that increased fatty acid levels in the circulation can rewire the metabolism of non-activated T cells and poise them to particularly differentiate toward T_H9 cells, for example, when the cells infiltrate diseased tissues, including atherosclerotic plaques, and become activated.

Our results showed that cholesterol biosynthesis was the primary transcriptionally upregulated pathway in oleic acid-exposed non-activated $CD4^+$ T cells (15 out of 20 genes). This upregulation is of particular interest because of this pathway's role in producing the necessary metabolites required for T cell activation[54]. Cholesterol biosynthesis is upregulated in activated T cells to support membrane production, cell signaling through the formation of lipid rafts, and prenylation of signaling proteins[55]. Additionally, intracellular cholesterol sensing has also been found to play a role in T cell differentiation, particularly toward pro-inflammatory subsets. For example, sterols were found to bind the T_H17 transcription factor RORγt and could promote its activity[56]. Thus, the upregulation of gene expression in the cholesterol biosynthesis pathway due to oleic acid exposure may be indicative of a metabolic reprogramming of the non-activated $CD4^+$ T cells toward an activated state and may lead to the differentiation toward pro-inflammatory subsets post-activation.

Additionally, expression of the two genes comprising the de novo fatty acid biosynthesis pathway was upregulated (*ACACA* and *FASN*). Together, cholesterol and fatty acid biosynthesis comprise part of the process known as lipogenesis, the synthesis of novel lipids in a cell. Lipogenesis is

induced by the activation of the transcription factor SREBP1, which was associated with the upregulated transcripts in our RNA-seq data. Enrichment analysis of our transcripts also revealed upregulated genes in mTORC1 signaling, which is known to induce the activation of SREBP1[57]. Although this effect is usually insulin dependent, obesity and overfeeding have been shown to hyperactivate mTORC1[58]. Thus, it is possible that oleic acid alone could induce the activation of mTORC1, which in turn activates SREBP1, leading to lipogenesis and expression of cholesterol and fatty acid biosynthesis-related genes.

Fatty acid biosynthesis has also been related to the development of T_H17 cells[17, 32]. Specifically, the mRNA expression of genes *ACACA*, encoding for acetyl-CoA carboxylase 1 (ACC1), and *FASN*, encoding fatty acid synthase, was increased in our dataset. These genes are key determinants in the development of the pro-inflammatory subset T_H17 cells over the anti-inflammatory subset T_{reg} cells[22, 31, 39, 46, 59]. Correspondingly, *FOXP3*, the key transcription factor of T_{reg} cells, was downregulated in oleic acid-exposed non-activated $CD4^+$ T cells. Upregulated transcripts were found to be associated with the transcription factor PU.1. PU.1 is the key transcription factor in the development of T_H9 cells. This subset is a highly pro-inflammatory subset related to T_H2 cells[60]. This further supports the idea that oleic acid exposure leads to a cellular metabolic reprogramming that could promote the development of pro-inflammatory T cell subsets, specifically T_H9, and possibly also T_H17 and T_H2 cells. These results indicate that oleic acid-exposed non-activated $CD4^+$ T cells were upregulating genes involved in metabolism to initiate/prepare for the selective differentiation into T_H9/T_H17/T_H2 cells post-activation. Moreover, the metabolic processes being enhanced due to oleic acid exposure hint that the cells may preferentially differentiate toward T_H9, T_H17, and T_H2 cells upon activation.

Importantly, we provide evidence that the oleic acid-induced metabolic rewiring underpins the observed enhanced T_H9, T_H17, and T_H2 differentiation as exposing non-activated $CD4^+$ T cells to oleic acid in combination with cholesterol or fatty acid synthesis inhibitors decreased the frequencies of IL-9^+, IL-$17A^+$, and IL-13^+ cells. While the role of T_H17 and T_H2 cells in atherosclerosis has not been resolved, these cell types have been identified as pro-inflammatory in other diseases such as autoimmune encephalomyelitis and allergy, respectively[35, 61]. In contrast, T_H9 cells have been implicated in atherosclerosis pathogenesis[62-64]. Additionally, statins have been hypothesized to have protective effects independent of cholesterol reduction[65]; our study hints that effect of statins on T cell responses could contribute to this protective role.

Immune-lipid interactions occur in the circulation, which is a complex environment comprising many factors that can affect T cell function prior to their recruitment to disease site like the atherosclerotic plaque[66]. Fatty acids are a significant component of this environment and have been found to exert their effect not only on atherosclerosis but also on T cell function[2]. Our model was designed to determine the effect of oleic acid exposure on non-activated $CD4^+$ T cells. Here, we focus solely on the interaction between oleic acid and $CD4^+$ T cells and thus make no claim to what effects this fatty acid might have in relation to atherosclerotic cardiovascular disease as a component of more complex lipids, like olive oil. Our study only focuses on oleic acid as

it was shown to have both pro- and anti-inflammatory effects on T cells in previous studies[10-12, 39-43]. Circulating levels of oleic acid have been found to be related to pro-atherogenic effects[37, 38], and oleic acid is one of the most abundant fatty acids in the human circulation[36]. However, this does not preclude any effects *in vivo* or of other types of fatty acids on non-activated T cells.

Taken together, our results suggest that oleic acid can rewire the metabolism of non-activated $CD4^+$ T cells, as they exist in the circulation. This metabolic rewiring induces a preferential differentiation in particular toward T_H9 cell types following activation. Since T_H9 cell have proatherogenic effects[62-64] and we show that the oleic acid-induced differentiation into T_H9 cells can be inhibited by statins, our study indicates a new route by which fatty acids can contribute to atherosclerosis through modifiable effects on the immune system.

Limitations of the study

Although our experiments show that non-activated $CD4^+$ T cells exposed to oleic acid undergo distinct changes in the expression of genes encoding key enzymes constituting core metabolic pathways, and that subsequent activation of pre-exposed cells results in a differentiation that is skewed toward IL-9^+- producing T cells, our study used an *in vitro* model to establish these relationships and lacked an in-depth functional and mechanistic characterization of the metabolic changes involved. First, studies *in vivo* will be required to determine the relevance of our findings to the etiology of inflammatory diseases including atherosclerosis. Second, additional functional support for the occurrence of metabolic rewiring by oleic acid as implied by our results will be important. However, it will be challenging to assay functional effects. The T cells exposed to oleic acid were in a non-activated state and hence are unlikely to display functional differences in cell metabolism. Metabolic pathways are involved in the differentiation of $CD4^+$ T cells into specific subsets, and functional metabolic differences in T cells generally emerge only post-activation. Cell-subtype-specific and single-cell approaches can be informative to overcome the limitations of the bulk sequencing and spectrometry experiments as we performed in this study[18], including flow cytometry-based methods to functionally profile energy metabolism[67], mass spectrometry, and proteomics. Nevertheless, pharmacological inhibition of fatty acid and cholesterol metabolism in non-activated T cells abolished the oleic acid-induced skew toward IL-9^+-producing T cells upon activation, supporting our overall interpretation that metabolism is mechanistically involved in the effects we observed.

Acknowledgements

The authors' work is supported by the Dutch Cardiovascular Alliance (The Dutch Heart Foundation, Dutch Federation of University Medical Centers, the Netherlands Organization for Health Research and Development, and the Royal Netherlands Academy of Sciences) for the GENIUSI and GENIUSII projects Generating the Best Evidence-Based Pharmaceutical Targets for Atherosclerosis (CVON2011-19, CVON2017-20, respectively) and the Joint Programming Initiative A healthy diet for a healthy life (JPI HDHL) administered by ZonMW, the Netherlands (grant 529051021).

Author contributions

B.T.H. and J.W.J. conceived the project. N.A.R. designed and conducted the experiments, analyzed the results, and drafted the manuscript. F.S. designed and analyzed the spectral flow cytometry experiments. K.F.D. designed the *in vitro* model and analyzed the RNA-seq data. J.C.K. and H.M.S. designed the *in vitro* model. L.S. helped with the data analysis. S.H. designed the functional assays. M.A.H. performed and analyzed the transcription factor footprint analysis. H.M. aligned the RNA-seq data. E.W.v.Z. conceived the statistical model used in the analysis of the RNA sequencing. B.E. conceived and interpreted the functional assays and spectral flow cytometry data. A.I.-F. conceived and designed the *in vitro* model. All authors contributed to the writing of the manuscript.

Competing interests

The authors declare no competing interests.

References

1 Schaftenaar, F., Frodermann, V., Kuiper, J. & Lutgens, E. Atherosclerosis: the interplay between lipids and immune cells. *Curr. Opin. Lipidol.* **27**, 209-215, (2016).

2 Reilly, N. A., Lutgens, E., Kuiper, J., Heijmans, B. T. & Wouter Jukema, J. Effects of fatty acids on T cell function: role in atherosclerosis. *Nat. Rev. Cardiol.* **18**, 824–837, (2021).

3 Winkels, H. *et al.* Atlas of the immune cell repertoire in mouse atherosclerosis defined by single-cell RNA-sequencing and mass cytometry. *Circ. Res.* **122**, 1675-1688, (2018).

4 Fernandez, D. M. *et al.* Single-cell immune landscape of human atherosclerotic plaques. *Nat. Med.* **25**, 1576-1588, (2019).

5 Depuydt, M. A. *et al.* Microanatomy of the human atherosclerotic plaque by single-cell transcriptomics. *Circ. Res.* **127**, 1437-1455, (2020).

6 Zernecke, A. *et al.* Meta-analysis of leukocyte diversity in atherosclerotic mouse aortas. *Circ. Res.* **127**, 402-426, (2020).

7 Ketelhuth, D. F. & Hansson, G. K. Adaptive response of T and B cells in atherosclerosis. *Circ. Res.* **118**, 668-678, (2016).

8 Saigusa, R., Winkels, H. & Ley, K. T cell subsets and functions in atherosclerosis. *Nat. Rev. Cardiol.* **17**, 387-401, (2020).

9 Zhou, X., Robertson, A. K., Hjerpe, C. & Hansson, G. K. Adoptive transfer of CD4+ T cells reactive to modified low-density lipoprotein aggravates atherosclerosis. *Arterioscler. Thromb. Vasc. Biol.* **26**, 864-870, (2006).

10 Angela, M. *et al.* Fatty acid metabolic reprogramming via mTOR-mediated inductions of PPARγ directs early activation of T cells. *Nat. Commun.* **7**, 13683, (2016).

11 Ioan-Facsinay, A. *et al.* Adipocyte-derived lipids modulate CD4+ T-cell function. *Eur. J. Immunol.* **43**, 1578-1587, (2013).

12 Hossein zade, A. *et al.* Fatty acids effect on T helper differentiation in vitro. *Int. J. Food Sci. Nutr.* **5**, (2016).

13 Bi, X. *et al.* ω-3 polyunsaturated fatty acids ameliorate type 1 diabetes and autoimmunity. *J. Clin. Invest.* **127**, 1757-1771, (2017).

14 Raphael, I., Nalawade, S., Eagar, T. N. & Forsthuber, T. G. T cell subsets and their signature cytokines in autoimmune and inflammatory diseases. *Cytokine* **74**, 5-17, (2015).

15 Grivel, J. C. *et al.* Activation of T lymphocytes in atherosclerotic plaques. *Arterioscler. Thromb. Vasc. Biol.* **31**, 2929-2937, (2011).

16 Geltink, R. I. K., Kyle, R. L. & Pearce, E. L. Unraveling the complex interplay between T cell metabolism and function. *Annu. Rev. Immunol.* **36**, 461-488, (2018).

17 Chapman, N. M., Boothby, M. R. & Chi, H. Metabolic coordination of T cell quiescence and activation. *Nat. Rev. Immunol.* **20**, 55-70, (2020).

18 MacIver, N. J., Michalek, R. D. & Rathmell, J. C. Metabolic regulation of T lymphocytes. *Annu. Rev. Immunol.* **31**, 259-283, (2013).

19 Warburg, O., Gawehn, K. & Geissler, A. W. Metabolism of leukocytes [German]. *Z. Naturforsch. B* **13B**, 515-516, (1958).

20 Vander Heiden, M. G., Cantley, L. C. & Thompson, C. B. Understanding the Warburg effect: the metabolic requirements of cell proliferation. *Science* **324**, 1029-1033, (2009).

21 Howie, D., Ten Bokum, A., Necula, A. S., Cobbold, S. P. & Waldmann, H. The role of lipid metabolism in T lymphocyte differentiation and survival. *Front. Immunol.* **8**, 1949, (2018).

22 Cluxton, D., Petrasca, A., Moran, B. & Fletcher, J. M. Differential regulation of human Treg and Th17 cells by fatty acid synthesis and glycolysis. *Front. Immunol.* **10**, 115, (2019).

23 Michalek, R. D. *et al.* Cutting edge: distinct glycolytic and lipid oxidative metabolic programs are essential for effector and regulatory CD4+ T cell subsets. *J. Immunol.* **186**, 3299-3303, (2011).

24 Fullerton, M. D., Steinberg, G. R. & Schertzer, J. D. Immunometabolism of AMPK in insulin resistance and atherosclerosis. *Mol. Cell Endocrinol.* **366**, 224-234, (2013).

25 Maganto-García, E., Tarrio, M. L., Grabie, N., Bu, D. X. & Lichtman, A. H. Dynamic changes in regulatory T cells are linked to levels of diet-induced hypercholesterolemia. *Circulation* **124**, 185-195, (2011).

26 Delgoffe, G. M. *et al.* mTOR differentially regulates effector and regulatory T cell lineage commitment. *Immunity* **30**, 832-844, (2009).

27 Korn, T., Bettelli, E., Oukka, M. & Kuchroo, V. K. IL-17 and Th17 cells. *Annu. Rev. Immunol.* **27**, 485-517, (2009).

28 Zhu, J., Yamane, H. & Paul, W. E. Differentiation of effector CD4 T cell populations*. *Annu. Rev. Immunol.* **28**, 445-489, (2010).

29 Delgoffe, G. M. *et al.* The kinase mTOR regulates the differentiation of helper T cells through the selective activation of signaling by mTORC1 and mTORC2. *Nat. Immunol.* **12**, 295-303, (2011).

30 Shi, L. Z. *et al.* HIF1α-dependent glycolytic pathway orchestrates a metabolic checkpoint for the differentiation of TH17 and Treg cells. *J. Exp. Med.* **208**, 1367-1376, (2011).

31 Young, K. E., Flaherty, S., Woodman, K. M., Sharma-Walia, N. & Reynolds, J. M. Fatty acid synthase regulates the pathogenicity of Th17 cells. *J. Leukoc. Biol.* **102**, 1229-1235, (2017).

32 Berod, L. *et al.* De novo fatty acid synthesis controls the fate between regulatory T and T helper 17 cells. *Nat. Med.* **20**, 1327-1333, (2014).

33 O'Sullivan, D. & Pearce, E. L. Fatty acid synthesis tips the TH17-Treg cell balance. *Nat. Med.* **20**, 1235-1236, (2014).

34 Gerriets, V. A. & Rathmell, J. C. Metabolic pathways in T cell fate and function. *Trends Immunol.* **33**, 168-173, (2012).

35 Nakayama, T. *et al.* Th2 cells in health and disease. *Annu. Rev. Immunol.* **35**, 53-84, (2017).

36 Bicalho, B., David, F., Rumplel, K., Kindt, E. & Sandra, P. Creating a fatty acid methyl ester database for lipid profiling in a single drop of human blood using high resolution capillary gas chromatography and mass spectrometry. *J. Chromatogr. A* **1211**, 120-128, (2008).

37 Steffen, B. T., Duprez, D., Szklo, M., Guan, W. & Tsai, M. Y. Circulating oleic acid levels are related to greater risks of cardiovascular events and all-cause mortality: The Multi-Ethnic Study of Atherosclerosis. *J. Clin. Lipidol.* **12**, 1404-1412, (2018).

38 Delgado, G. E. *et al.* Individual omega-9 monounsaturated fatty acids and mortality – the Ludwigshafen Risk and Cardiovascular Health Study. *J. Clin. Lipidol.* **11**, 126-135, (2017).

39 Endo, Y. *et al.* Obesity drives Th17 cell differentiation by inducing the lipid metabolic kinase, ACC1. *Cell Rep.* **12**, 1042-1055, (2015).

40 Moussa, M. *et al.* In vivo effects of olive oil-based lipid emulsion on lymphocyte activation in rats. *Clin. Nutr.* **19**, 49-54, (2000).

41 Miura, S. *et al.* Increased proliferative response of lymphocytes from intestinal lymph during long chain fatty acid absorption. *Immunology* **78**, 142-146, (1993).

42 Stentz, F. B. & Kitabchi, A. E. Palmitic acid-induced activation of human T-lymphocytes and aortic endothelial cells with production of insulin receptors, reactive oxygen species, cytokines, and lipid peroxidation. *Biochem. Biophys. Res. Commun.* **346**, 721-726, (2006).

43 Passos, M. E. *et al.* Differential effects of palmitoleic acid on human lymphocyte proliferation and function. *Lipids Health Dis.* **15**, 217, (2016).

44 Verlengia, R. *et al.* Effect of arachidonic acid on proliferation, cytokines production and pleiotropic genes expression in Jurkat cells - a comparison with oleic acid. *Life Sci.* **73**, 2939-2951, (2003).

45 Gorjão, R., Cury-Boaventura, M. F., de Lima, T. M. & Curi, R. Regulation of human lymphocyte proliferation by fatty acids. *Cell Biochem. Funct.* **25**, 305-315, (2007).

46 Endo, Y. *et al.* ACC1 determines memory potential of individual CD4+ T cells by regulating de novo fatty acid biosynthesis. *Nat. Metab.* **1**, 261-275, (2019).

47 Abdelmagid, S. A. *et al.* Comprehensive profiling of plasma fatty acid concentrations in young healthy Canadian adults. *PLoS One* **10**, 0116195, (2015).

48 Lin, C. C. *et al.* IL-1-induced Bhlhe40 identifies pathogenic T helper cells in a model of autoimmune neuroinflammation. *J. Exp. Med.* **213**, 251-271, (2016).

49 Nechanitzky, R. *et al.* Cholinergic control of Th17 cell pathogenicity in experimental autoimmune encephalomyelitis. *Cell Death Differ.* **30**, 407-416, (2023).

50 Kidani, Y. *et al.* Sterol regulatory element-binding proteins are essential for the metabolic programming of effector T cells and adaptive immunity. *Nat. Immunol.* **14**, 489-499, (2013).

51 Shin, H. J., Lee, J. B., Park, S. H., Chang, J. & Lee, C. W. T-bet expression is regulated by EGR1-mediated signaling in activated T cells. *Clin. Immunol.* **131**, 385-394, (2009).

52 Allan, S. E. *et al.* Activation-induced FOXP3 in human T effector cells does not suppress proliferation or cytokine production. *Int. Immunol.* **19**, 345-354, (2007).

53 Cai, F., Jin, S. & Chen, G. The effect of lipid metabolism on CD4+ T cells. *Mediators Inflamm.* **2021**, 6634532, (2021).

54 Smith-Garvin, J. E., Koretzky, G. A. & Jordan, M. S. T cell activation. *Annu. Rev. Immunol.* **27**, 591-619, (2009).

55 Shyer, J. A., Flavell, R. A. & Bailis, W. Metabolic signaling in T cells. *Cell Res.* **30**, 649-659, (2020).

56 Santori, F. R. *et al.* Identification of natural RORγ ligands that regulate the development of lymphoid cells. *Cell Metab.* **21**, 286-298, (2015).

57 Laplante, M. & Sabatini, D. M. An emerging role of mTOR in lipid biosynthesis. *Curr. Biol.* **19**, 1046-1052, (2009).

58 Khamzina, L., Veilleux, A., Bergeron, S. & Marette, A. Increased activation of the mammalian target of rapamycin pathway in liver and skeletal muscle of obese rats: possible involvement in obesity-linked insulin resistance. *Endocrinology* **146**, 1473-1481, (2005).

59 Sun, L., Fu, J. & Zhou, Y. Metabolism controls the balance of Th17/T-regulatory cells. *Front. Immunol.* **8**, 1632, (2017).

60 Angkasekwinai, P. & Dong, C. IL-9-producing T cells: potential players in allergy and cancer. *Nat Rev Immunol* **21**, 37-48, (2021).

61 Schnell, A., Littman, D. R. & Kuchroo, V. K. Th17 cell heterogeneity and its role in tissue inflammation. *Nat. Immunol.* **24**, 19-29, (2023).

62 Zhang, W. *et al.* IL-9 aggravates the development of atherosclerosis in ApoE2/2 mice. *Cardiovasc. Res.* **106**, 453-464, (2015).

63 Gregersen, I. *et al.* Increased systemic and local interleukin 9 levels in patients with carotid and coronary atherosclerosis. *PLoS One* **8**, 72769, (2013).

64 Li, Q. *et al.* Increased Th9 cells and IL-9 levels accelerate disease progression in experimental atherosclerosis. *Am. J. Transl. Res.* **9**, 1335-1343, (2017).

65 Oesterle, A., Laufs, U. & Liao, J. K. Pleiotropic effects of statins on the cardiovascular system. *Circ. Res.* **120**, 229-243, (2017).

66 Visscher, M. *et al.* Data processing pipeline for lipid profiling of carotid atherosclerotic plaque with mass spectrometry imaging. *J. Am. Soc. Mass. Spectrom.* **30**, 1790-1800, (2019).

67 Argüello, R. J. *et al.* SCENITH: a flow cytometry-based method to functionally profile energy metabolism with single-cell resolution. *Cell Metab.* **32**, 1063-1075, (2020).

68 van der Vusse, G. J. Albumin as fatty acid transporter. *Drug Metab. Pharmacokinet.* **24**, 300-307, (2009).

69 Su, B. *et al.* A DMS shotgun lipidomics workflow application to facilitate high-throughput, comprehensive lipidomics. *J. Am. Soc. Mass Spectrom.* **32**, 2655-2663, (2021).

70 Ghorasaini, M. *et al.* Congruence and complementarity of differential mobility spectrometry and NMR spectroscopy for plasma lipidomics. *Metabolites* **12**, 1030, (2022).

71 Ledderose, C., Heyn, J., Limbeck, E. & Kreth, S. Selection of reliable reference genes for quantitative real-time PCR in human T cells and neutrophils. *BMC Res. Notes* **4**, 427, (2011).

72 Mandala, W., Harawa, V., Munyenyembe, A., Soko, M. & Longwe, H. Optimization of stimulation and staining conditions for intracellular cytokine staining (ICS) for determination of cytokine-producing T cells and monocytes. *Curr. Res. Immunol.* **2**, 184-193, (2021).

73 Love, M. I., Huber, W. & Anders, S. Moderated estimation of fold change and dispersion for RNA-seq data with DESeq2. *Genome Biol.* **15**, 550, (2014).

74 Kassambara, A. & Mundt, F. Extract and visualize the results of multivariate data analyses. (2020).

75 Gu, Z., Eils, R. & Schlesner, M. Complex heatmaps reveal patterns and correlations in multidimensional genomic data. *Bioinformatics* **32**, 2847-2849, (2016).

76 Yu, G., Wang, L. G., Han, Y. & He, Q. Y. clusterProfiler: an R package for comparing biological themes among gene clusters. *OMICS* **16**, 284-287, (2012).

77 Wishart, D. S. *et al.* PathBank: a comprehensive pathway database for model organisms. *Nucleic Acids Res.* **48**, 470-478, (2020).

78 Heinz, S. *et al.* Simple combinations of lineage-determining transcription factors prime cis-regulatory elements required for macrophage and B cell identities. *Mol. Cell* **38**, 576-589, (2010).

Supplemental information

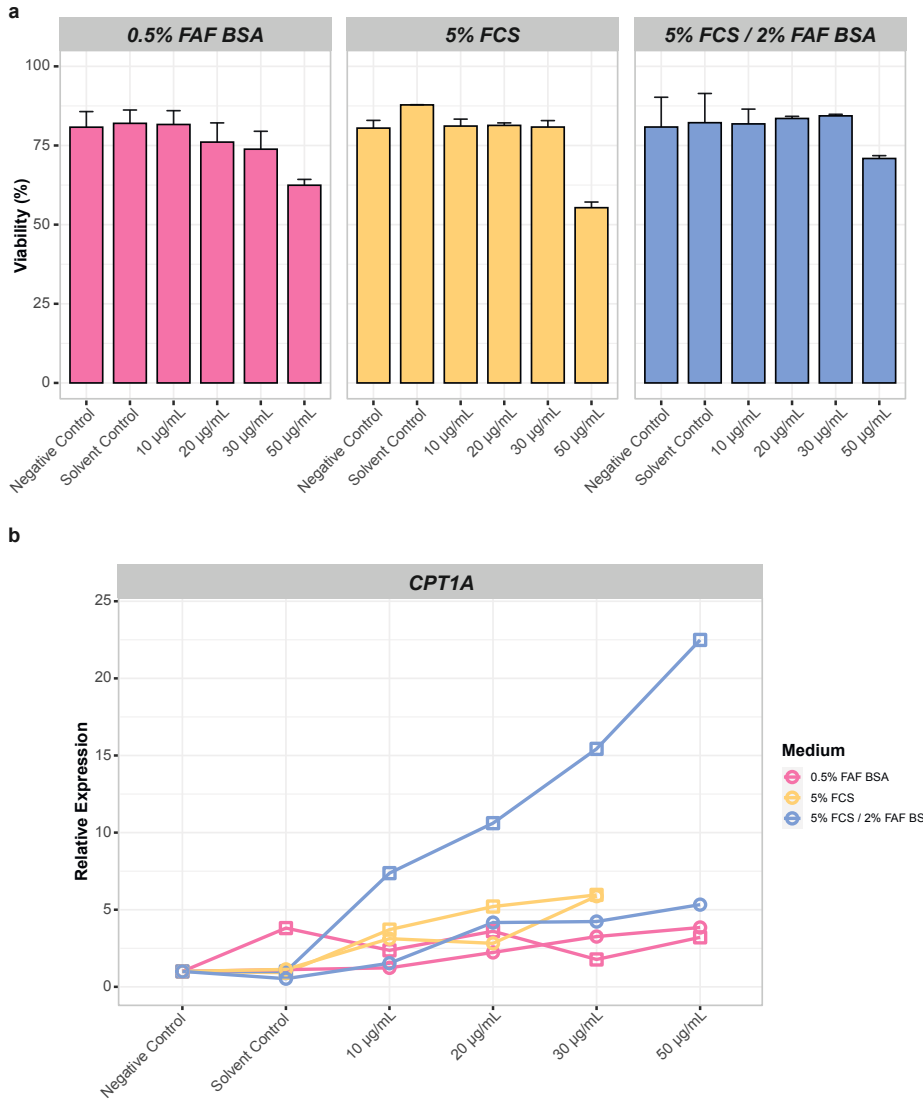

Supplemental Fig. 1 | Determination of culture medium type and concentration of oleic acid to use in the *in vitro* model by viability and *CPT1A* expression. Three different medium types were tested. First, cells cultured in and oleic acid dissolved in FAF BSA only. Second, cells cultured in and oleic acid dissolved in 5% FCS only. Third, cells cultured in 5% FCS and oleic acid dissolved in FAF BSA. Non-activated $CD4^+$ T cells were exposed to 10, 20, 30, or 50µg/mL oleic acid for 48 h. Conditions are labelled by color. The greatest upregulation while maintaining cell viability occurred at 30µg/mL oleic acid in the 5% FCS / 2% FAF BSA medium combination, n = 2. **(a)** Bar plot showing the average cell viability and standard error in percent, as determined by trypan blue staining, for 2 donors for each medium and concentration tested after 48 h exposure. For FAF BSA medium only, the average viability was 80.79 SE 4.93% at negative control, 82.00

SE 4.22% at solvent control, 81.64 SE 4.37% at 10µg/mL, 76.07 SE 6.07% at 20µg/mL, 73.84 SE 5.66% at 30µg/mL, and 62.45 SE 1.84% at 50µg/mL. For 5% FCS medium only, the average viability was 80.49 SE 2.44% at negative control, 87.82 SE 0.06% at solvent control, 81.14 SE 2.19% at 10µg/mL, 81.35 SE 0.79% at 20µg/mL, 80.83 SE 2.04% at 30µg/mL, and 55.36 SE 1.79% at 50µg/mL. For the combination of 5% FCS and FAF BSA, the average cell viability was 80.84 SE 9.41% at negative control, 82.20 SE 9.23% at solvent control, 81.82 SE 43.68% at 10µg/mL, 83.54 SE 0.68% at 20µg/mL, 84.36 SE 0.49% at 30µg/mL, and 70.90 SE 0.90% at 50µg/mL. The solvent control had no effect on $CD4^+$ T cell viability as expected. Oleic acid had no effect on $CD4^+$ T cell viability until 50µg/mL. **(b)** Line plot showing the relative expression of ***CPT1A***, as determined by RT-qPCR, per donor for each medium and concentration tested after 48 h exposure. Data is shown relative to the negative control condition. As expected, the solvent was not found to have any effect on ***CPT1A*** expression, in any of the medium types tested (3.81 fold for FAF BSA only, 1.02 SE 0.11 fold for 5% FCS only, and 0.76 SE 0.23 fold for the combination of 5% FCS and FAF BSA). No RNA was extracted from the second donor in the solvent control condition making the mean only the mean of the first donor and therefore also no SE could be calculated. For FAF BSA medium only, on average, oleic acid exposure caused ***CPT1A*** to be upregulated 1.80 SE 0.57 fold at 10µg/mL, 2.92 SE 0.69 fold at 20µg/mL, and 2.52 SE 0.74 fold at 30µg/mL, and 3.53 SE 0.32 fold at 50µg/mL. ***CPT1A*** expression increased inconsistently, most likely due to insufficient nutrients (often supplied by FCS) for the cells to survive and behave as they normally would. For 5% FCS medium only, on average, oleic acid exposure caused ***CPT1A*** to be upregulated 3.42 SE 0.29 fold at 10µg/mL, 4.01 SE 1.19 fold at 20µg/mL, and 5.92 SE 0.04 fold at 30µg/mL. Oleic acid exposure increased the expression of ***CPT1A*** gradually with increasing concentrations until 50µg/mL where the lack of albumin bound oleic acid became toxic and the cells died, making it impossible to extract sufficient quality RNA for RT-qPCR analysis. For the combination of 5% FCS and FAF BSA, on average, oleic acid exposure caused ***CPT1A*** to be upregulated 4.45 SE 2.92 fold at 10µg/mL, 7.39 SE 3.22 fold at 20µg/mL, 9.83 SE 5.60 fold at 30µg/mL, and 13.91 SE 8.58 fold at 50µg/mL. Oleic acid exposure increased the expression of ***CPT1A*** gradually with increasing concentrations.

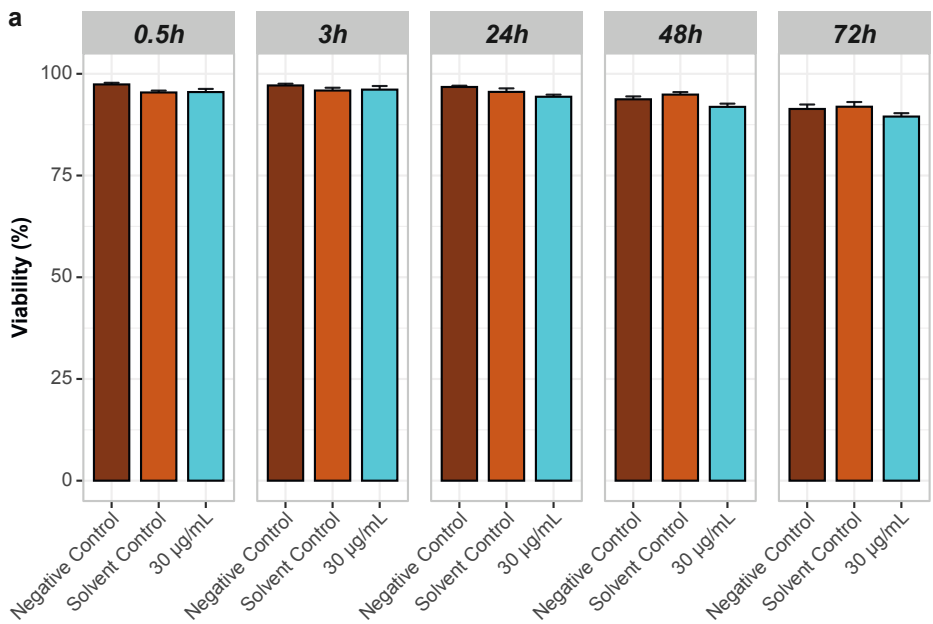

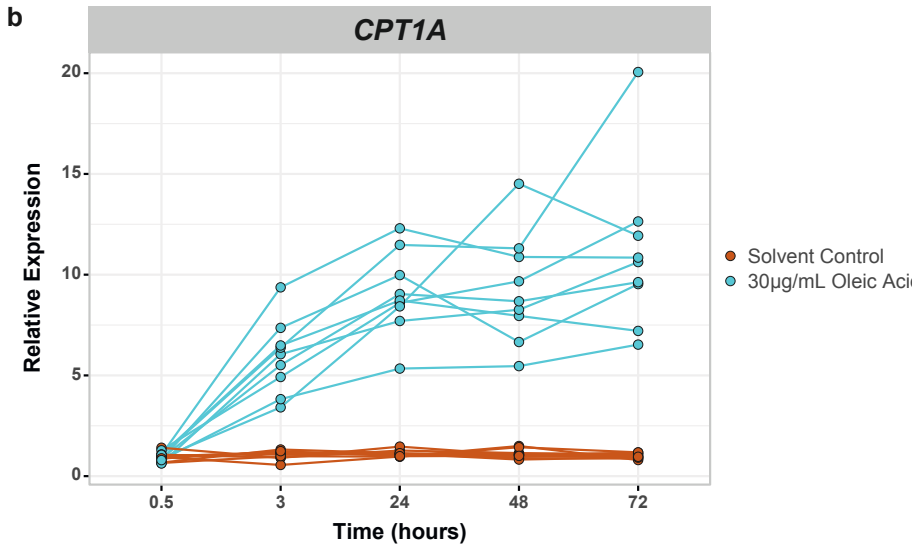

Supplemental Fig. 2 | Verification of *in vitro* model prior to RNA sequencing by viability and *CPT1A* expression. (a) Bar plot showing the average cell viability and standard error in percent, as determined by trypan blue exclusion. On average the cell viability of the negative control exposed cells was 97.4 SE 0.4% at 0.5h, 97.1 SE 0.4% at 3h, 96.8 SE 0.3% at 24h, 93.7 SE 0.7% at 48h, and 91.4 SE 1.1% at 72h. On average the cell viability of the solvent control exposed cells was 95.4 SE 0.5% at 0.5h, 95.9 SE 0.7% at 3h, 95.6 SE 0.9% at 24h, 94.9 SE 0.6% at 48h, and 91.9 SE 1.2% at 72h. On average the cell viability of the oleic acid exposed cells was 95.5 SE 0.8% at 0.5h, 96.1 SE 0.9% at 3h, 94.4 SE 0.5% at 24h, 91.8 SE 0.8% at 48h, and 89.4 SE 0.8% at 72h. Thus, neither the controls nor the exposure had an effect on $CD4^+$ T cell viability, as expected, n = 9. **(b)** Line plot showing the relative expression of ***CPT1A*** per donor across time by RT-qPCR confirming the effect of oleic acid on $CD4^+$ T cells in the ***in vitro*** model and the absence of an effect of solvent. Values are colored by exposure across time. In solvent control exposed samples, there was no effect on ***CPT1A*** expression with a relative expression of 1.0 SE 0.07 fold at 0.5h, 1.0 SE 0.08 fold at 3h, 1.1 SE 0.05 fold at 24h, 1.1 SE 0.08 fold at 48h, and 1.0 SE 0.04 fold at 72h as compared to the negative control. In oleic acid exposed samples, on average ***CPT1A*** was upregulated 0.9 SE 0.07 fold at 0.5h, 5.9 SE 0.61 fold at 3h, 9.1 SE 0.68 fold at 24h, 9.3 SE 0.90 fold at 48h, and 11.0 SE 1.30 fold at 72h as compared to the negative control. The solvent control has no effect gene expression and can therefore be used as a comparison for the differential gene expression analysis, n = 9.

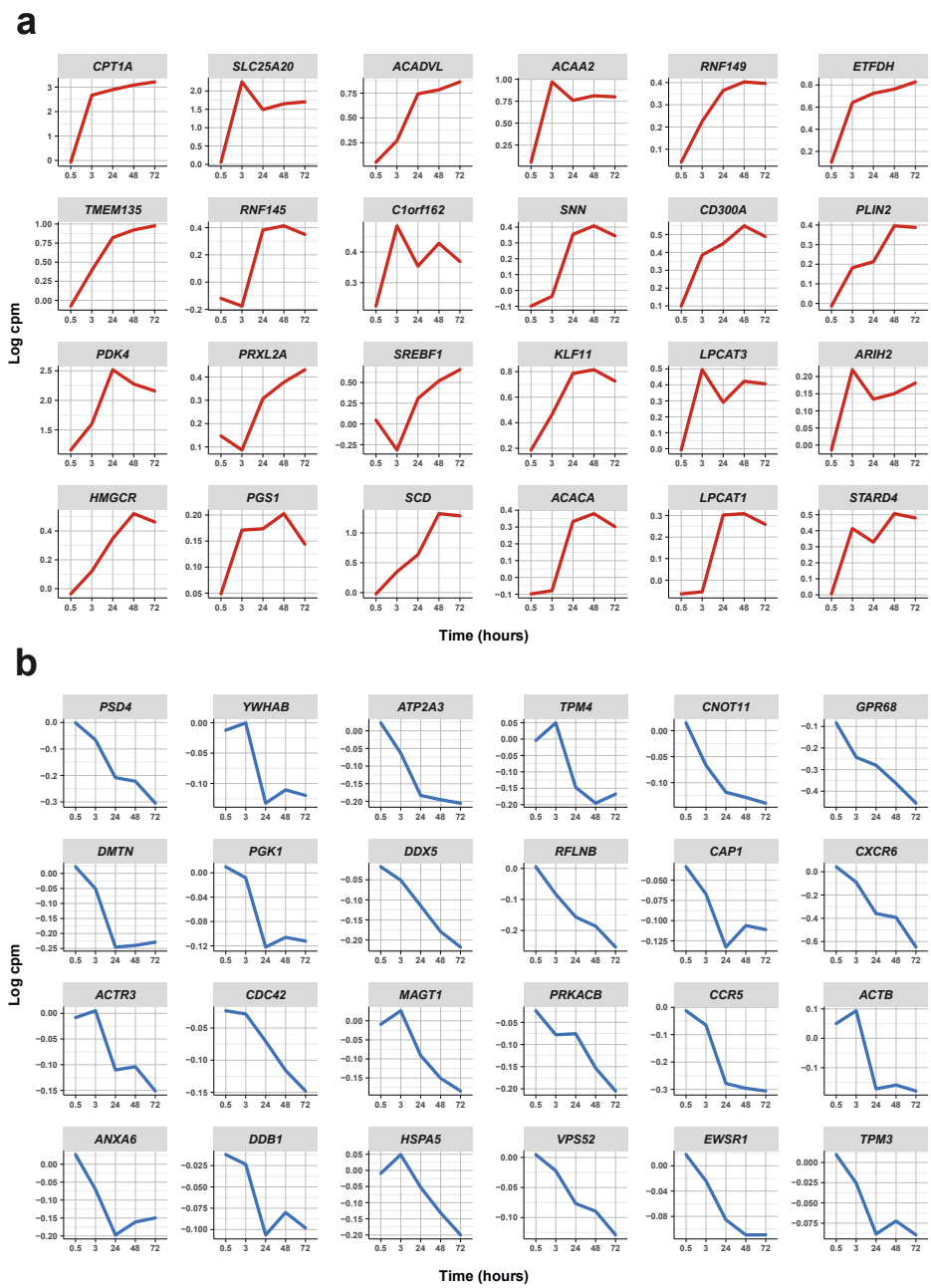

Supplemental Fig. 3 | Top differentially expressed genes from cluster 1 and 2. (a) Cluster 1 differentially expressed genes. Line plots showing mean expression values (read counts) of indicated genes from cluster 1 across time analyzed by RNA-Seq. **(b)** Cluster 2 differentially expressed genes. Line plots showing mean expression values (read counts) of indicated genes from cluster 2 across time analyzed by RNA-Seq.

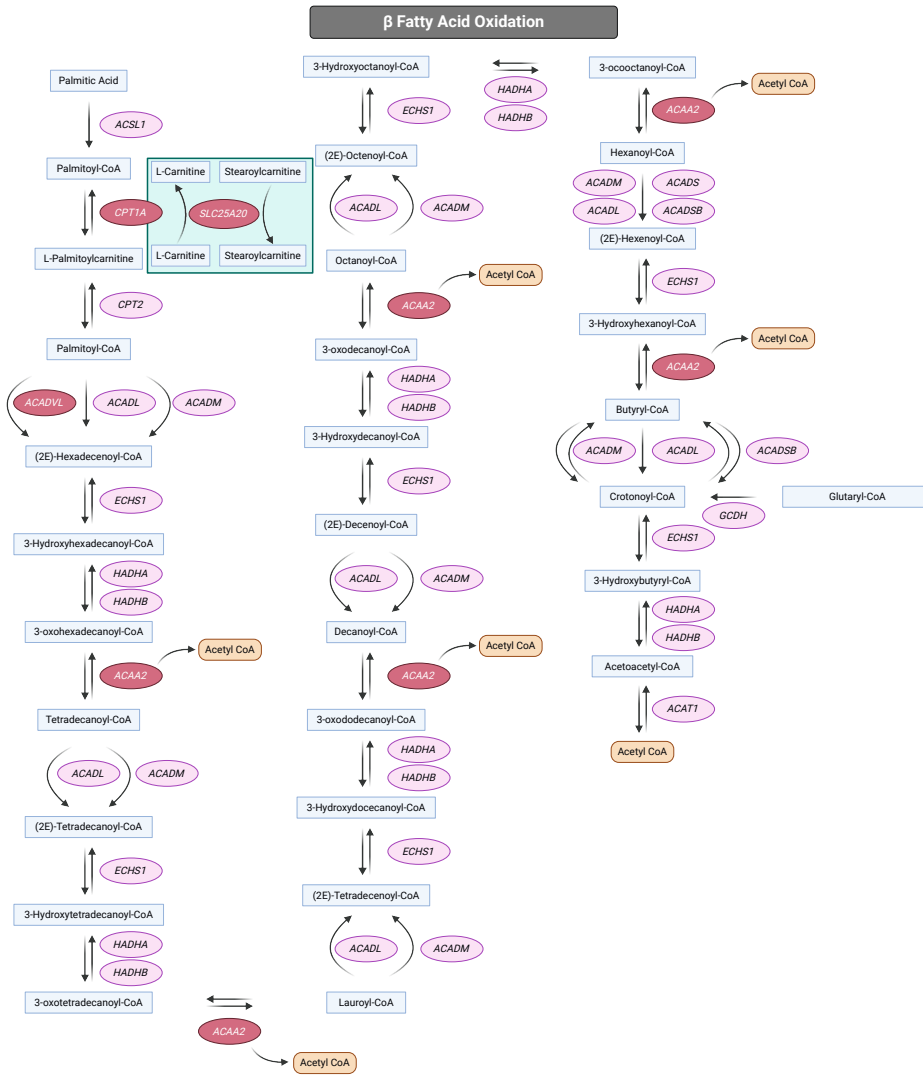

Supplemental Fig. 4 | Visualization of the Path-MAP identified overlap of differentially expressed genes within the β fatty acid oxidation pathway. Overall, a total of 4 out of 16 enzymes involved in the β fatty acid oxidation were upregulated in our oleic acid exposed non-activated $CD4^+$ T cells. Compounds are in blue boxes, enzymes not differentially expressed in the RNA sequencing data are in light pink ovals, enzymes present in the RNA sequencing data are in red ovals, the arrows indicate the direction of movement of the process. Visualization created in BioRender.com.

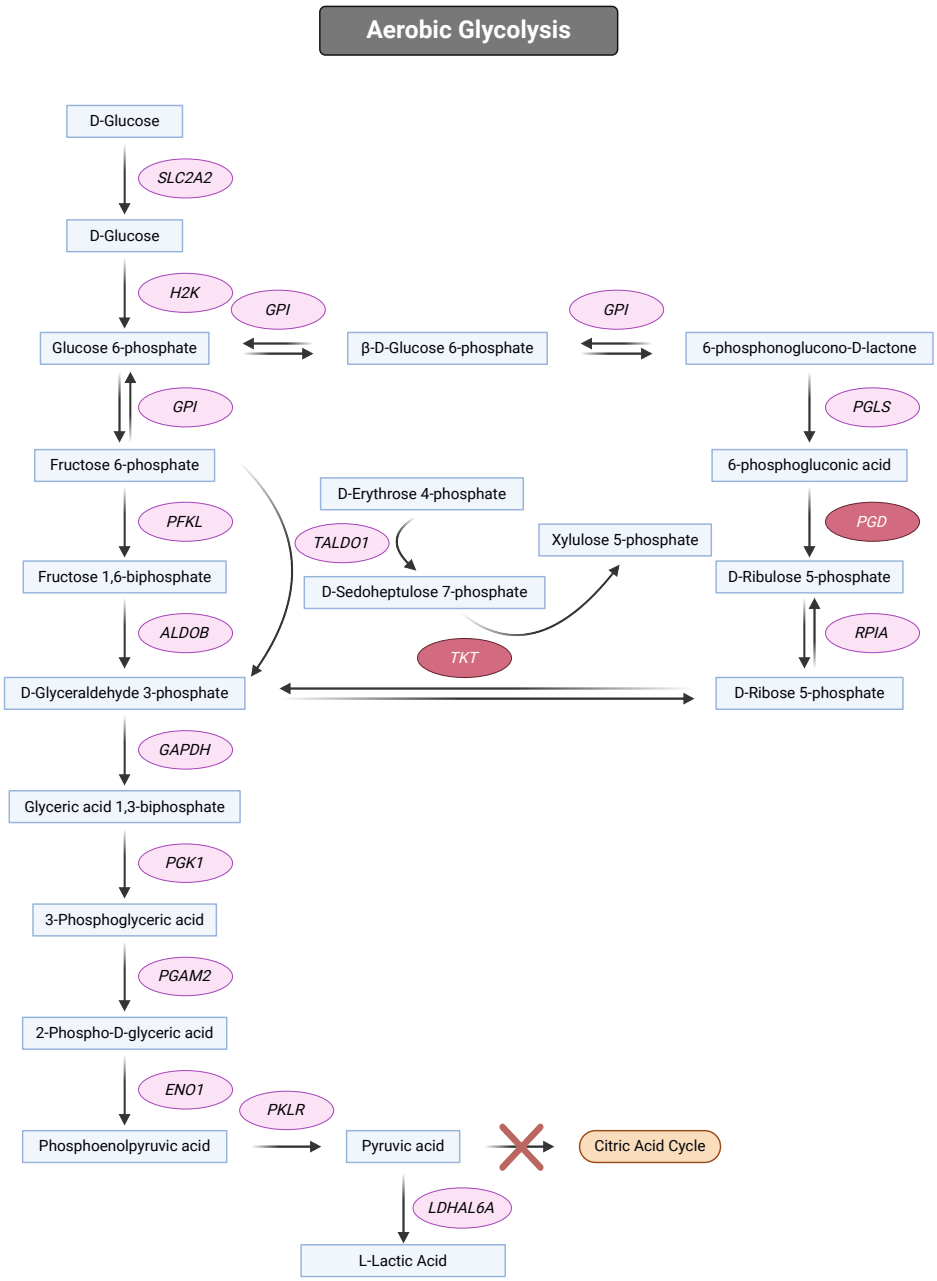

Supplemental Fig. 5 | Visualization of the Path-MAP identified overlap of differentially expressed genes within the aerobic glycolysis pathway. Overall, a total of 2 out of 15 enzymes involved in aerobic glycolysis were upregulated in our oleic acid exposed non-activated $CD4^+$ T cells. Compounds are in blue boxes, enzymes not differentially expressed in the RNA sequencing data are in light pink ovals, enzymes present in the RNA sequencing data are in red ovals, the arrows indicate the direction of movement of the process. Visualization created in BioRender.com.

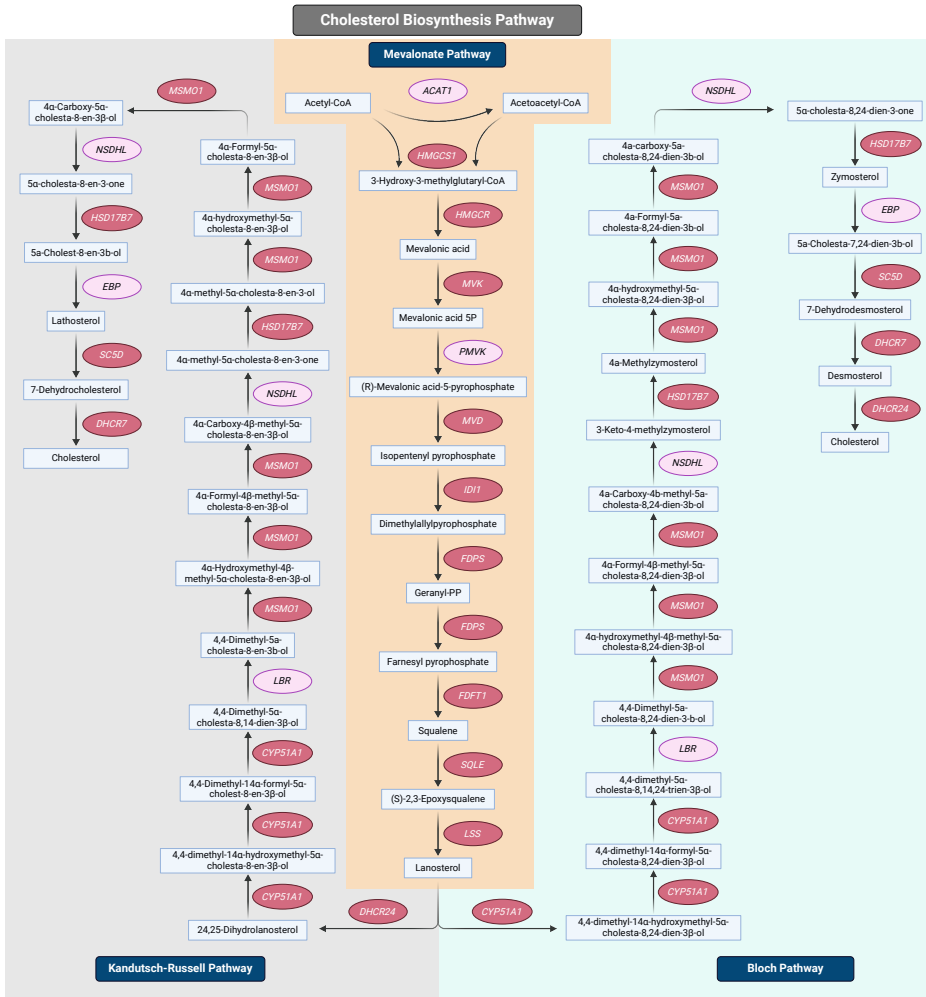

Supplemental Fig. 6 | Visualization of the Path-MAP identified overlap of differentially expressed genes within the cholesterol biosynthesis pathway. Path-MAP showed an overlap between 9 of 11 enzymes within the mevalonate pathway, 6 out of 9 enzymes within the Bloch Pathway, and 6 of 9 enzymes within the Kandutch-Russel Pathway. Overall, a total of 15 out of 20 enzymes involved in cholesterol biosynthesis were upregulated in our oleic acid exposed non-activated $CD4^+$ T cells. Compounds are in blue boxes, enzymes not differentially expressed in the RNA sequencing data are in light pink ovals, enzymes present in the RNA sequencing data are in red ovals, the arrows indicate the direction of movement for cholesterol production, the orange background indicates enzymes and compounds involved in the mevalonate pathway, the grey background indicates enzymes and compounds involved in the Kandutch-Russell pathway, and the light green background indicates enzymes and compounds involved in the Bloch pathway. Visualization created in BioRender.com.

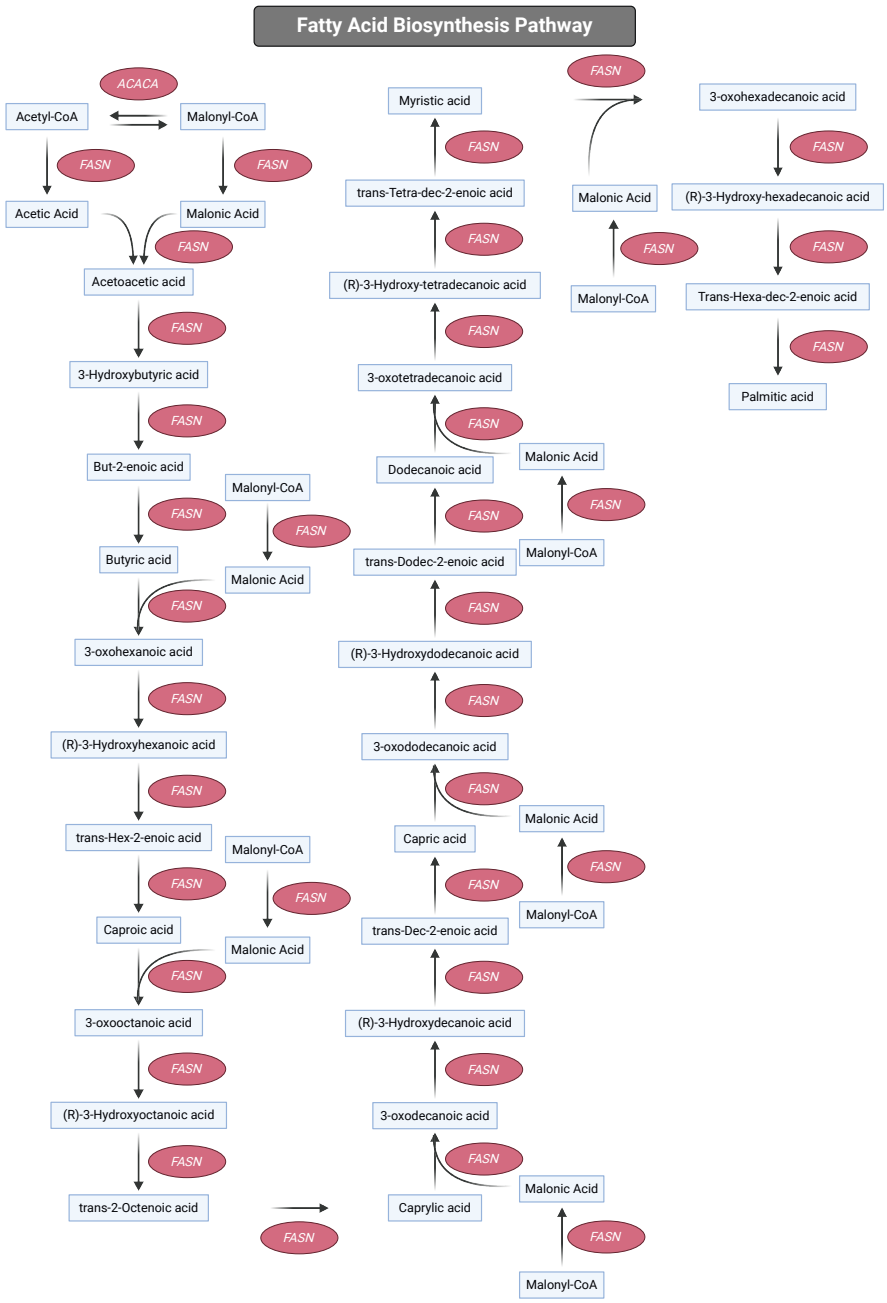

Supplemental Fig. 7 | Visualization of the Path-MAP identified overlap of differentially expressed genes within the fatty acid biosynthesis pathway. Overall, a total of 2 out of 2 enzymes involved in fatty acid biosynthesis were upregulated in our oleic acid exposed non-activated $CD4^+$ T cells. Compounds are in blue boxes, enzymes not differentially expressed in the RNA sequencing data are in light pink ovals, enzymes present in the RNA sequencing data are in red ovals, the arrows indicate the direction of movement for fatty acid production. Visualization created in BioRender.com.

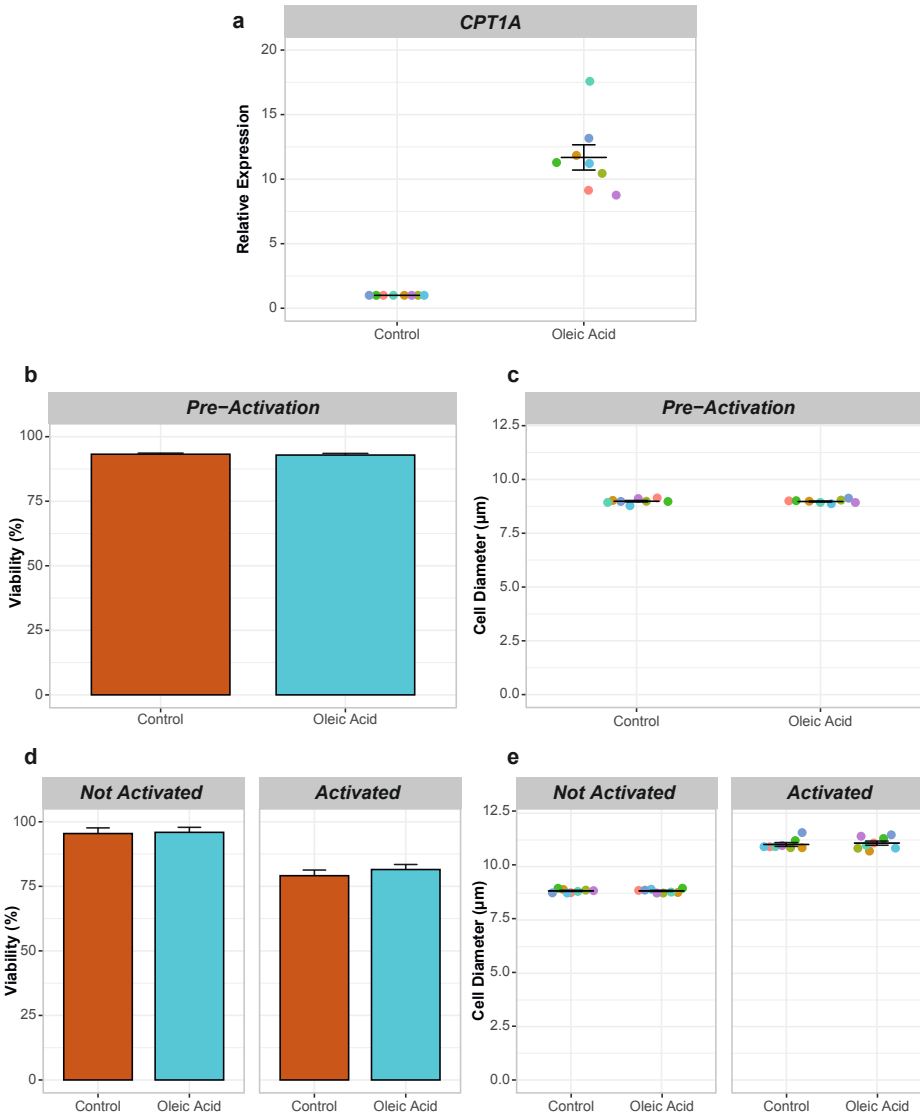

Supplemental Fig. 8 | Verification of viability, cell diameter and *CPT1A* expression post-exposure and post-activation for spectral cytometry. (a) Dot plot showing the relative expression of *CPT1A* per donor after 48h of oleic acid exposure as a confirmation of the *in vitro* model by RT-qPCR. Values are colored by donor and shown relative to the control condition. On average *CPT1A* expression of 30µg/mL oleic acid exposed cells was upregulated by 11.68 SE 0.98 fold after 48h ($p < 0.0001$), n =8. **(b)** Bar plot showing the average cell viability and standard error in percent, as determined by Via1-Cassette™ on a NucleoCounter® NC-200™. On average the cell viability of control exposed cells was 93.21 SE 0.43% and of oleic acid exposed cells was 92.89 SE 0.64%. Thus, The solvent control had no effect on $CD4^+$ T cell viability, as expected, at 48h. Thus, there was no effect on $CD4^+$ T cell viability after 48h exposure, n =8. **(c)** Dot plot showing the average cell diameter and standard error in µm, as determined by Via1-Cassette™ on a NucleoCounter® NC-200™. On average the cell diameter of control exposed cells was 8.99 SE 0.04µm and of oleic acid exposed was 8.98 SE 0.03µm. Thus, there was no effect on $CD4^+$ T cell diameter after 48h exposure, n =8. **(d)** Bar plot showing the average cell viability and standard error in percent, as determined by Via1-Cassette™ on a NucleoCounter®

NC-200™. Left plot shows the cell viability for non-activated cells and right plot shows the cell viability for activated cells. On average, the cell viability of control pre-exposed non-activated cells was 95.45 SE 2.19% and for 30µg/mL oleic acid pre-exposed non-activated cells was 95.91 SE 1.95% after 72h. The cell viability of control pre-exposed activated cells was 79.13 SE 2.19% and for 30µg/mL oleic acid pre-exposed activated cells was 81.51 SE 1.95% after 72h activation with CD3-CD28 beads. Thus, there was no effect on $CD4^+$ T cell viability between the different pre-exposures. However, activation did affect $CD4^+$ T cell viability, where the activated cells were less viable than the not activated cells, n =8. **(e)** Dot plot showing the average cell diameter and standard error in µm, as determined by Via1-Cassette™ on a NucleoCounter® NC-200™. Left plot shows the cell diameter for non-activated cells and right plot shows the cell diameter for activated cells. On average, the cell diameter of control pre-exposed non-activated cells was 8.86 SE 0.03 µm and for 30µg/mL oleic acid pre-exposed non-activated cells was 8.86 SE 0.03µm after 72h. The cell diameter of control pre-exposed activated cells was 11.04 SE 0.09µm and for 30µg/mL oleic acid pre-exposed activated cells was 11.10 SE 0.10µm after 72h activation with CD3-CD28 beads. Thus, there was no effect on $CD4^+$ T cell diameter between the different pre-exposures. However, activation did affect $CD4^+$ T cell diameter, where the activated cells were larger than the not activated cells, n =8.

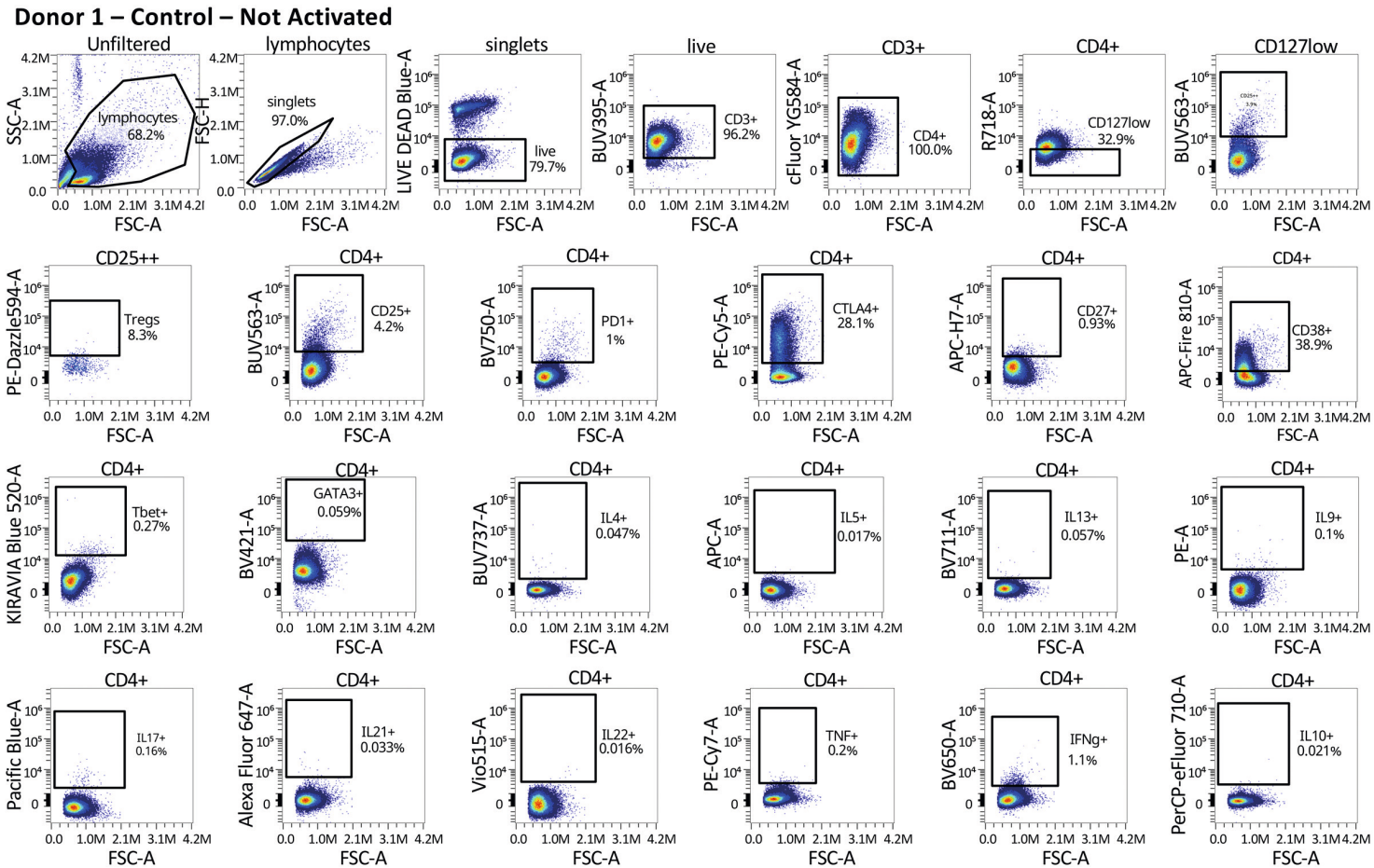
Donor 1 – Control – Not Activated
Unfiltered
SSC-A
FSC-H
FSC-A
lymphocytes
68.2%
lymphocytes
singlets
97.0%
singlets
LIVE DEAD Blue-A
live
79.7%
live
BUV395-A
CD3+
96.2%
CD3+
cFluor YG584-A
CD4+
100.0%
CD4+
R718-A
CD127low
32.9%
CD127low
BUV563-A
CD25++
PE-Dazzle594-A
Tregs
8.3%
CD4+
BUV563-A
CD25+
4.2%
CD4+
BV750-A
PD1+
1%
CD4+
PE-Cy5-A
CTLA4+
28.1%
CD4+
APC-H7-A
CD27+
0.93%
CD4+
APC-Fire 810-A
CD38+
38.9%
CD4+
KIRAVIA Blue 520-A
Tbet+
0.27%
CD4+
BV421-A
GATA3+
0.059%
CD4+
BUV737-A
IL4+
0.047%
CD4+
APC-A
IL5+
0.017%
CD4+
BV711-A
IL13+
0.057%
CD4+
PE-A
IL9+
0.1%
CD4+
Pacific Blue-A
IL17+
0.16%
CD4+
Alexa Fluor 647-A
IL21+
0.033%
CD4+
Vio515-A
IL22+
0.016%
CD4+
PE-Cy7-A
TNF+
0.2%
CD4+
BV650-A
IFNg+
1.1%
CD4+
PerCP-eFluor 710-A
IL10+
0.021%
CD4+
FSC-A

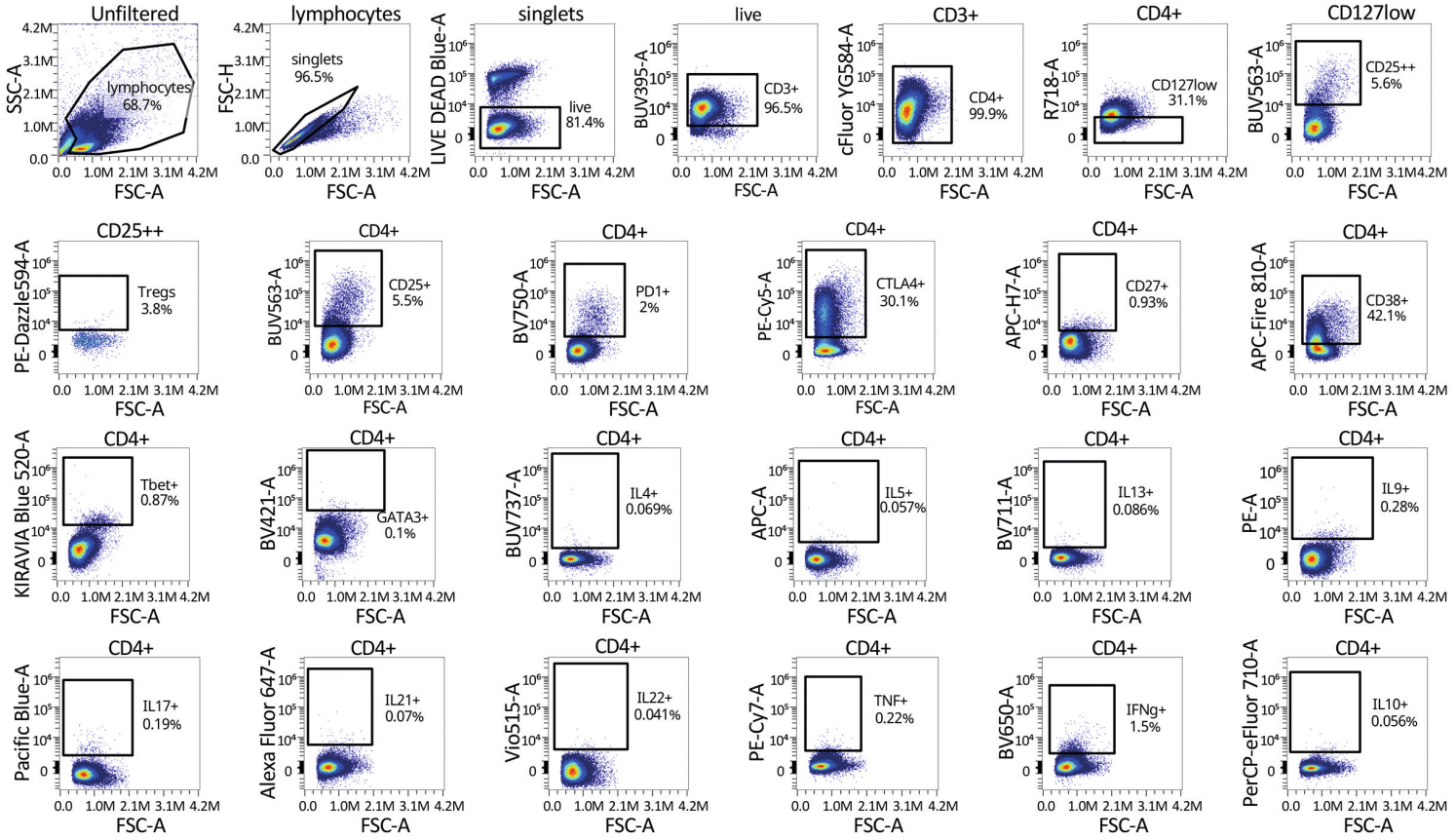

Supplemental Fig. 9 (partial) | Gating strategy for the primary spectral cytometry analysis of non-activated CD4⁺ T cells pre-exposed to oleic acid, n = 8. Gating strategy is the same for all 8 donors analyzed and includes gates set for all markers measured in the panel. Gating strategy for one donor and both exposures are shown here, the rest of the figure can be found in the online supplement: https://doi.org/10.1016/j.isci.2024.109496.

Donor 1 – Control – Activated
Unfiltered
Lymphocytes
73.6%
SSC-A
FSC-A
Lymphocytes
Singlets
97.1%
FSC-H
FSC-A
Singlets
Live
76.8%
LIVE DEAD Blue-A
FSC-A
Live
CD3+CD4+
99.1%
BUV395-A
cFluor YG584-A
CD3+CD4+
CD127low
4.6%
R718-A
FSC-A
CD127low
CD25++
68.9%
BUV563-A
FSC-A
CD25++
Tregs
7.1%
PE-DazzleI594-A
FSC-A
CD3+CD4+
CD25+
72.2%
BUV563-A
FSC-A
CD3+CD4+
PD1+
60.4%
BV750-A
FSC-A
CD3+CD4+
CTLA4+
66.5%
PE-Cy5-A
FSC-A
CD3+CD4+
CD27+
14.6%
APC-H7-A
FSC-A
CD3+CD4+
CD38+
52.3%
APC-Fire 810-A
FSC-A
CD3+CD4+
Tbet+
0.42%
KIRAVIA Blue 520-A
FSC-A
CD3+CD4+
GATA3+
0.63%
BV421-A
FSC-A
CD3+CD4+
IL4+
0.018%
BUV737-A
FSC-A
CD3+CD4+
IL5+
0.023%
APC-A
FSC-A
CD3+CD4+
IL13+
0.059%
BV711-A
FSC-A
CD3+CD4+
IL9+
0.68%
PE-A
FSC-A
CD3+CD4+
IL17A+
0.29%
Pacific Blue-A
FSC-A
CD3+CD4+
IL21+
0.21%
Alexa Fluor 647-A
FSC-A
CD3+CD4+
IL22+
0.12%
Vio515-A
FSC-A
CD3+CD4+
TNF+
0.65%
PE-Cy7-A
FSC-A
CD3+CD4+
IFNg+
2.8%
BV650-A
FSC-A
CD3+CD4+
IL10+
0.12%
PerCP-eFluor 710-A
FSC-A

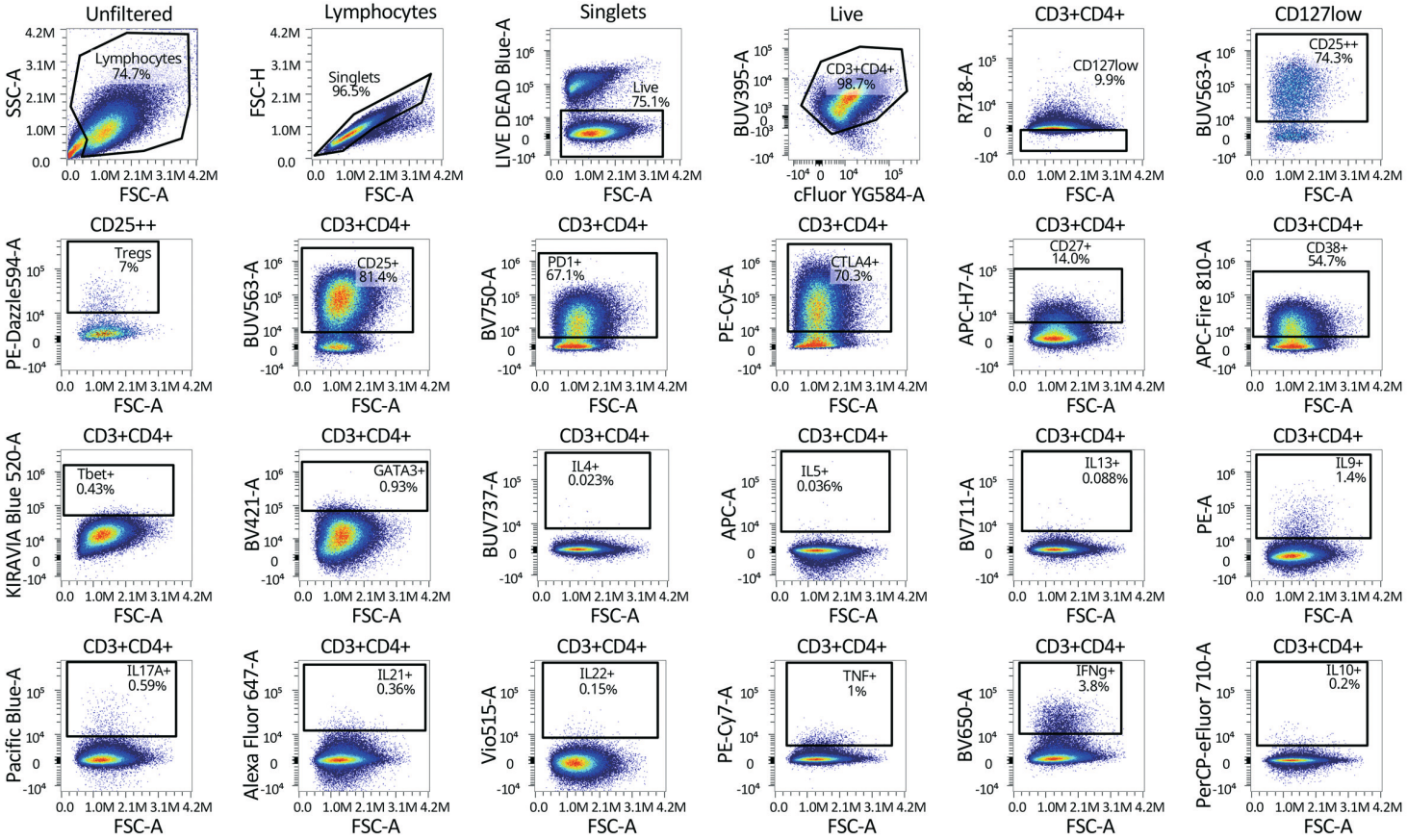

Supplemental Fig. 10 (partial) | Gating strategy for the primary spectral cytometry analysis of activated CD4⁺ T cells pre-exposed to oleic acid, n = 8. Gating strategy is the same for all 8 donors analyzed and includes gates set for all markers measured in the panel. Gating strategy for 2 different donors and exposures are shown here, the rest of the figure can be found in the online supplement: https://doi.org/10.1016/j.isci.2024.109496.

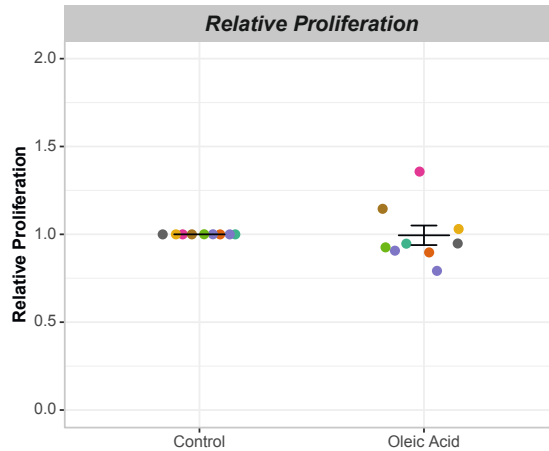

Supplemental Fig. 11 | Relative proliferation post-activation of oleic acid pre-exposed CD4⁺ T cells. Dot plot showing the relative proliferation, as determined by ^{3}H incorporation, per donor after 48h exposure to control or 30µg/mL oleic acid, where the solvent was completely evaporated prior to addition to the cells, and subsequent activation by CD3/CD28 activation beads for 72h. ^{3}H was added post 72h activation and cells were left to proliferate for 18h. Data is shown relative to the Control condition. Points are colored by donor with mean and standard error. No difference in proliferative capacity was observed between the oleic acid and control pre-exposed conditions. On average the relative proliferation of oleic acid exposed cells was 0.99 SE 0.06 ($p > 0.92$), $n = 9$.

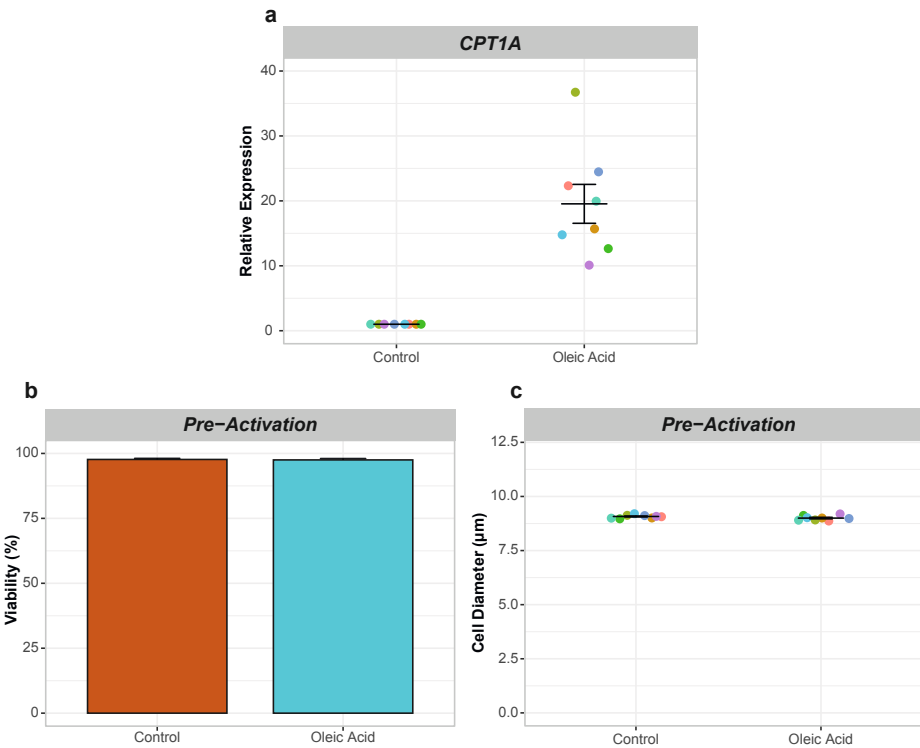

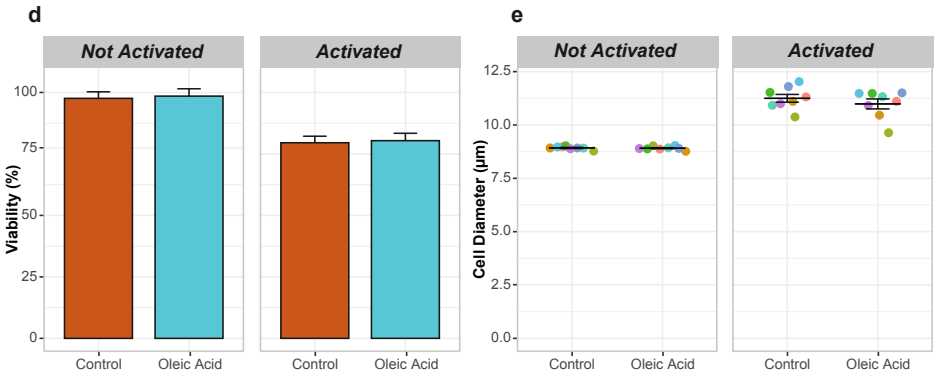

Supplemental Fig. 12 | Verification of viability, cell diameter and *CPT1A* expression post-exposure and post-activation for spectral cytometry. (a) Dot plot showing the relative expression of ***CPT1A*** per donor after 48h of oleic acid exposure as a confirmation of the ***in vitro*** model by RT-qPCR. Values are colored by donor and shown relative to the control condition. On average ***CPT1A*** expression of 28µg/mL oleic acid exposed cells was upregulated by 19.5 SE 3.00 fold after 48h ($p < 0.0001$), n = 8. **(b)** Bar plot showing the average cell viability and standard error in percent, as determined by Via1-Cassette™ on a NucleoCounter® NC-200™. On average the cell viability of control exposed cells was 93.21 SE 0.43% and of oleic acid exposed cells was 92.89 SE 0.64%. Thus, The solvent control had no effect on $CD4^+$ T cell viability, as expected, at 48h. Thus, there was no effect on $CD4^+$ T cell viability after 48h exposure, n = 8. **(c)** Dot plot showing the average cell diameter and standard error in µm, as determined by Via1-Cassette™ on a NucleoCounter® NC-200™. On average the cell diameter of control exposed cells was 8.99 SE 0.04µm and of oleic acid exposed was 8.98 SE 0.03µm. Thus, there was no effect on $CD4^+$ T cell diameter after 48h exposure, n = 8. **(d)** Bar plot showing the average cell viability and standard error in percent, as determined by Via1-Cassette™ on a NucleoCounter® NC-200™. Left plot shows the cell viability for non-activated cells and right plot shows the cell viability for activated cells. On average, the cell viability of control pre-exposed non-activated cells was 95.45 SE 2.19% and for 28µg/mL oleic acid pre-exposed non-activated cells was 95.91 SE 1.95% after 72h. The cell viability of control pre-exposed activated cells was 79.13 SE 2.19% and for 28µg/mL oleic acid pre-exposed activated cells was 81.51 SE 1.95% after 72h activation with CD3-CD28 beads. Thus, there was no effect on $CD4^+$ T cell viability between the different pre-exposures. However, activation did affect $CD4^+$ T cell viability, where the activated cells were less viable than the not activated cells, n = 8. **(e)** Dot plot showing the average cell diameter and standard error in µm, as determined by Via1-Cassette™ on a NucleoCounter® NC-200™. Left plot shows the cell diameter for non-activated cells and right plot shows the cell diameter for activated cells. On average, the cell diameter of control pre-exposed non-activated cells was 8.86 SE 0.03 µm and for 28µg/mL oleic acid pre-exposed non-activated cells was 8.86 SE 0.03µm after 72h. The cell diameter of control pre-exposed activated cells was 11.04 SE 0.09µm and for 28µg/mL oleic acid pre-exposed activated cells was 11.10 SE 0.10µm after 72h activation with CD3-CD28 beads. Thus, there was no effect on $CD4^+$ T cell diameter between the different pre-exposures. However, activation did affect $CD4^+$ T cell diameter, where the activated cells were larger than the not activated cells, n = 8.

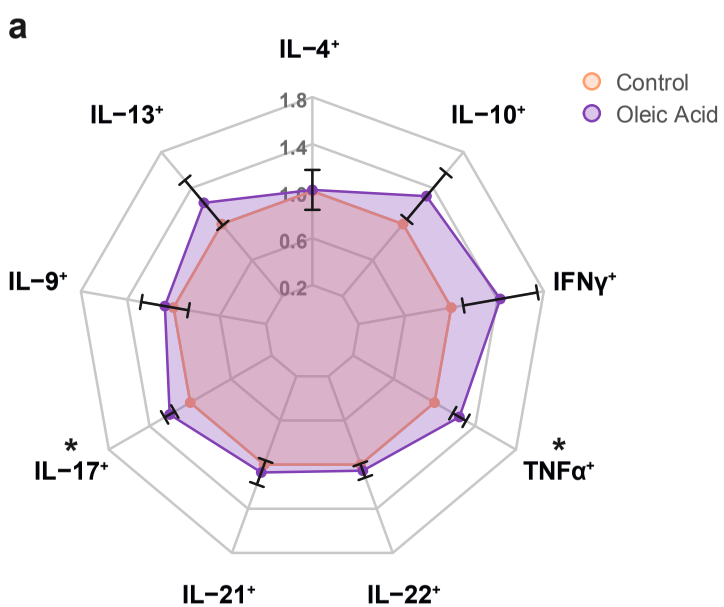
a
IL−4+
IL−10+
IFNγ+
*
TNFα+
IL−22+
IL−21+
*
IL−17+
IL−9+
IL−13+
1.8
1.4
1.0
0.6
0.2
Control
Oleic Acid

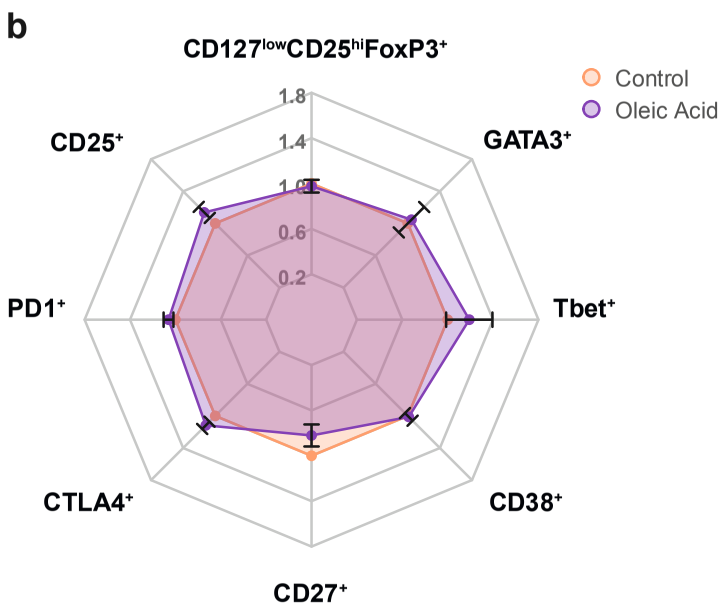
b
CD127lowCD25hiFoxP3+
GATA3+
Tbet+
CD38+
CD27+
CTLA4+
PD1+
CD25+
1.8
1.4
1.0
0.6
0.2
Control
Oleic Acid

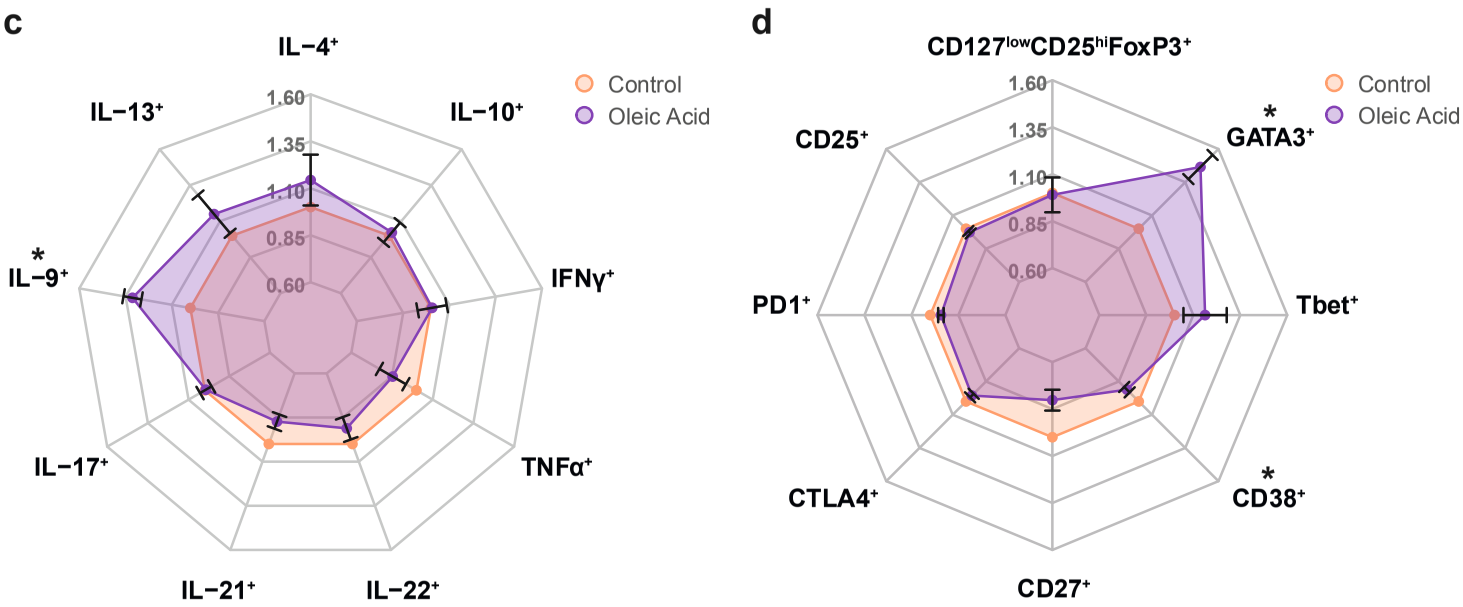

Supplemental Fig. 13 | Oleic acid pre-exposure leads to changes in expression of extracellular markers, transcription factors, and intracellular cytokines. (*) $P_{FDR} < 0.05$, n = 8. **(a)** Radar plot of various $CD4^+$ T cell internal cytokines expressed in $CD4^+$ T cells after 48h of oleic acid exposure or control followed by 72h of rest and 4h stimulus with PMA/ionomycin. Values are expressed as fold change and standard error relative to control. **(b)** Radar plot of various $CD4^+$ T cell external markers and transcription factors expressed in $CD4^+$ T cells after 48h of oleic acid exposure or control followed by 72h of rest and 4h stimulus with PMA/ionomycin. Values are expressed as fold change and standard error relative to control. **(c)** Radar plot of various $CD4^+$ T cell internal cytokines expressed in $CD4^+$ T cells after 48h of oleic acid exposure or control followed by 72h of activation with CD3/CD28 activation beads and 4h additional stimulus with PMA/ionomycin. Values are expressed as fold change and standard error relative to control. **(d)** Radar plot of various $CD4^+$ T cell external markers and transcription factors expressed in $CD4^+$ T cells after 48h of oleic acid exposure or control followed by 72h of activation with CD3/CD28 activation beads and 4h additional stimulus with PMA/ionomycin. Values are expressed as fold change and standard error relative to control.

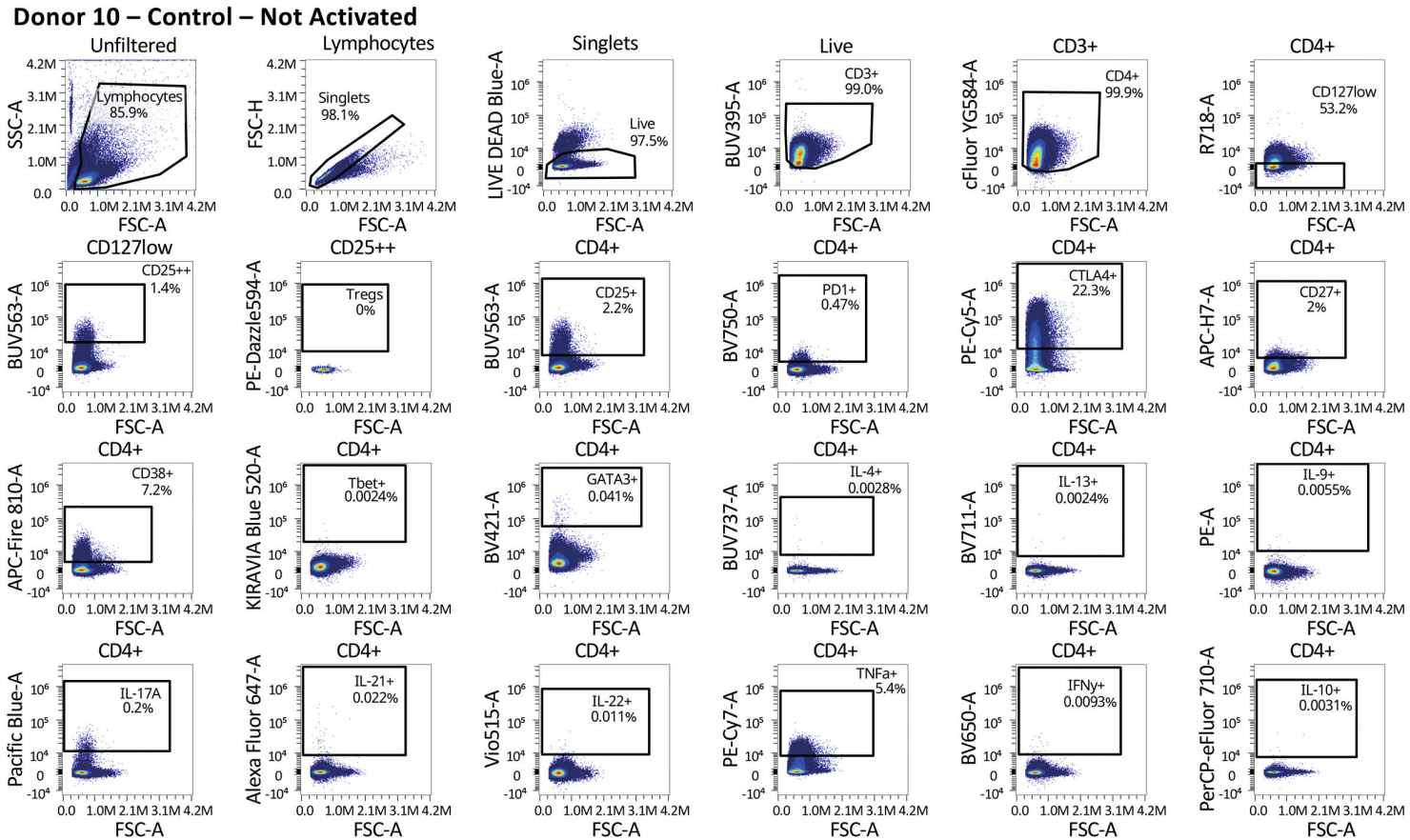
Donor 10 – Control – Not Activated
Unfiltered
Lymphocytes
85.9%
Lymphocytes
Singlets
98.1%
Singlets
Live
97.5%
Live
CD3+
99.0%
CD3+
CD4+
99.9%
CD4+
CD127low
53.2%
CD127low
CD25++
1.4%
CD25++
Tregs
0%
CD4+
CD25+
2.2%
CD4+
PD1+
0.47%
CD4+
CTLA4+
22.3%
CD4+
CD27+
2%
CD4+
CD38+
7.2%
CD4+
Tbet+
0.0024%
CD4+
GATA3+
0.041%
CD4+
IL-4+
0.0028%
CD4+
IL-13+
0.0024%
CD4+
IL-9+
0.0055%
CD4+
IL-17A
0.2%
CD4+
IL-21+
0.022%
CD4+
IL-22+
0.011%
CD4+
TNFa+
5.4%
CD4+
IFNy+
0.0093%
CD4+
IL-10+
0.0031%
SSC-A
FSC-H
LIVE DEAD Blue-A
BUV395-A
cFluor YG584-A
R718-A
BUV563-A
PE-Dazzle594-A
BUV563-A
BV750-A
PE-Cy5-A
APC-H7-A
APC-Fire 810-A
KIRAVIA Blue 520-A
BV421-A
BUV737-A
BV711-A
PE-A
Pacific Blue-A
Alexa Fluor 647-A
Vio515-A
PE-Cy7-A
BV650-A
PerCP-eFluor 710-A
FSC-A

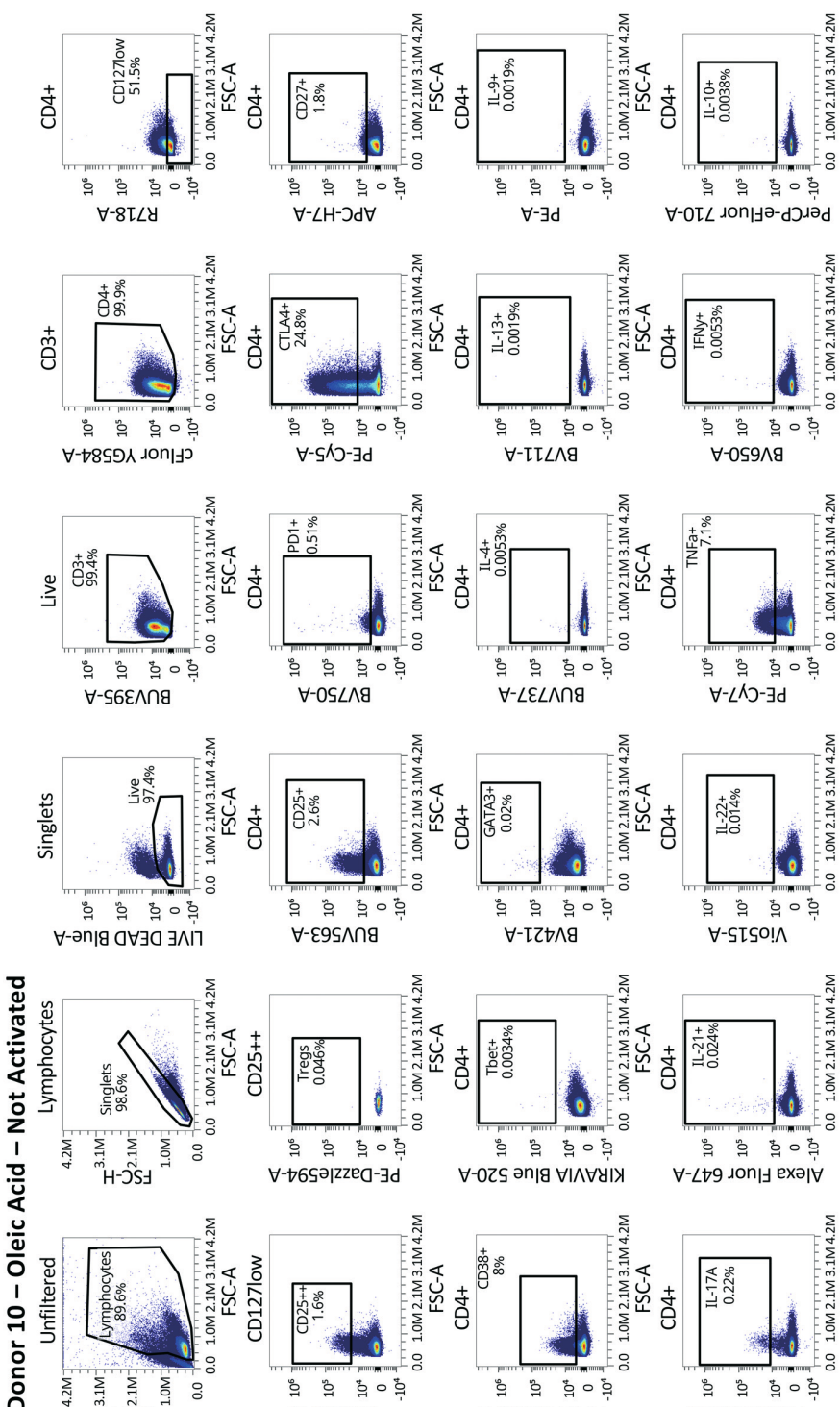

Supplemental Fig. 14 (partial) | Gating strategy for the second spectral cytometry analysis of non-activated CD4⁺ T cells pre-exposed to oleic acid from 8 independent donors, n = 8. Gating strategy is the same for all 8 independent donors analyzed and includes gates set for all markers measured in the panel. Gating strategy for 2 different donors and exposures are shown here, the rest of the figure can be found in the online supplement: https://doi.org/10.1016/j.isci.2024.109496.

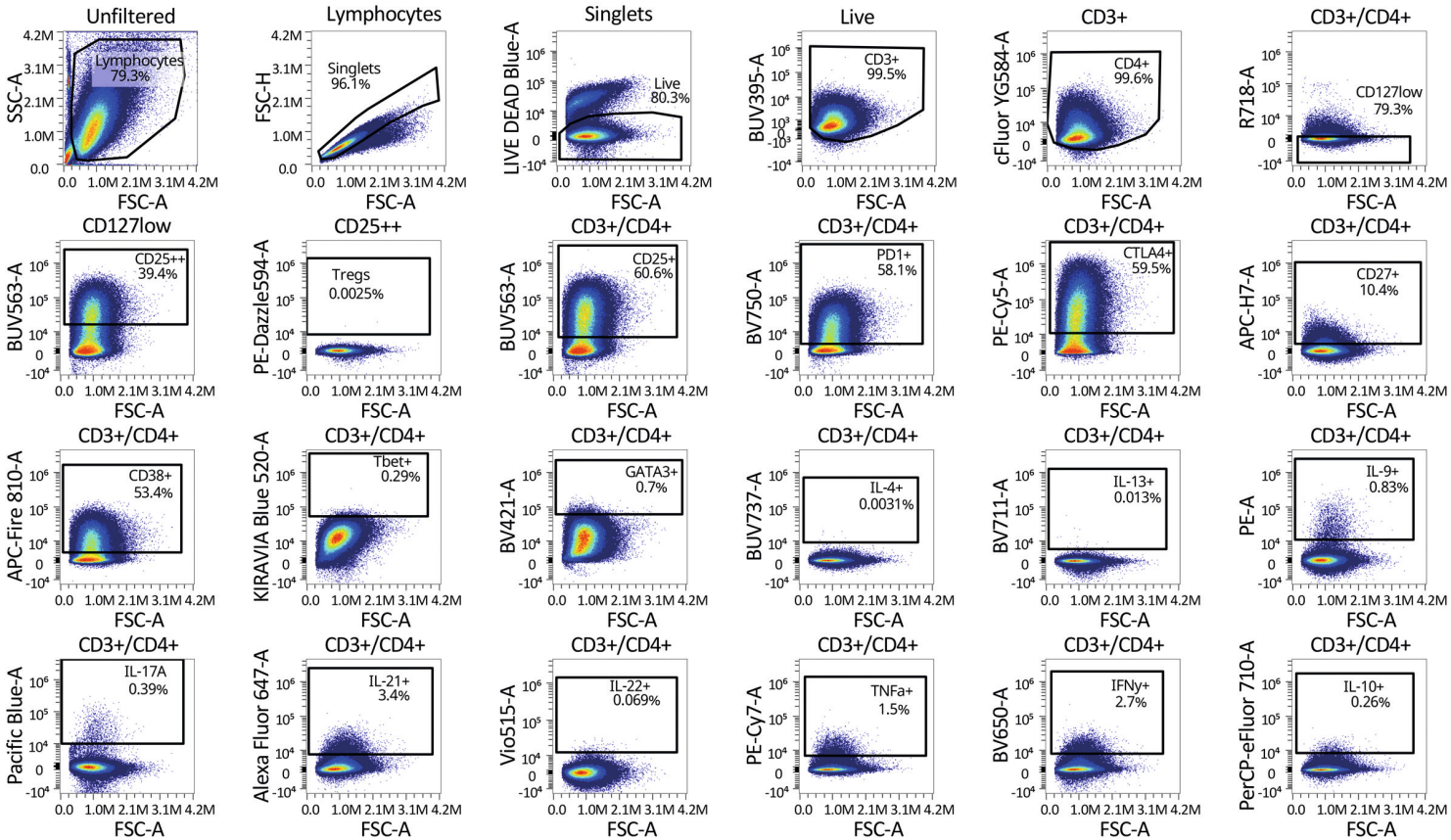
Donor 10 – Control – Activated
Unfiltered
Lymphocytes
79.3%
SSC-A
FSC-A
Lymphocytes
Singlets
96.1%
FSC-H
FSC-A
Singlets
Live
80.3%
LIVE DEAD Blue-A
FSC-A
Live
CD3+
99.5%
BUV395-A
FSC-A
CD3+
CD4+
99.6%
cFluor YG584-A
FSC-A
CD3+/CD4+
CD127low
79.3%
R718-A
FSC-A
CD127low
CD25++
39.4%
BUV563-A
FSC-A
CD25++
Tregs
0.0025%
PE-Dazzle594-A
FSC-A
CD3+/CD4+
CD25+
60.6%
BUV563-A
FSC-A
CD3+/CD4+
PD1+
58.1%
BV750-A
FSC-A
CD3+/CD4+
CTLA4+
59.5%
PE-Cy5-A
FSC-A
CD3+/CD4+
CD27+
10.4%
APC-H7-A
FSC-A
CD3+/CD4+
CD38+
53.4%
APC-Fire 810-A
FSC-A
CD3+/CD4+
Tbet+
0.29%
KIRAVIA Blue 520-A
FSC-A
CD3+/CD4+
GATA3+
0.7%
BV421-A
FSC-A
CD3+/CD4+
IL-4+
0.0031%
BUV737-A
FSC-A
CD3+/CD4+
IL-13+
0.013%
BV711-A
FSC-A
CD3+/CD4+
IL-9+
0.83%
PE-A
FSC-A
CD3+/CD4+
IL-17A
0.39%
Pacific Blue-A
FSC-A
CD3+/CD4+
IL-21+
3.4%
Alexa Fluor 647-A
FSC-A
CD3+/CD4+
IL-22+
0.069%
Vio515-A
FSC-A
CD3+/CD4+
TNFa+
1.5%
PE-Cy7-A
FSC-A
CD3+/CD4+
IFNy+
2.7%
BV650-A
FSC-A
CD3+/CD4+
IL-10+
0.26%
PerCP-eFluor 710-A
FSC-A

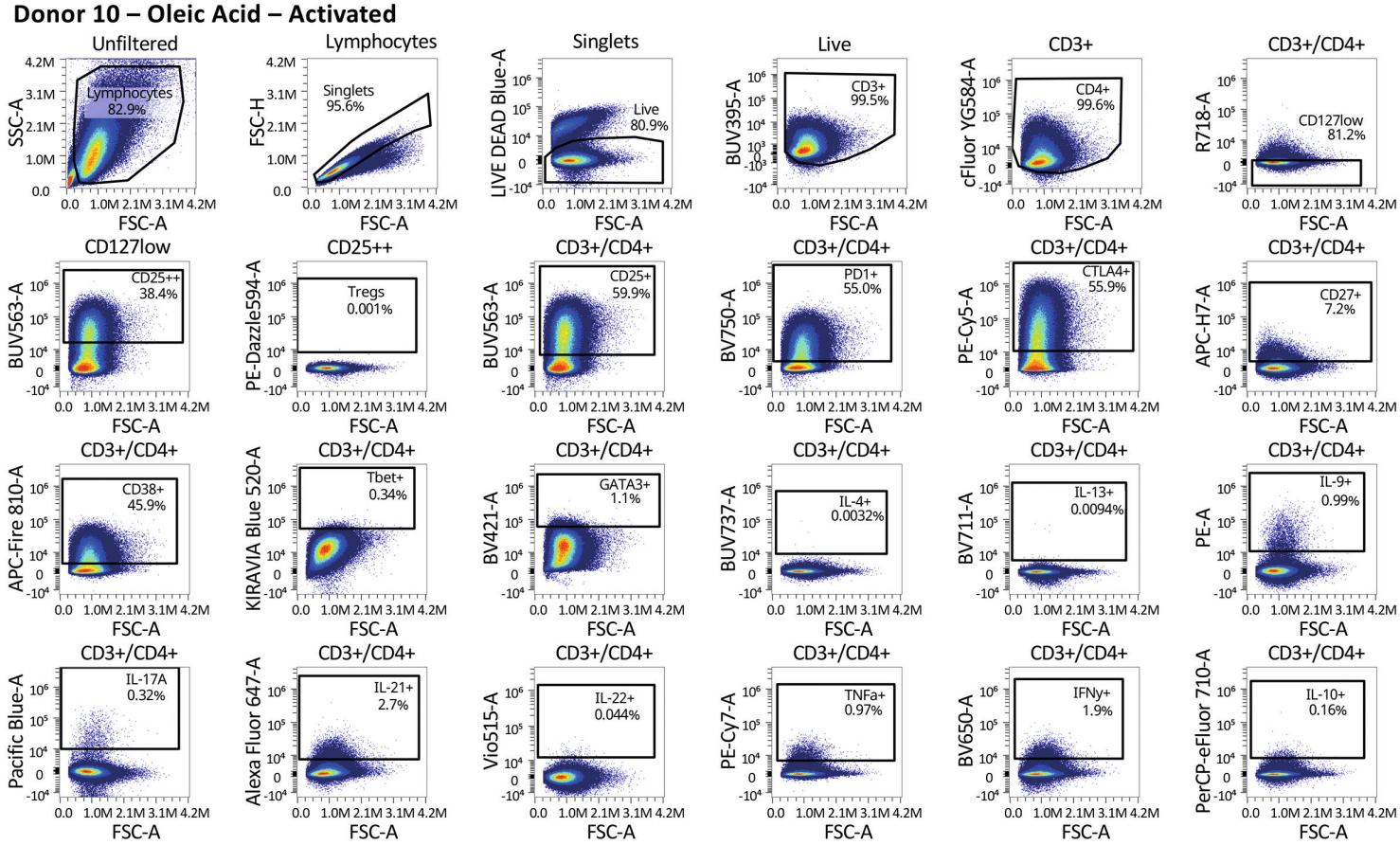

Supplemental Fig. 15 (partial) | Gating strategy for the second spectral cytometry analysis of activated $CD4^+$ T cells pre-exposed to oleic acid from 8 independent donors, n = 8. Gating strategy is the same for all 8 independent donors analyzed and includes gates set for all markers measured in the panel. Gating strategy for 2 different donors and exposures are shown here, the rest of the figure can be found in the online supplement: https://doi.org/10.1016/j.isci.2024.109496.

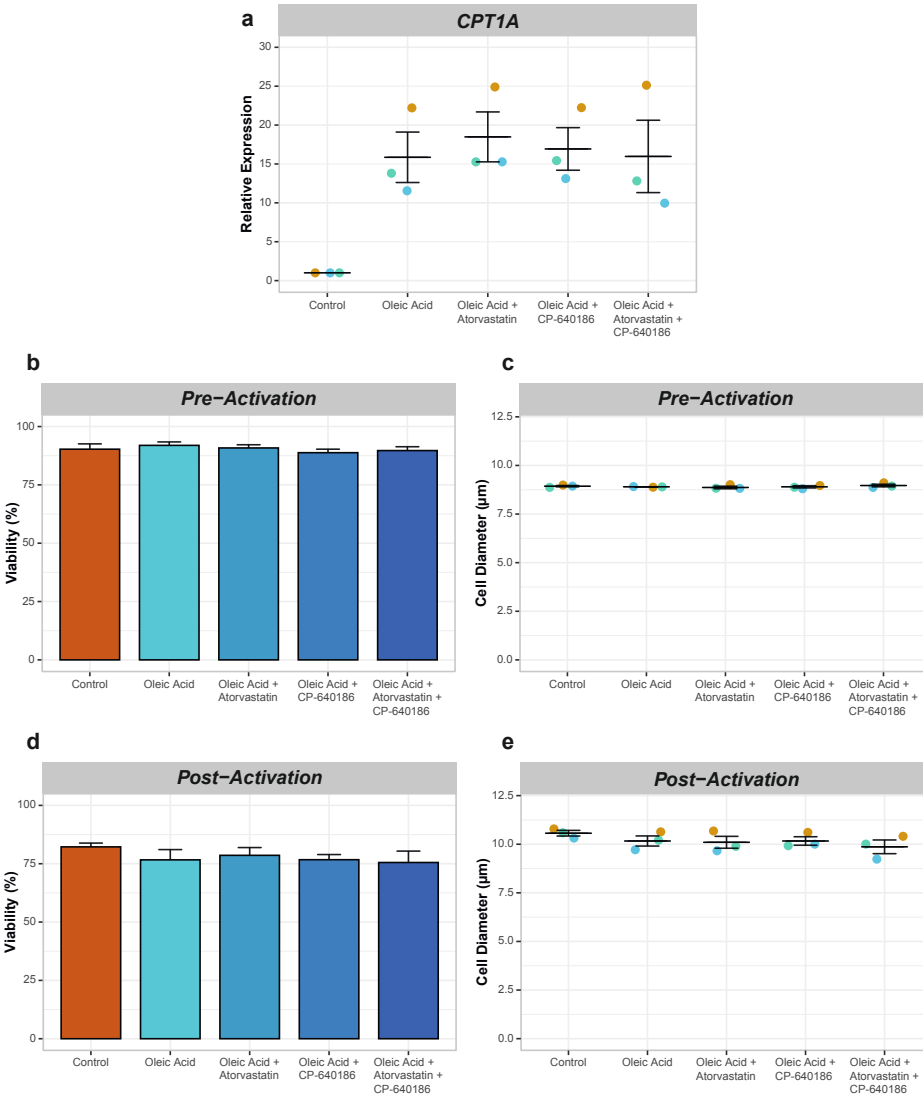

Supplemental Fig. 16 | Verification of viability, cell diameter and *CPT1A* expression post-exposure and post-activation for spectral cytometry with metabolic inhibitors. (a) Dot plot showing the relative expression of *CPT1A* per donor after 48h of oleic acid exposure, with or without inhibitors added as a confirmation of the ***in vitro*** model by RT-qPCR. Values are colored by donor and shown relative to the control condition. On average *CPT1A* was upregulated 15.86 SE 3.24 fold when exposed to oleic acid, 18.48 SE 3.21 fold when exposed to oleic acid + atorvastatin, 16.93 SE 2.74 fold when exposed to oleic acid + CP-640186, and 15.97 SE 4.65 fold when exposed to oleic acid + atorvastatin + CP-640186. Atorvastatin is an HMGCR inhibitor, blocking cholesterol biosynthesis, and CP-640186 is an ACC inhibitor, blocking fatty acid biosynthesis. As CPT1A is a part of the fatty acid oxidation pathway there was no influence of the inhibitors on *CPT1A* expression, n = 3. **(b)** Bar plot showing the average cell viability and standard error in percent, as determined by Via1-Cassette™ on a NucleoCounter® NC-200™. On average the cell viability of control exposed cells was 90.30 SE 2.27%, oleic acid exposed cells was 91.93 SE 1.48%, oleic acid + atorvastatin exposed cells was 90.83 SE 1.37%, oleic acid + CP-640186 exposed cells was 88.80 SE 1.50%, and oleic acid + atorvastatin + CP-640186 exposed cells was

89.70 SE 2.86% at 48h. Thus, there was no effect on $CD4^+$ T cell viability after 48h exposure, n = 3. **(c)** Dot plot showing the average cell diameter and standard error in µm, as determined by Via1-Cassette™ on a NucleoCounter® NC-200™. On average the cell diameter of control exposed cells was 8.93 SE 0.03µm, oleic acid exposed cells was 8.90 SE 0.0µm, oleic acid + atorvastatin exposed cells was 8.87 SE 0.07µm, oleic acid + CP-640186 exposed cells was 8.90 SE 0.0µm, and oleic acid + atorvastatin + CP-640186 exposed cells was 8.97 SE 0.07µm after 48h exposure. Thus, there was no effect on $CD4^+$ T cell diameter after 48h exposure, n = 3. **(d)** Bar plot showing the average cell viability and standard error in percent, as determined by Via1-Cassette™ on a NucleoCounter® NC-200™ after 72h activation with CD3-CD28 activation beads. On average the cell viability of control exposed cells was 82.23 SE 1.62%, oleic acid exposed cells was 76.67 SE 7.61%, oleic acid + atorvastatin exposed cells was 78.60 SE 3.33%, oleic acid + CP-640186 exposed cells was 76.73 SE 2.20%, and oleic acid + atorvastatin + CP-640186 exposed cells was 75.53 SE 4.88% after 72h activation. Thus, there was no effect on $CD4^+$ T cell viability after 72h activation between the different conditions. However, the cells were slightly less viable after activation than before activation, n = 3. **(e)** Dot plot showing the average cell diameter and standard error in µm, as determined by Via1-Cassette™ on a NucleoCounter® NC-200™. On average the cell diameter of control exposed cells was 10.57 SE 0.15µm, oleic acid exposed cells was 10.17 SE 0.26µm, oleic acid + atorvastatin exposed cells was 10.10 SE 0.31µm, oleic acid + CP-640186 exposed cells was 10.17 SE 0.22µm, and oleic acid + atorvastatin + CP-640186 exposed cells was 9.87 SE 0.61µm after 72h activation. Thus, there was no effect on $CD4^+$ T cell diameter after 48h exposure. However, the cells were larger after activation than before activation as was expected, n = 3.

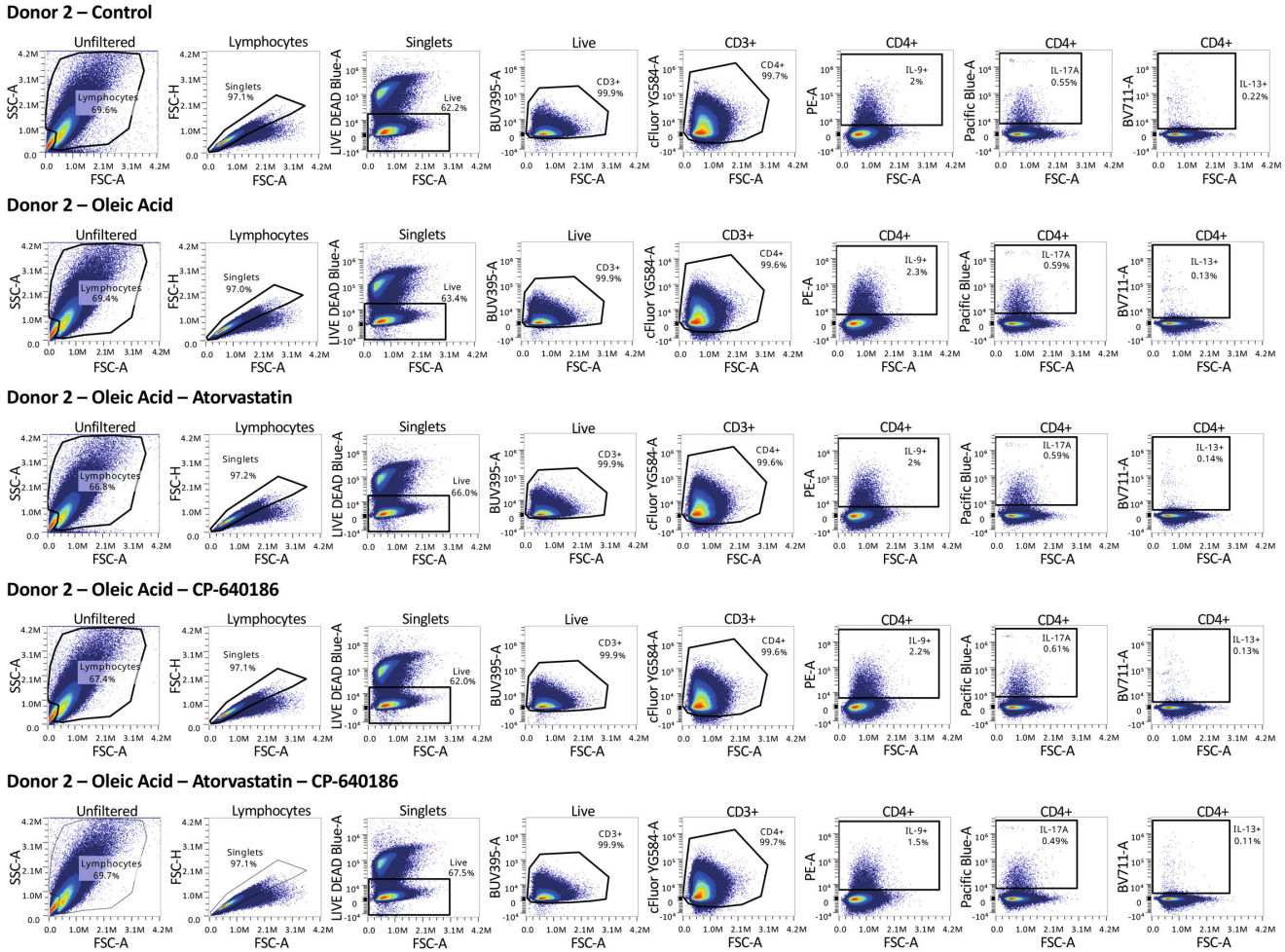

Supplemental Fig. 17 (partial) | Gating strategy for the inhibitor spectral cytometry analysis of activated CD4⁺ T cells pre-exposed to oleic acid with or without metabolic inhibitors, n = 3. Gating strategy is the same for all 3 donors analyzed and includes gates set for all markers measured. Gating strategy for 2 different donors and 5 different exposures are shown here, the rest of the figure can be found in the online supplement: https://doi.org/10.1016/j.isci.2024.109496.

Supplemental Table 1 | Changes in gene expression and $CD4^+$ T cell markers due to oleic acid pre-exposure.

Supplemental Table 1 | (a) (partial) Upregulated differentially expressed genes in order of significance along with their Ensembl ID, gene symbol, UniProt ID, base mean, log2 fold change, log2 fold change at 0.5h, log2 fold change at 3h, log2 fold change at 24h, log2 fold change at 48h, log2 fold change at 72h, p value, and adjusted p value (FDR). The log2FoldChange at specific time points were used to create the heatmap and the UniProt ID was used for Path-MAP in PathBank. Top 30 most significantly expressed genes are shown here, the rest of the table can be found in the online supplement: https://doi.org/10.1016/j.isci.2024.109496.

Order	Ensembl ID	Gene Symbol	UniProt	baseMean	log2FC	log2FC 0.5h	log2FC 3h	log2FC 24h	log2FC 48h	log2FC 72h	P value	P_{FDR}
1	ENSG00000110090	*CPT1A*	P50416	3804.649	-0.066	-0.067	2.669	2.897	3.095	3.228	0	0
2	ENSG00000178537	*SLC25A20*	O43772	931.641	0.064	0.062	2.254	1.491	1.662	1.715	0	0
3	ENSG00000072778	*ACADVL*	P49748	8010.624	0.057	0.057	0.270	0.739	0.791	0.875	5.190E-260	2.237E-256
4	ENSG00000167315	*ACAA2*	P42765	905.165	0.067	0.060	0.972	0.757	0.821	0.812	3.568E-206	1.153E-202
5	ENSG00000163162	*RNF149*	Q8NC42	5125.409	0.047	0.047	0.226	0.360	0.409	0.406	2.302E-111	5.955E-108
6	ENSG00000171503	*ETFDH*	Q16134	801.658	0.111	0.109	0.641	0.721	0.772	0.840	4.397E-97	9.477E-94
7	ENSG00000166575	*TMEM135*	Q86UB9	403.428	-0.053	-0.065	0.390	0.822	0.936	0.995	9.506E-82	1.756E-78
8	ENSG00000145860	*RNF145*	Q96MT1	5873.733	-0.112	-0.115	-0.176	0.379	0.421	0.361	9.517E-65	1.539E-61
9	ENSG00000143110	*C1orf162*	Q8NEQ5	2052.143	0.231	0.228	0.485	0.349	0.437	0.380	2.701E-60	3.881E-57
10	ENSG00000184602	*SNN*	O75324	2253.209	-0.096	-0.095	-0.036	0.351	0.416	0.356	4.913E-57	6.354E-54
11	ENSG00000167851	*CD300A*	Q9UGN4	573.914	0.102	0.105	0.381	0.443	0.555	0.498	1.443E-45	1.697E-42
12	ENSG00000147872	*PLIN2*	Q99541	1591.102	-0.005	-0.009	0.183	0.211	0.403	0.400	6.864E-41	7.397E-38
13	ENSG00000004799	*PDK4*	Q16654	5.514	3.381	3.071	4.328	5.433	4.714	3.357	8.302E-41	8.258E-38

[continued on next page]

Supplemental Table 1 *[continued]*

Order	Ensembl ID	Gene Symbol	UniProt	baseMean	log2FC	log2FC 0.5h	log2FC 3h	log2FC 24h	log2FC 48h	log2FC 72h	P value	P_{FDR}
14	ENSG00000122378	*PRXL2A*	Q9BRX8	387.115	0.148	0.151	0.090	0.303	0.383	0.445	6.621E-39	6.116E-36
15	ENSG00000072310	*SREBF1*	P36956	964.618	0.052	0.051	-0.319	0.301	0.527	0.665	2.790E-38	2.405E-35
16	ENSG00000172059	*KLF11*	O14901	578.566	0.199	0.193	0.469	0.787	0.829	0.740	2.566E-37	2.074E-34
17	ENSG00000111684	*LPCAT3*	Q6P1A2	720.001	0.004	-0.002	0.495	0.288	0.431	0.416	7.622E-34	5.798E-31
18	ENSG00000177479	*ARIH2*	O95376	6202.269	-0.008	-0.010	0.220	0.130	0.157	0.192	2.752E-28	1.977E-25
19	ENSG00000113161	*HMGCR*	P04035	2667.317	-0.037	-0.032	0.121	0.343	0.528	0.474	9.134E-28	6.217E-25
20	ENSG00000087157	*PGS1*	Q32NB8	2240.393	0.052	0.053	0.172	0.170	0.210	0.155	3.379E-26	2.185E-23
21	ENSG00000099194	*SCD*	O00767	452.316	-0.042	-0.025	0.353	0.633	1.341	1.301	6.064E-25	3.734E-22
22	ENSG00000278540	*ACACA*	Q13085	944.923	-0.093	-0.093	-0.079	0.329	0.387	0.313	1.338E-23	7.864E-21
23	ENSG00000153395	*LPCAT1*	Q8NF37	3186.515	-0.058	-0.059	-0.054	0.298	0.316	0.270	2.971E-23	1.671E-20
24	ENSG00000164211	*STARD4*	Q96DR4	712.106	0.016	0.015	0.419	0.324	0.516	0.496	3.675E-23	1.980E-20
25	ENSG00000104823	*ECH1*	Q13011	1348.019	0.115	0.108	0.288	0.245	0.310	0.324	4.264E-23	2.206E-20
26	ENSG00000198911	*SREBF2*	Q12772	8317.191	-0.009	-0.009	0.132	0.227	0.471	0.408	1.458E-21	6.985E-19
27	ENSG00000186480	*INSIG1*	O15503	2865.535	-0.010	-0.007	0.169	0.249	0.531	0.554	4.234E-21	1.956E-18
28	ENSG00000130164	*LDLR*	P01130	2737.906	-0.051	-0.055	0.327	0.448	0.989	0.885	4.431E-21	1.976E-18
29	ENSG00000112972	*HMGCS1*	Q01581	1968.928	-0.021	-0.022	0.225	0.313	0.519	0.424	9.547E-21	4.115E-18
30	ENSG00000116133	*DHCR24*	Q15392	1436.170	-0.078	-0.078	0.216	0.446	0.860	0.715	5.054E-20	2.108E-17

Supplemental Table 1 | (b) (partial) Downregulated differentially expressed genes in order of significance along with their Ensembl ID, gene symbol, UniProt ID, base mean, log2 fold change, log2 fold change at 0.5h, log2 fold change at 3h, log2 fold change at 24h, log2 fold change at 48h, log2 fold change at 72h, p value, and adjusted p value (FDR). The log2FoldChange at specific time points were used to create the heatmap and the UniProt ID was used for Path-MAP in PathBank. Top 30 most significantly expressed genes are shown here, the rest of the table can be found in the online supplement: https://doi.org/10.1016/j.isci.2024.109496.

Order	Ensembl ID	Gene Symbol	UniProt	baseMean	log2FC	log2FC 0.5h	log2FC 3h	log2FC 24h	log2FC 48h	log2FC 72h	P value	P_{FDR}
1	ENSG00000125637	*PSD4*	Q8NDX1	7753.592	0.002	0.003	-0.066	-0.213	-0.215	-0.294	2.682E-22	1.334E-19
2	ENSG00000166913	*YWHAB*	P31946	16988.864	-0.006	-0.008	0.000	-0.137	-0.104	-0.109	1.123E-15	3.459E-13
3	ENSG00000074370	*ATP2A3*	Q93084	8314.894	0.027	0.027	-0.063	-0.187	-0.189	-0.194	1.915E-13	4.586E-11
4	ENSG00000167460	*TPM4*	P67936	4348.318	0.003	0.001	0.049	-0.152	-0.189	-0.157	5.491E-13	1.255E-10
5	ENSG00000158435	*CNOT11*	Q9UKZ1	3021.238	0.019	0.019	-0.065	-0.123	-0.121	-0.129	8.453E-12	1.562E-09
6	ENSG00000119714	*GPR68*	Q15743	556.312	-0.080	-0.079	-0.236	-0.283	-0.362	-0.439	3.278E-11	5.729E-09
7	ENSG00000158856	*DMTN*	Q08495	527.740	0.025	0.026	-0.050	-0.249	-0.233	-0.217	2.851E-10	4.552E-08
8	ENSG00000102144	*PGK1*	P00558	9599.530	0.019	0.015	-0.008	-0.126	-0.099	-0.101	4.516E-10	6.876E-08
9	ENSG00000108654	*DDX5*	P17844	53321.550	-0.012	-0.013	-0.051	-0.119	-0.172	-0.207	4.519E-10	6.876E-08
10	ENSG00000183688	*RFLNB*	Q8N5W9	4685.097	0.010	0.009	-0.082	-0.162	-0.179	-0.241	4.641E-10	6.979E-08
11	ENSG00000131236	*CAP1*	Q01518	12576.054	-0.027	-0.029	-0.067	-0.137	-0.099	-0.100	1.042E-09	1.481E-07
12	ENSG00000172215	*CXCR6*	O00574	270.089	0.046	0.045	-0.094	-0.364	-0.386	-0.621	1.587E-09	2.147E-07
13	ENSG00000115091	*ACTR3*	P61158	8483.351	-0.001	-0.004	0.005	-0.114	-0.097	-0.140	2.746E-09	3.586E-07
14	ENSG00000070831	*CDC42*	P60953	9857.088	-0.016	-0.018	-0.028	-0.075	-0.109	-0.137	2.997E-09	3.876E-07

[continued on next page]

Supplemental Table 1 | (b) (partial) *[continued]*

Order	Ensembl ID	Gene Symbol	UniProt	baseMean	log2FC	log2FC 0.5h	log2FC 3h	log2FC 24h	log2FC 48h	log2FC 72h	P value	P_{FDR}
15	ENSG00000102158	*MAGT1*	Q9H0U3	1961.500	-0.003	-0.004	0.025	-0.095	-0.144	-0.173	3.736E-09	4.784E-07
16	ENSG00000142875	*PRKACB*	P22694	6088.499	-0.016	-0.018	-0.078	-0.080	-0.147	-0.195	4.829E-09	6.063E-07
17	ENSG00000160791	*CCR5*	P51681	445.160	-0.016	-0.015	-0.063	-0.275	-0.288	-0.297	5.118E-09	6.364E-07
18	ENSG00000075624	*ACTB*	P60709	90701.100	0.062	0.055	0.094	-0.176	-0.152	-0.168	1.135E-08	1.346E-06
19	ENSG00000197043	*ANXA6*	P08133	12140.502	0.030	0.031	-0.070	-0.201	-0.154	-0.139	1.230E-08	1.446E-06
20	ENSG00000167986	*DDB1*	Q16531	7313.881	-0.008	-0.008	-0.023	-0.111	-0.073	-0.088	1.322E-08	1.527E-06
21	ENSG00000044574	*HSPA5*	P11021	10108.431	-0.002	-0.004	0.049	-0.056	-0.125	-0.189	2.223E-08	2.457E-06
22	ENSG00000223501	*VPS52*	Q8N1B4	3308.603	0.010	0.010	-0.021	-0.081	-0.082	-0.119	3.427E-08	3.724E-06
23	ENSG00000182944	*EWSR1*	Q01844	13959.893	0.022	0.022	-0.024	-0.090	-0.102	-0.098	4.940E-08	5.237E-06
24	ENSG00000143549	*TPM3*	P06753	12626.672	0.017	0.014	-0.025	-0.093	-0.066	-0.079	5.965E-08	6.272E-06
25	ENSG00000072818	*ACAP1*	Q15027	14390.199	0.055	0.054	-0.039	-0.050	-0.112	-0.126	6.646E-08	6.821E-06
26	ENSG00000128340	*RAC2*	P15153	10806.212	0.042	0.040	-0.074	-0.139	-0.139	-0.162	9.966E-08	9.914E-06
27	ENSG00000198176	*TFDP1*	Q14186	1798.488	-0.028	-0.028	-0.010	-0.144	-0.137	-0.187	1.484E-07	1.443E-05
28	ENSG00000143870	*PDIA6*	Q15084	3458.824	0.043	0.040	-0.002	-0.027	-0.096	-0.185	2.079E-07	1.948E-05
29	ENSG00000138071	*ACTR2*	P61160	15672.838	-0.061	-0.063	0.022	-0.108	-0.107	-0.133	2.356E-07	2.176E-05
30	ENSG00000120798	*NR2C1*	P13056	1981.007	-0.016	-0.016	0.063	0.054	-0.073	-0.156	3.371E-07	3.027E-05

Supplemental Table 1 | (c) Transcription factors, extracellular markers, and intracellular markers measured in non-activated $CD4^+$ T cell after pre-exposure to oleic acid. Values are shown as a percent of the parent, n = 8.

Donor	Exposure	$CD127^{low}$ $CD25^{hi}$ $FoxP3^+$	$CD25^+$	$PD1^+$	$CTLA4^+$	$CD27^+$	$CD38^+$	$Tbet^+$	$GATA3^+$	$IL\text{-}4^+$	$IL\text{-}5^+$	$IL\text{-}13^+$	$IL\text{-}9^+$	$IL\text{-}17A^+$	$IL\text{-}21^+$	$IL\text{-}22^+$	$TNF\alpha^+$	$IFN\gamma^+$	$IL\text{-}10^+$
1	Control	0.619	4.210	1.010	28.10	0.934	38.90	0.271	0.059	0.047	0.017	0.057	0.103	0.160	0.033	0.016	0.200	1.070	0.021
1	Oleic Acid	0.501	5.540	1.980	30.10	0.925	42.10	0.869	0.103	0.069	0.057	0.087	0.284	0.193	0.070	0.041	0.225	1.530	0.056
2	Control	0.380	1.750	0.401	42.60	0.104	33.40	0.058	0.027	0.046	0.026	0.026	0.034	0.257	0.043	0.082	1.130	1.360	0.027
2	Oleic Acid	0.195	1.520	0.331	42.60	0.041	29.90	0.056	0.011	0.042	0.027	0.020	0.030	0.264	0.051	0.070	1.080	1.580	0.028
3	Control	0.903	5.080	2.620	39.30	1.730	31.40	0.813	0.147	0.068	0.103	0.049	0.242	0.178	0.159	0.073	0.812	3.650	0.102
3	Oleic Acid	0.437	2.950	0.747	38.90	0.888	29.40	0.072	0.016	0.045	0.072	0.031	0.028	0.184	0.064	0.027	0.872	4.220	0.058
4	Control	0.786	2.180	1.340	42.40	0.484	27.50	0.051	0.023	0.045	0.070	0.036	0.016	0.121	0.094	0.031	0.748	4.390	0.061
4	Oleic Acid	0.445	1.890	1.130	43.90	0.258	24.90	0.048	0.019	0.040	0.075	0.024	0.017	0.099	0.125	0.038	0.845	5.490	0.096
5	Control	2.350	5.090	0.646	12.20	0.166	47.80	0.011	0.024	0.015	0.002	0.030	0.010	0.081	0.041	0.005	0.007	0.103	0.005
5	Oleic Acid	2.280	5.350	0.547	12.50	0.099	47.90	0.035	0.022	0.020	0.009	0.020	0.014	0.084	0.055	0.003	0.013	0.088	0.005
6	Control	7.770	7.380	1.780	23.00	0.284	37.40	0.023	0.036	0.016	0.007	0.066	0.012	0.075	0.038	0.006	0.011	0.231	0.005
6	Oleic Acid	6.210	7.120	1.640	22.80	0.255	37.60	0.018	0.024	0.021	0.049	0.051	0.006	0.117	0.047	0.003	0.007	0.240	0.003
7	Control	0.798	1.310	0.638	13.40	0.227	51.10	0.016	0.024	0.020	0.002	0.015	0.010	0.086	0.044	0.007	0.005	0.030	0.003
7	Oleic Acid	0.452	1.210	0.572	13.00	0.142	51.20	0.033	0.017	0.019	0.009	0.018	0.010	0.056	0.039	0.008	0.012	0.028	0.004
8	Control	4.540	5.990	1.740	16.30	1.800	38.80	0.039	0.021	0.020	0.009	0.022	0.013	0.080	0.042	0.005	0.011	0.067	0.006
8	Oleic Acid	3.800	6.230	1.500	16.40	1.450	39.70	0.039	0.019	0.018	0.015	0.025	0.015	0.079	0.049	0.004	0.014	0.075	0.004

Supplemental Table 1 | (d) Transcription factors, extracellular markers, and intracellular markers measured in activated $CD4^+$ T cell after pre-exposure to oleic acid. The concentration of oleic acid was 30µg/mL. Values are shown as a percent of the parent, n = 8.

Donor	Exposure	$CD127^{low}$ $CD25^{hi}$ $FoxP3^+$	$CD25^+$	$PD1^+$	$CTLA4^+$	$CD27^+$	$CD38^+$	$Tbet^+$	$GATA3^+$	$IL\text{-}4^+$	$IL\text{-}5^+$	$IL\text{-}13^+$	$IL\text{-}9^+$	$IL\text{-}17A^+$	$IL\text{-}21^+$	$IL\text{-}22^+$	$TNF\alpha^+$	$IFN\gamma^+$	$IL\text{-}10^+$
1	Control	7.120	72.20	60.40	66.50	14.60	52.30	0.421	0.629	0.018	0.023	0.059	0.680	0.292	0.208	0.117	0.648	2.770	0.124
1	Oleic Acid	6.960	81.40	67.10	70.30	14.00	54.70	0.427	0.930	0.023	0.037	0.089	1.440	0.595	0.362	0.148	1.040	3.840	0.203
2	Control	4.560	62.80	55.30	80.30	2.140	54.20	0.213	1.470	0.041	0.055	0.067	0.595	0.302	0.520	0.219	2.640	4.010	0.138
2	Oleic Acid	5.980	67.50	58.00	80.30	1.440	51.40	0.244	1.780	0.019	0.097	0.115	0.889	0.389	0.828	0.304	2.610	4.600	0.150
3	Control	9.610	68.10	60.70	66.90	4.580	58.40	0.513	1.020	0.019	0.039	0.094	0.563	0.361	0.322	0.189	1.730	8.310	0.144
3	Oleic Acid	11.20	69.80	60.50	68.10	2.760	53.50	0.807	1.470	0.066	0.078	0.219	1.110	0.633	0.438	0.180	2.160	8.850	0.213
4	Control	6.860	59.90	54.20	71.80	1.850	53.00	0.415	0.698	0.022	0.104	0.158	1.040	0.181	0.475	0.104	1.740	13.20	0.151
4	Oleic Acid	8.570	60.20	53.20	69.70	1.400	50.10	0.539	0.905	0.018	0.119	0.320	2.010	0.322	0.743	0.139	2.100	13.40	0.217
5	Control	6.270	79.10	66.60	80.00	6.090	49.90	1.690	1.850	0.039	0.103	0.047	2.110	0.350	0.217	0.032	0.610	1.530	0.130
5	Oleic Acid	7.070	79.60	68.10	79.30	5.580	45.30	1.540	3.320	0.046	0.134	0.077	3.360	0.456	0.250	0.032	0.682	1.670	0.144
6	Control	9.420	85.40	76.70	80.00	2.250	60.90	1.490	1.480	0.093	0.244	0.245	3.060	1.250	0.585	0.118	1.580	3.100	0.245
6	Oleic Acid	10.50	85.30	75.10	79.50	1.660	52.90	1.090	1.390	0.080	0.245	0.199	3.660	1.410	0.544	0.115	1.630	2.810	0.250
7	Control	3.660	84.40	75.80	88.30	15.30	72.40	0.726	0.952	0.035	0.146	0.051	0.559	0.186	0.247	0.030	0.570	0.703	0.121
7	Oleic Acid	4.470	80.90	70.30	86.70	12.70	63.90	0.725	1.370	0.045	0.168	0.077	0.736	0.205	0.229	0.030	0.776	0.823	0.112
8	Control	12.00	85.30	79.70	82.20	4.720	72.80	2.780	0.434	0.135	0.332	0.264	1.960	0.868	0.594	0.124	1.640	4.200	0.392
8	Oleic Acid	13.30	85.10	79.30	82.20	3.550	70.00	2.690	0.450	0.134	0.390	0.378	2.690	1.090	0.600	0.132	1.580	4.490	0.327

Supplemental Table 1 | (e) Coexpression analysis of various $CD4^+$ T cell markers in activated $CD4^+$ T cells after pre-exposure to oleic acid. The concentration of oleic acid was 30µg/mL. Values are shown as a percent of the parent, n = 8.

Donor	Exposure	$IFNy^+$ OR TNF^+	$IFNy^+$ AND $TNFα^+$	$IL\text{-}5^+$ OR $IL\text{-}4^+$ OR $IL\text{-}13^+$	$IL\text{-}13^+$ AND $IL\text{-}4^+$ AND $IL\text{-}5^+$	$IL\text{-}5^+$ OR $IL\text{-}4^+$ OR $IL\text{-}13^+$ AND $IL\text{-}9^+$	$PD1^+$ AND $CTLA4^+$	$PD1^+$ OR $CTLA4^+$
1	Control	3.22	0.20	0.09	0	0.020	44.9	82.1
1	Oleic Acid	4.54	0.34	0.15	0	0.020	50.2	87.3
2	Control	5.89	0.76	0.16	0	0.005	45.2	90.3
2	Oleic Acid	6.32	0.89	0.22	0.001	0.020	48.2	90.1
3	Control	9.30	0.73	0.15	0	0.006	43.6	84.1
3	Oleic Acid	10.1	0.95	0.35	0	0.010	43.4	85.1
4	Control	14.0	0.96	0.27	0.002	0.020	40.3	85.7
4	Oleic Acid	14.4	1.09	0.42	0	0.040	39.3	83.7
5	Control	2.03	0.10	0.18	0.0009	0.010	55.1	91.4
5	Oleic Acid	2.22	0.13	0.23	0	0.040	56.1	91.4
6	Control	4.33	0.34	0.50	0.004	0.050	64.0	92.7
6	Oleic Acid	4.07	0.36	0.45	0.001	0.040	62.5	92.1
7	Control	1.20	0.07	0.22	0	0.007	68.4	95.6
7	Oleic Acid	1.48	0.12	0.27	0.0009	0.007	62.5	94.5
8	Control	5.44	0.39	0.64	0.003	0.030	67.4	94.4
8	Oleic Acid	5.66	0.42	0.77	0.001	0.060	67.3	94.2

Supplemental Table 1 | (e) continued

Donor	Exposure	PD1$^+$ AND CTLA4$^+$ AND CD38$^+$	PD1$^+$ AND CTLA4$^+$ AND CD38$^+$ AND IFNy$^+$ OR TNFα$^+$	PD1$^+$ AND CTLA4$^+$ AND CD38$^+$ AND IL-5$^+$ OR IL-4$^+$ OR IL-13$^+$	PD1$^+$ AND CTLA4$^+$ AND CD38$^+$ AND IL-9$^+$	IFNy$^+$ OR TNFα$^+$ AND IL-9$^+$
1	Control	33.4	1.73	0.05	0.35	0.16
1	Oleic Acid	34.2	2.32	0.07	0.72	0.32
2	Control	38.2	3.76	0.10	0.40	0.21
2	Oleic Acid	36.9	3.78	0.12	0.54	0.31
3	Control	37.7	5.88	0.08	0.44	0.19
3	Oleic Acid	33.6	5.66	0.21	0.68	0.31
4	Control	34.1	7.84	0.18	0.63	0.6
4	Oleic Acid	31.9	7.78	0.28	1.25	1.12
5	Control	36.2	0.84	0.08	0.84	0.24
5	Oleic Acid	32.9	0.80	0.09	1.00	0.40
6	Control	45.3	2.56	0.27	1.62	0.47
6	Oleic Acid	38.2	2.00	0.19	1.43	0.53
7	Control	60.3	0.87	0.16	0.42	0.05
7	Oleic Acid	51.0	0.94	0.18	0.48	0.09
8	Control	58.5	4.15	0.46	1.53	0.40
8	Oleic Acid	56.4	4.17	0.5	2.02	0.46

Supplemental Table 1 | (f) Transcription factors, extracellular markers, and intracellular markers measured in non-activated $CD4^+$ T cell after pre-exposure to oleic acid. The concentration of oleic acid was 28µg/mL. Values are shown as a percent of the parent, n = 8. In order to calculate the fold change of $CD127^{low}CD25^{hi}FoxP3^+$ for D10, D11 and D12 add a "1" to each value for that donor.

Donor	Exposure	$CD127^{low}$ $CD25^{hi}$ $FoxP3^+$	$CD25^+$	$PD1^+$	$CTLA4^+$	$CD27^+$	$CD38^+$	$Tbet^+$	$GATA3^+$	$IL\text{-}4^+$	$IL\text{-}13^+$	$IL\text{-}9^+$	$IL\text{-}17A^+$	$IL\text{-}21^+$	$IL\text{-}22^+$	$TNF\alpha^+$	$IFN\gamma^+$	$IL\text{-}10^+$
10	Control	0.000	2.210	0.470	22.30	2.050	7.250	0.002	0.041	0.003	0.002	0.006	0.195	0.022	0.011	5.410	0.009	0.003
10	Oleic Acid	0.046	2.560	0.512	24.80	1.830	8.020	0.003	0.020	0.005	0.002	0.002	0.216	0.024	0.014	7.120	0.005	0.004
11	Control	0.000	2.000	0.240	23.00	0.328	8.700	0.007	0.026	0.003	0.001	0.006	0.573	0.023	0.037	5.390	0.008	0.002
11	Oleic Acid	0.000	2.750	0.316	24.30	0.459	10.80	0.002	0.038	0.002	0.002	0.007	0.653	0.028	0.038	7.510	0.010	0.005
12	Control	0.000	1.150	0.646	16.20	0.656	8.410	0.008	0.006	0.003	0.001	0.002	0.120	0.019	0.020	3.810	0.008	0.002
12	Oleic Acid	0.000	1.690	0.718	22.20	0.439	7.160	0.018	0.005	0.003	0.001	0.005	0.155	0.030	0.023	5.620	0.007	0.004
13	Control	41.70	3.160	0.790	47.50	0.387	1.890	0.021	0.009	0.008	0.004	0.094	0.920	0.026	0.289	21.20	0.116	0.011
13	Oleic Acid	45.00	3.230	0.741	47.30	0.324	1.890	0.032	0.015	0.010	0.004	0.103	1.020	0.031	0.359	19.80	0.378	0.011
14	Control	21.90	2.040	0.217	29.10	0.312	6.550	0.019	0.011	0.003	0.002	0.100	0.192	0.030	0.346	11.30	0.057	0.006
14	Oleic Acid	16.20	2.360	0.208	30.80	0.228	7.080	0.021	0.018	0.002	0.005	0.095	0.226	0.027	0.273	13.10	0.066	0.007
15	Control	31.20	1.480	0.095	44.10	0.569	4.830	0.013	0.017	0.005	0.002	0.072	0.146	0.023	0.239	5.550	0.049	0.005
15	Oleic Acid	27.50	1.460	0.095	43.30	0.500	4.310	0.017	0.017	0.005	0.003	0.077	0.155	0.027	0.210	5.860	0.110	0.005
16	Control	11.80	2.930	0.226	29.20	1.480	7.880	0.033	0.018	0.031	0.006	0.037	0.271	0.051	0.034	6.090	0.023	0.004
16	Oleic Acid	9.710	2.720	0.246	33.30	0.660	6.880	0.025	0.009	0.019	0.002	0.021	0.407	0.027	0.031	7.590	0.016	0.003
17	Control	5.990	4.520	0.552	21.60	0.537	11.70	0.280	0.018	0.021	0.006	0.022	0.808	0.032	0.027	11.30	0.015	0.004
17	Oleic Acid	7.450	4.520	0.542	26.40	0.382	12.30	0.254	0.015	0.021	0.004	0.025	0.992	0.029	0.033	15.60	0.020	0.002

Supplemental Table 1 | (g) Transcription factors, extracellular markers, and intracellular markers measured in activated $CD4^+$ T cell after pre-exposure to oleic acid. The concentration of oleic acid was 28µg/mL. Values are shown as a percent of the parent, n = 8. In order to calculate the fold change of $CD127^{low}CD25^{hi}FoxP3^+$ for D11 and D12 add a "1" to each value for that donor.

Donor	Exposure	$CD127^{low}$ $CD25^{hi}$ $FoxP3^+$	$CD25^+$	$PD1^+$	$CTLA4^+$	$CD27^+$	$CD38^+$	$Tbet^+$	$GATA3^+$	$IL\text{-}4^+$	$IL\text{-}13^+$	$IL\text{-}9^+$	$IL\text{-}17A^+$	$IL\text{-}21^+$	$IL\text{-}22^+$	$TNF\alpha^+$	$IFN\gamma^+$	$IL\text{-}10^+$
10	EtOH	0.003	60.60	58.10	59.50	10.40	53.40	0.287	0.700	0.003	0.013	0.831	0.394	3.380	0.069	1.540	2.680	0.258
10	Oleic Acid	0.001	59.90	55.00	55.90	7.230	45.90	0.341	1.060	0.003	0.009	0.986	0.319	2.750	0.044	0.967	1.860	0.160
11	EtOH	0.000	64.90	56.20	51.90	8.930	50.90	0.349	0.840	0.008	0.016	1.190	0.389	2.510	0.079	1.270	1.370	0.188
11	Oleic Acid	0.001	62.20	52.30	52.10	7.220	46.40	0.624	1.300	0.009	0.027	1.680	0.420	2.610	0.082	1.700	1.960	0.213
12	EtOH	0.000	64.20	57.80	69.80	14.20	53.50	0.370	0.613	0.003	0.030	0.816	0.133	2.580	0.082	1.400	1.890	0.123
12	Oleic Acid	0.002	63.50	54.20	65.20	9.220	49.10	0.435	1.000	0.004	0.024	1.190	0.137	2.240	0.069	0.896	2.040	0.134
13	EtOH	6.680	80.00	71.10	61.00	4.350	65.60	1.980	2.590	0.013	0.021	3.340	1.130	1.360	0.845	7.170	8.580	0.612
13	Oleic Acid	6.280	77.20	68.20	62.10	4.760	62.70	2.020	3.480	0.024	0.035	3.800	1.030	1.240	0.848	6.550	9.090	0.738
14	EtOH	5.560	72.50	61.60	62.90	6.150	61.40	1.020	1.220	0.010	0.034	1.030	0.596	1.000	0.658	6.830	4.720	0.801
14	Oleic Acid	5.400	71.20	60.00	59.70	5.690	57.70	0.927	2.190	0.014	0.036	1.170	0.616	0.905	0.615	4.700	4.540	0.764
15	EtOH	3.130	72.60	61.50	67.50	13.60	65.70	1.100	5.310	0.016	0.038	0.522	0.181	0.803	0.325	1.800	2.640	0.431
15	Oleic Acid	3.430	73.80	62.10	62.60	11.90	66.20	1.480	6.490	0.019	0.046	0.700	0.196	0.764	0.379	1.550	2.560	0.493
16	EtOH	3.810	86.60	77.30	70.50	18.70	71.00	1.510	4.780	0.205	0.240	0.402	0.507	0.571	0.143	2.020	0.859	0.047
16	Oleic Acid	4.840	82.40	70.90	64.00	13.80	59.00	1.030	4.820	0.158	0.232	0.574	0.546	0.372	0.140	1.670	0.669	0.042
17	EtOH	4.030	84.30	66.30	52.70	7.390	71.10	7.480	0.292	0.154	0.172	1.740	1.540	0.870	0.188	17.10	8.240	0.043
17	Oleic Acid	4.940	79.00	57.60	50.90	4.700	61.60	8.920	0.483	0.100	0.179	2.440	1.430	0.736	0.131	16.00	8.890	0.049

Supplemental Table 1 | (h) Intracellular markers measured in activated $CD4^+$ T cell after pre-exposure either oleic acid, oleic acid + atorvastatin, oleic acid + CP-640186, or oleic acid + atorvastatin + CP-640186. The concentration of oleic acid was 30µg/mL, atorvastatin was 10µM, and CP-640186 was 20µM. The donor numbers are labeled respectively of the donors used in the previous experiments. Values are shown as a percent of the parent, n = 3.

Donor	Exposure	Inhibitor	IL-9$^+$	IL-17A$^+$	IL-13$^+$
2	Control	None	2.000	0.555	0.222
2	Oleic Acid	None	2.280	0.588	0.127
2	Oleic Acid	Atorvastatin	2.030	0.585	0.138
2	Oleic Acid	CP-640186	2.170	0.615	0.126
2	Oleic Acid	Atorvastatin + CP-640186	1.480	0.486	0.115
5	Control	None	2.630	0.526	0.103
5	Oleic Acid	None	3.870	0.683	0.136
5	Oleic Acid	Atorvastatin	2.560	0.528	0.080
5	Oleic Acid	CP-640186	2.250	0.659	0.106
5	Oleic Acid	Atorvastatin + CP-640186	1.840	0.580	0.106
6	Control	None	4.630	1.950	0.287
6	Oleic Acid	None	5.520	2.480	0.365
6	Oleic Acid	Atorvastatin	4.020	1.970	0.271
6	Oleic Acid	CP-640186	3.350	1.800	0.283
6	Oleic Acid	Atorvastatin + CP-640186	2.750	1.470	0.317